

Measurements of Two-Particle Correlations with respect to Higher-Order Event Planes in $\sqrt{s}_{NN}=200$ GeV Au+Au Collisions at RHIC-PHENIX

**(RHIC-PHENIX $\sqrt{s}_{NN} = 200$ GeV 金・金衝突実験における
二粒子相関の反応平面依存性の測定)**

轟木 貴人
数理物質科学研究科 物理学専攻
高エネルギー原子核実験グループ
博士論文公開発表会 2014/1/27

Outline

✧ Introduction

- Quark Gluon Plasma (QGP)
- Higher-order event-planes & flow harmonics
- Previous two-particle correlation measurements and theoretical models

✧ Analysis

- Experimental set up
- Flow and two-particle correlation measurements
- Correlations with respect to event-planes

✧ Results & Discussion

- Two-particle correlations
- Event-plane dependent correlations

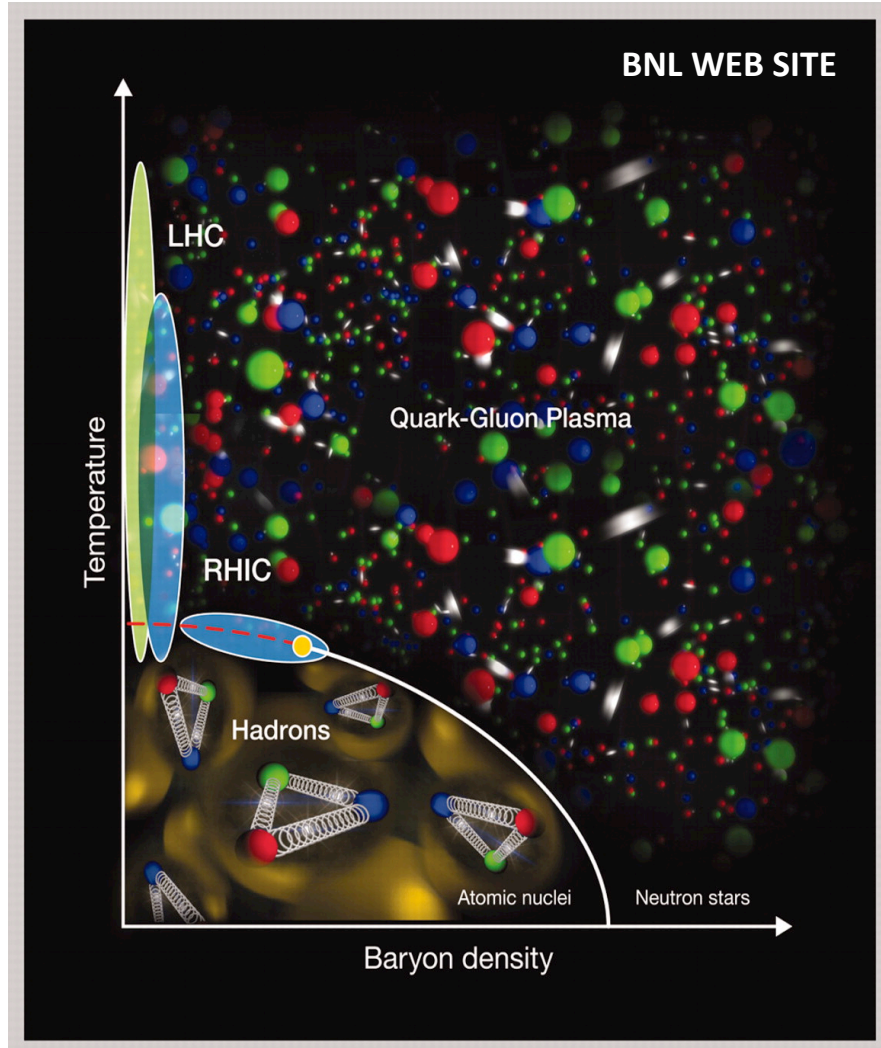
✧ Conclusion

INTRODUCTION

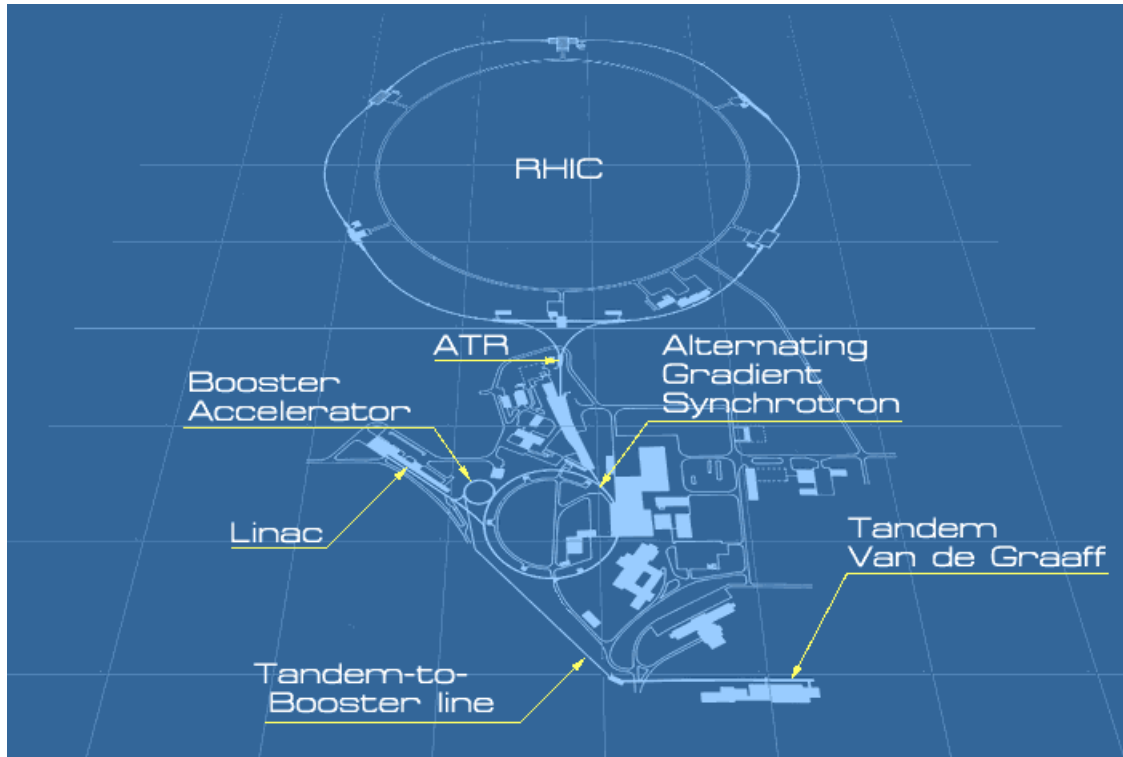
Quark Gluon Plasma (QGP)

- ✧ A fluid in which quark and gluons are deconfined from hadrons at high energy-density ε & temperature T
- ✧ Predicted transition ε & T by Lattice-QCD
 - $\varepsilon_c \sim 1.0$ [GeV/fm³]
 - $T_c \sim 170$ [MeV]

F. Karsch, Lect. Notes Phys. 583, 209 (2002)



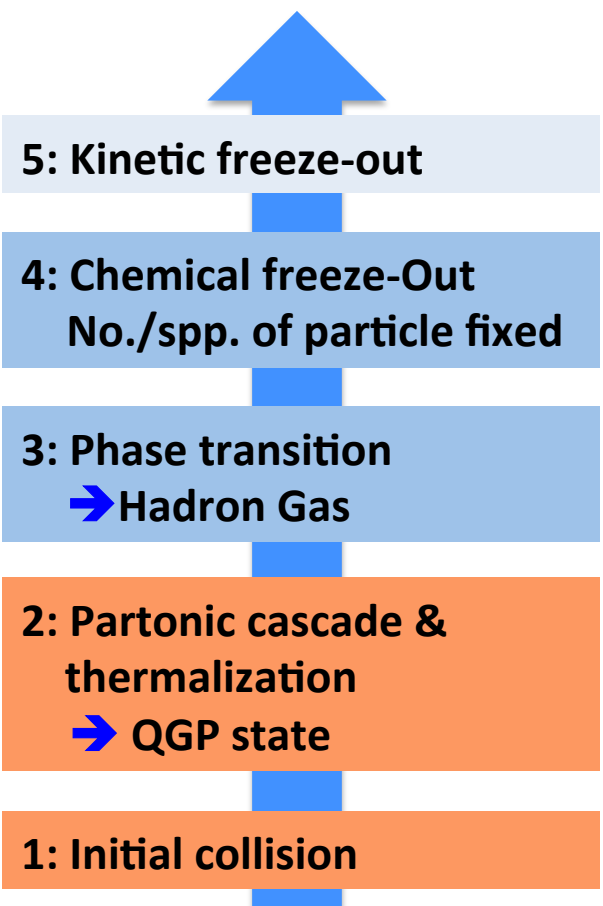
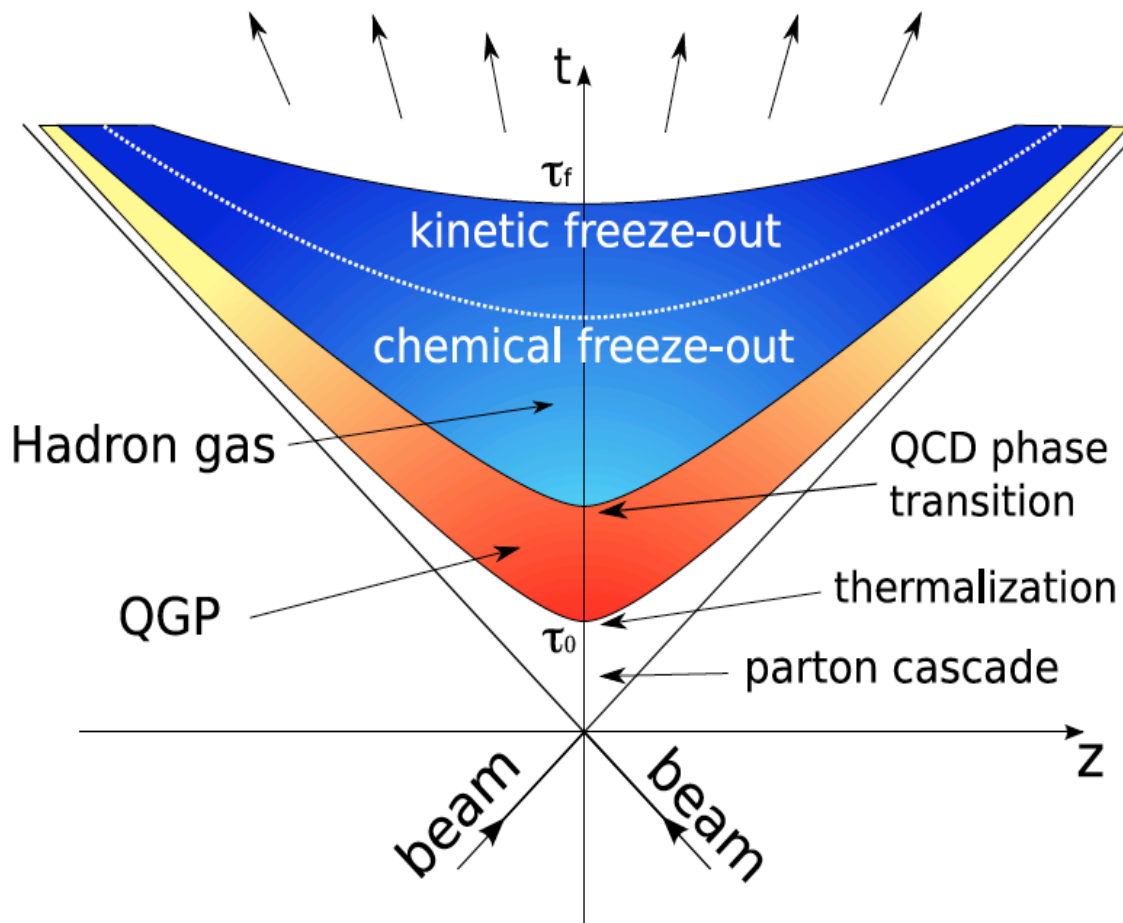
Relativistic Heavy Ion Collider (RHIC)



| Year | Collisions System |
|------|------------------------------|
| 2001 | Au+Au 130 GeV |
| 2002 | p+p, Au+Au 200 GeV |
| 2003 | p+p, d+Au 200 GeV |
| 2004 | Au+Au 62.4, 200 GeV |
| 2005 | Cu+Cu 22.4, 62.4, 200 GeV |
| 2006 | p+p 62.4, 200 GeV |
| 2007 | Au+Au 200 GeV |
| 2008 | p+p, d+Au 200 GeV |
| 2009 | p+p 200 500 GeV |
| 2010 | Au+Au 7.7, 39, 62.4, 200 GeV |
| 2011 | Au+Au 19.6, 27, 200 |
| 2012 | U+U 193GeV, Cu+Au 200 GeV |

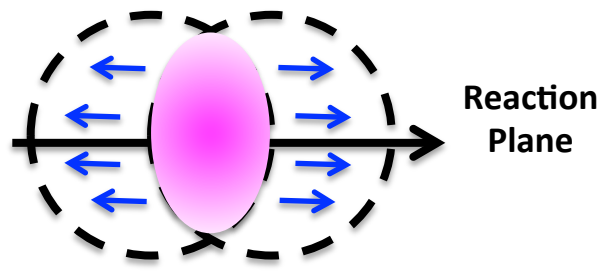
- Relativistic heavy ion collision is an unique tool to form QGP on the Earth
- Energy density at RHIC
 - $\varepsilon_{RHIC} \sim 5.0 - 15.0 \text{ [GeV/fm}^3\text{]}$
 - $\varepsilon_{RHIC} > \varepsilon_c$

Space-Time Evolution of Heavy Ion Collisions



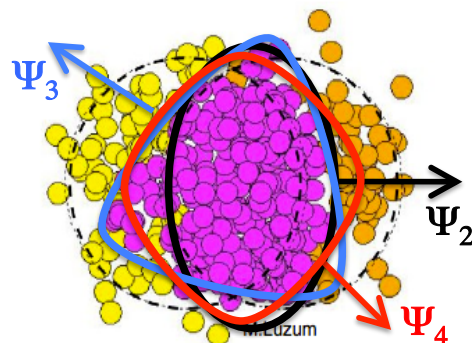
Higher-Order Event-Planes & Flow-Harmonics

Smooth participant density



Expansion to the short-axis direction by pressure gradient

Fluctuating participant density



Expansion to the short-axis directions of event-planes by pressure gradient

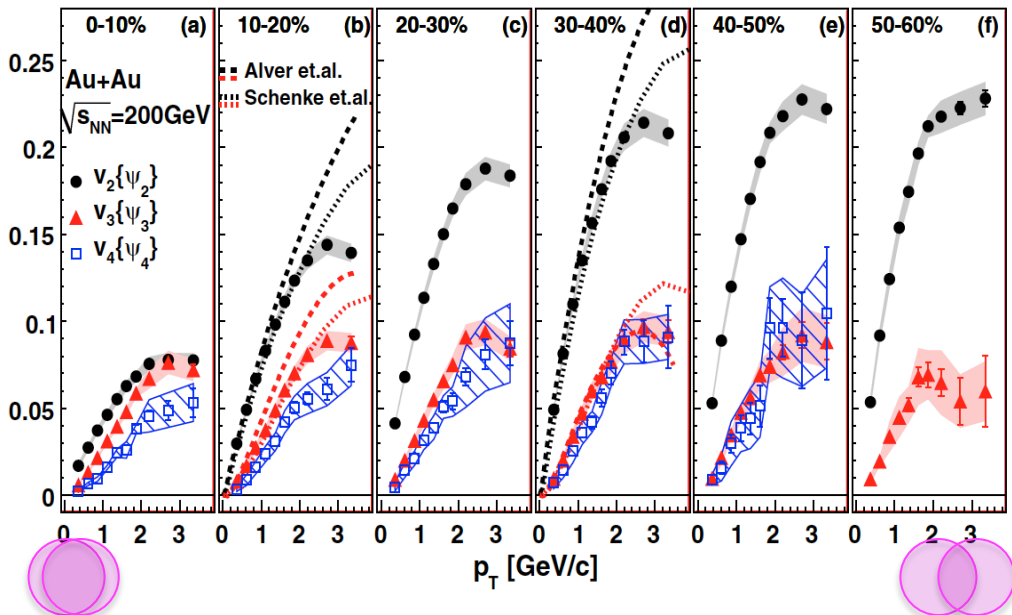
- ◊ Azimuthal distribution of emitted particles

$$\begin{aligned} \frac{dN}{d\phi} \propto & 1 + 2v_2 \cos 2(\phi - \Psi_2) \\ & + 2v_3 \cos 3(\phi - \Psi_3) \\ & + 2v_4 \cos 4(\phi - \Psi_4) \dots \\ v_n = & \langle \cos n(\phi - \Psi_n) \rangle \end{aligned}$$

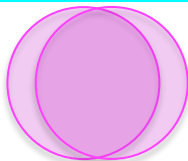
- v_n : Higher-order flow harmonics
- Ψ_n : Higher-order event planes
- ϕ : Azimuthal angle of emitted particles

Higher-Order Flow Harmonics

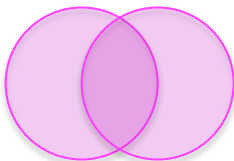
PRL107.252301 (2011)



Central Collisions



Peripheral Collisions

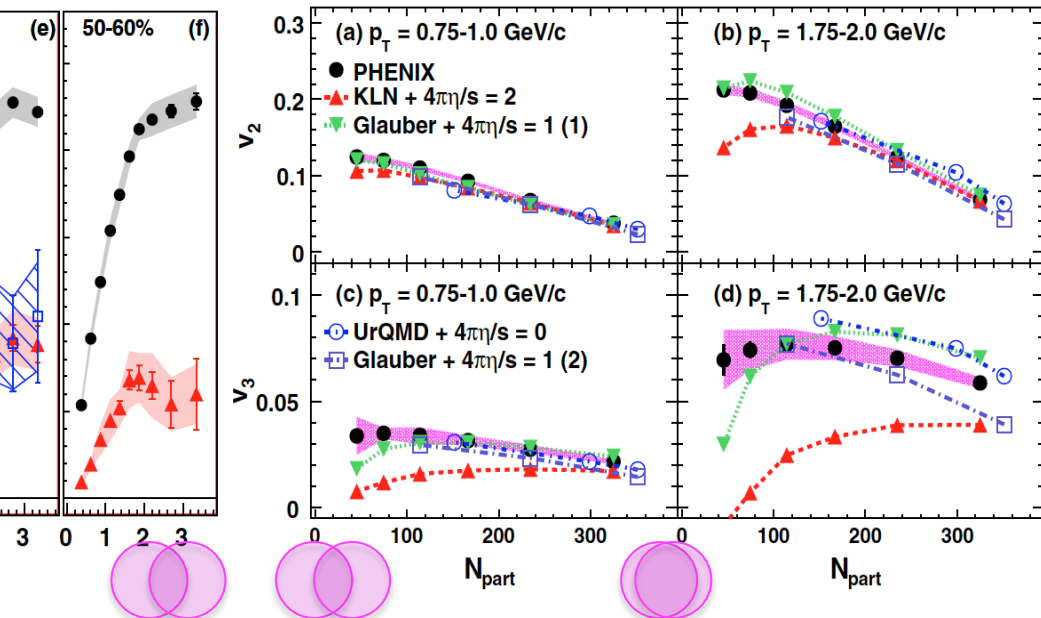


2014/1/27

N_{part} : # of participant nucleons in a collision

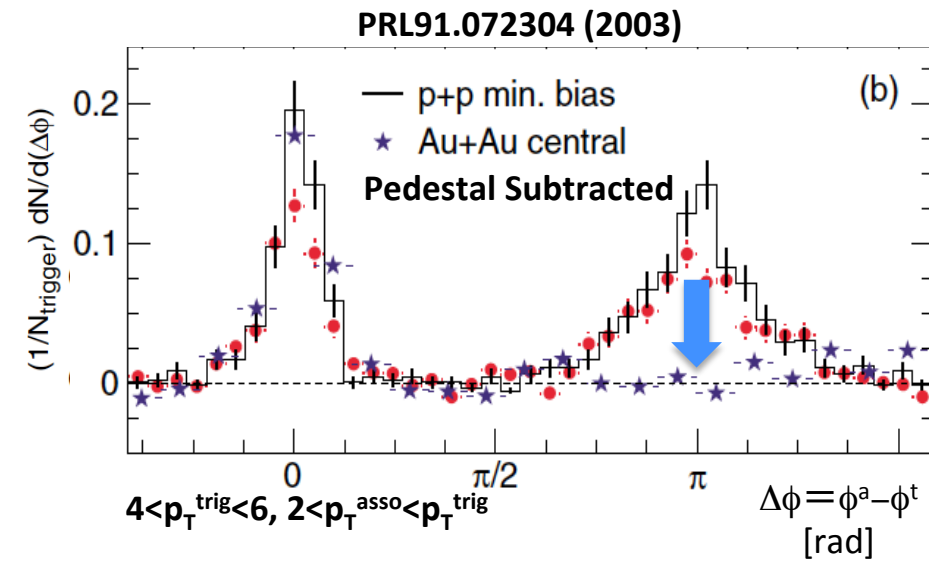
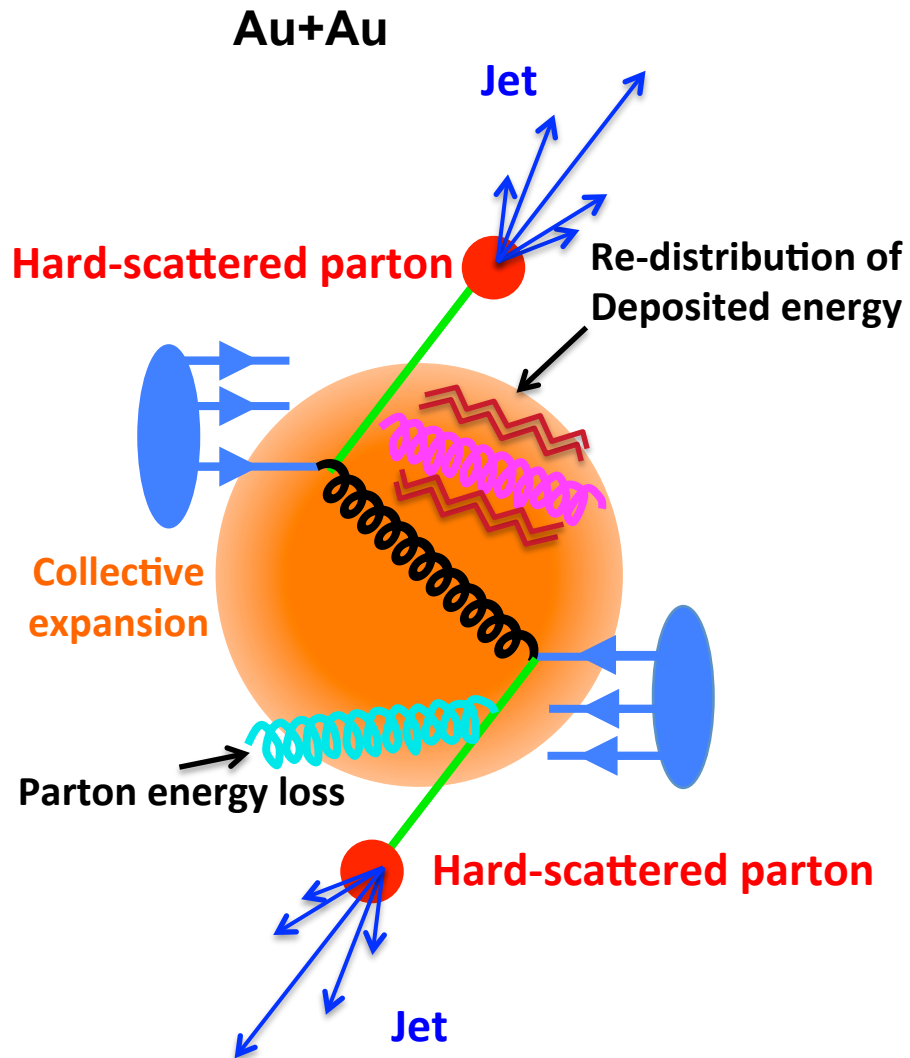
Centrality~0%

$N_{\text{part}} \sim 394$



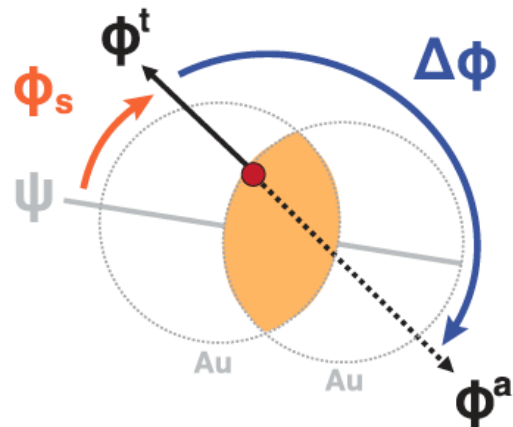
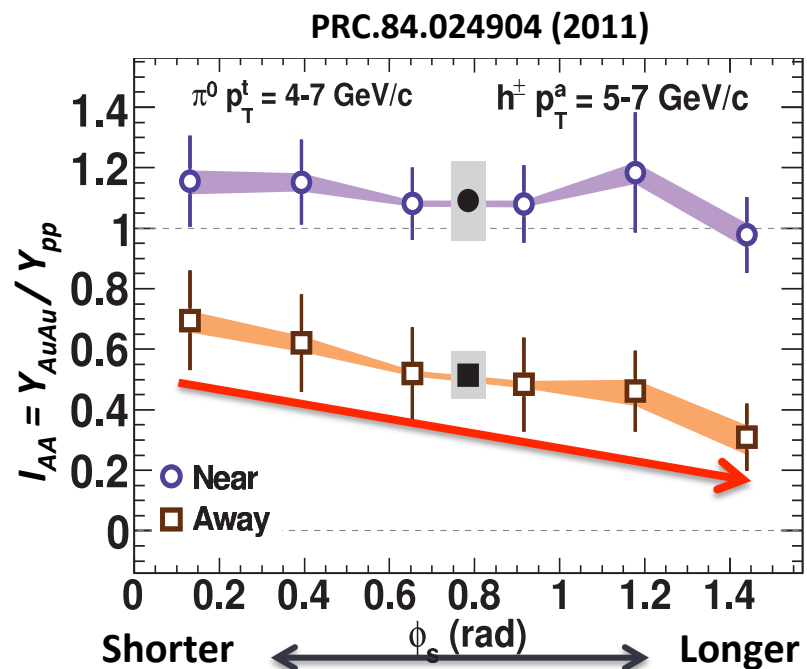
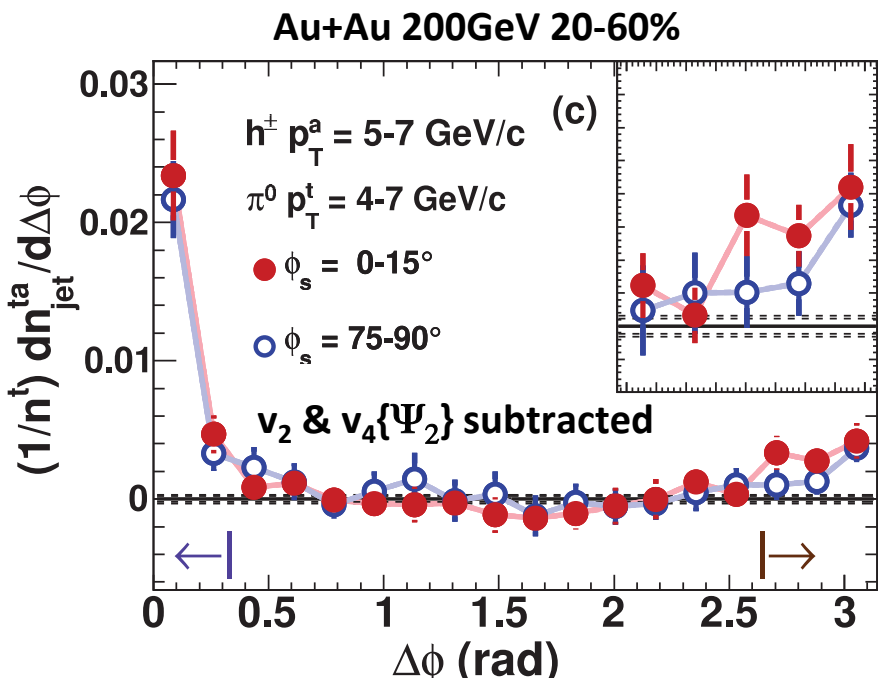
- ✧ None-zero $v_n(n>2)$ is observed
- ✧ Degeneracy of models disentangled
 - Initial Condition, shear viscosity of QGP, different expansion mechanism between v_2 & v_3
- ✧ Backgrounds in correlation functions

Jet-Quenching



- ❖ **p+p collisions : no suppression**
- ❖ **Suppression in away-side of high p_T correlations**

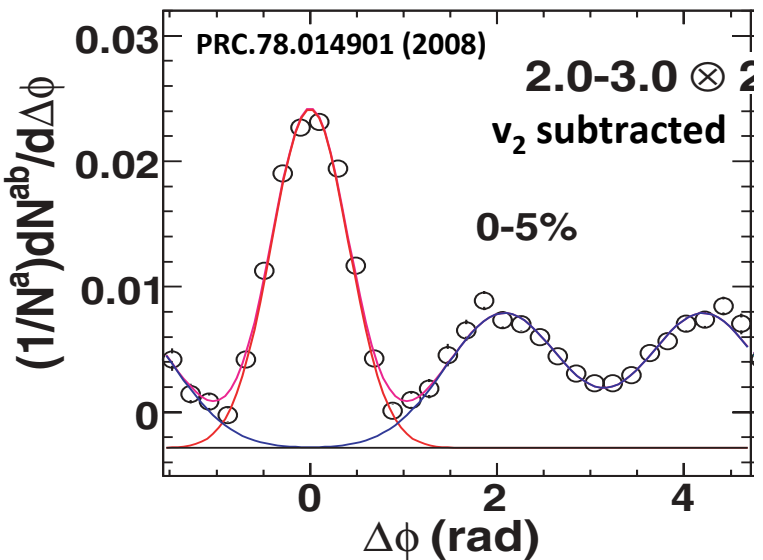
Ψ_2 Dependence of Away-Side Suppression of high p_T corrs.



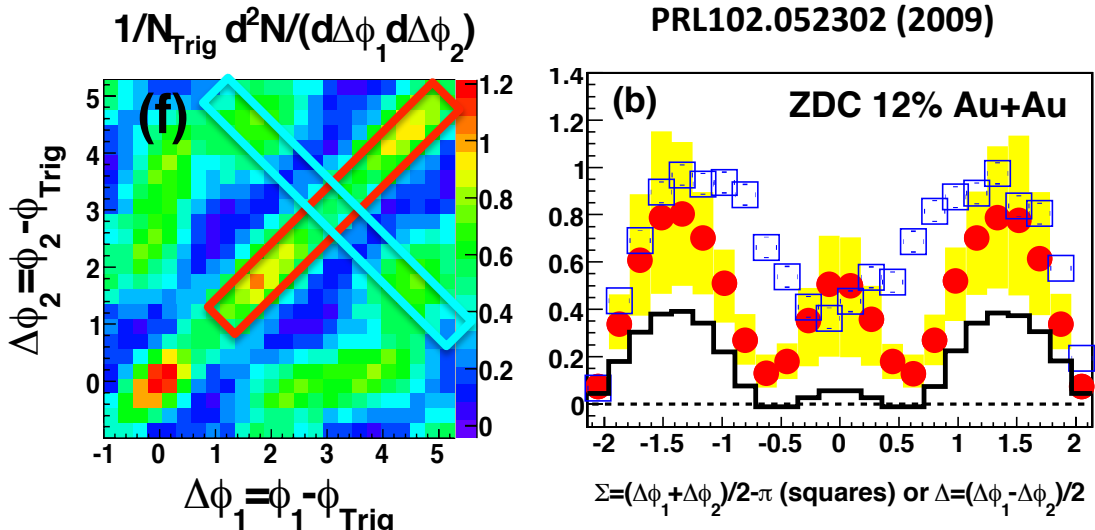
- ✧ Monotonic suppression with increase of path length
- ✧ Parton energy loss depending on path-length
- ✧ Similar trends seen in Ψ_3 dependence?

Conical Emission of Intermediate p_T correlations

Two-Particle Correlations



Three-Particle Correlations



- ✧ Away-side double hump in two-particle correlations
- ✧ Conical Emission confirmed via three-particle correlations



Models of Double-Hump : 1

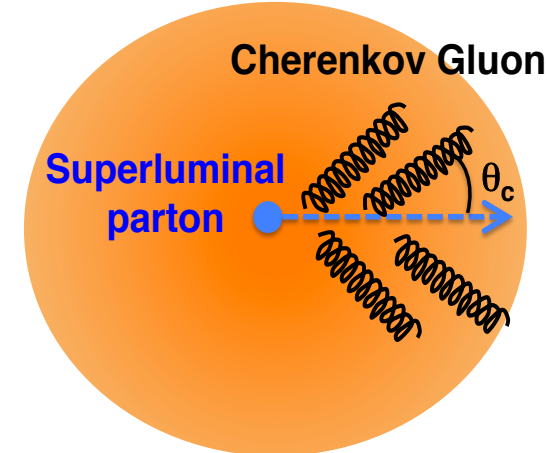
- ✧ Cherenkov gluon radiation by superluminal partons

$$\cos \theta_c = 1/n(p)$$

$n(p)$: Index of refraction

p : Gluon Momentum

PRL 96.172302 (2006)



- ✧ Shock-wave by supersonic partons

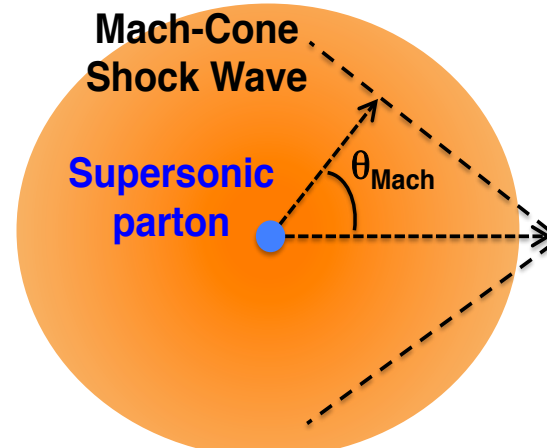
$$\cos \theta_{Mach} = c_s/v_{part}$$

c_s : Speed of sound

v_{part} : Speed of parton

Phys. Rev. C 73, 011901(R), (2006)

PRL 105.222301 (2010)



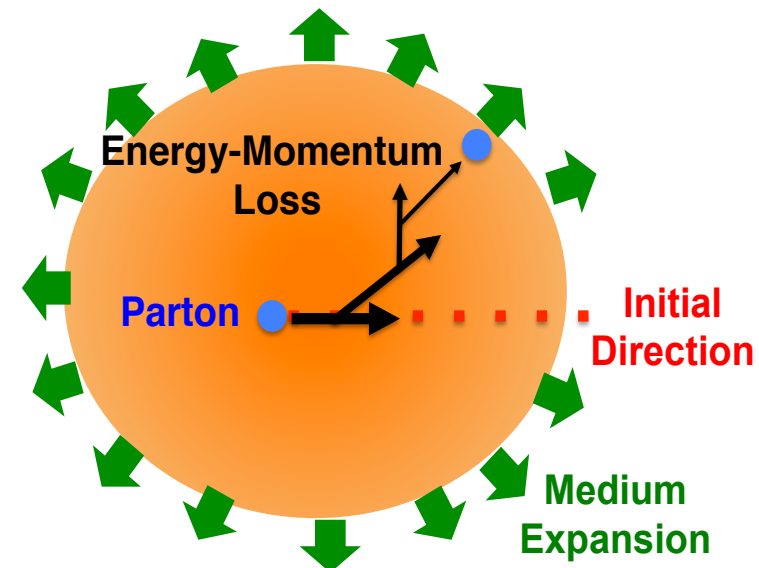
Models of Double-Hump : 2

- ◇ Energy-momentum loss + expanding medium

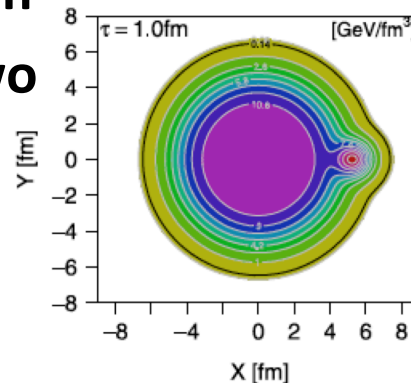
$$\partial_\mu T^{\mu\nu} = S^\nu$$

$$S^\nu(t, \vec{x}) = \frac{1}{(\sqrt{2\pi}\sigma)^3} \exp \left[-\frac{[\vec{x} - \vec{x}_{jet}(t)]^2}{2\sigma^2} \right] \\ \times \left(\frac{dE}{dt}, \frac{dM}{dt}, 0, 0 \right) \left[\frac{T(t, \vec{x})}{T_{max}} \right]^3$$

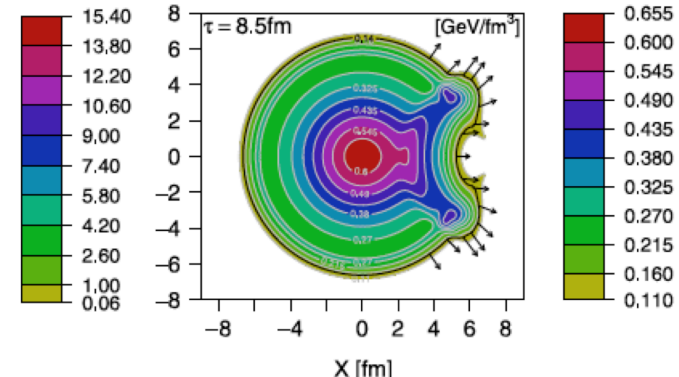
PRL 105.222301 (2010)



- ◇ Hot spot+ expanding medium
 - Split of the hot spot into two directions



Phys. Let. B 712 (2012) 226-230



Motivation of this Dissertation

- ✧ Provide experimental results after v_n subtraction
 - Centrality & p_T dependence, double-humps etc.
 - Revisit of previous models for double-humps
- ✧ Examine the path length dependence of Ψ_2 dependent correlations after v_n subtraction
- ✧ Search for differences between Ψ_2 & Ψ_3 dependent correlations which may reflects **possible different** evolution processes between the 2nd- and 3rd-order geometry planes

My Contributions

*Oral Presentation

*Collaboration work

*Analysis

M1,2 : AY
2008~2009

DNP-JPS Joint Meeting

PHENIX Run9 PHENIX Run10
Detector Maintenance

D2 (RIKEN JRA)
: AY 2011

JPS Fall
WPCF2011

D1 (RIKEN JRA)
: AY 2010

Heavy Ion Pub
preliminary approval
Au+Au ridge analysis

D3 (RIKEN JRA)
: AY 2012

JPS Spring
HIC/HIP
Hard Probes2012

Quark Matter2012
Nagoya-Mini Workshop2012
preliminary approval Au+Au
correlations with respect to EP

preliminary approval
Au+Au vn-correlation

PHENIX Run12
Detector Maintenance
preliminary approval
Au+Au PID vn

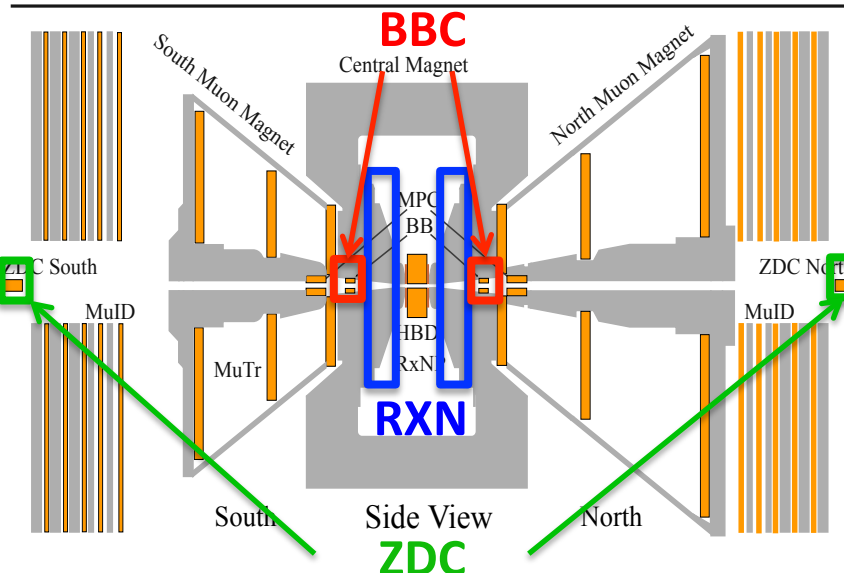
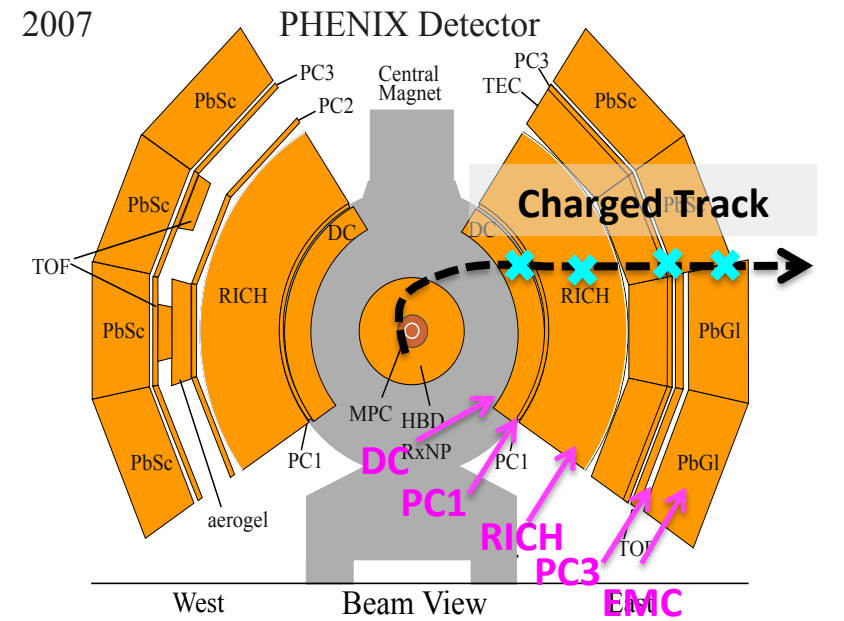
D3 (4) : AY 2013

PHENIX Run13
vn EP calibration
Detector Maintenance

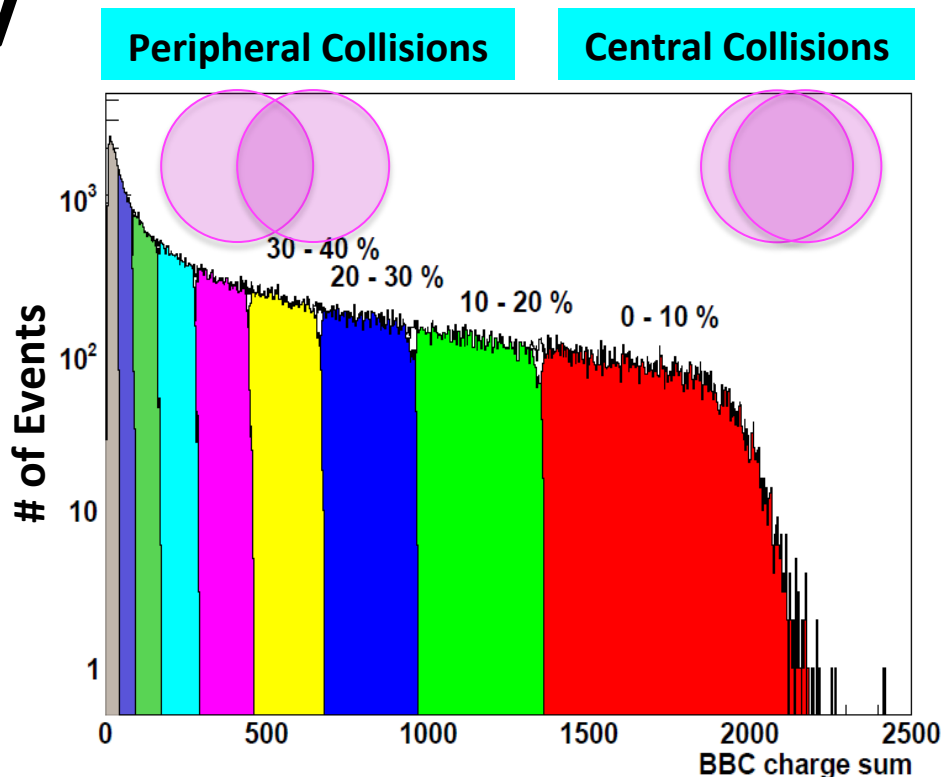
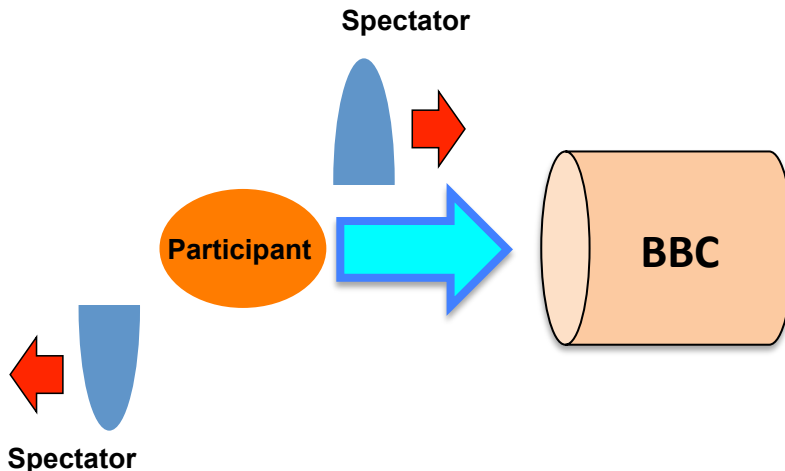
ANALYSYS

PHENIX 2007 Experiment: Au+Au 200 GeV Collisions

- ✧ Minimum Bias trigger : 4.4 billion events
- ✧ Trigger, collision vertex, centrality
 - Zero-Degree-Calorimeter(ZDC)
 - Beam-Beam-Counter (BBC)
- ✧ Event-plane
 - BBC
 - Reaction-Plane-Detector(RXN)
- ✧ Central Arm, $\Delta\phi=\pi$, $|\eta|<0.35$
 - Drift Chamber (DC)
 - Pad Chambers(PC)
 - Electromagnetic Calorimeter(EMC)
 - Momentum, charged particle tracking
 - Ring Image Cherenkov Detector(RICH)
 - Electron veto



Collision Centrality



- ✧ A degree of overlap of two colliding nuclei
 - Distance between center of the nuclei → multiplicity → charge deposited in BBC
- ✧ Require each percentile contains same # of events
 - Most-central Collision : 0%
 - Most-peripheral Collision : 100% (PHENIX determines it up to 92%)

Analysis Flow-Chart

Single-particle analysis

Event-Plane
(Resolution)

Flow harmonics v_n

Pure flow
backgrounds

Tracking efficiency

Two-particle analysis

Two-particle
correlations

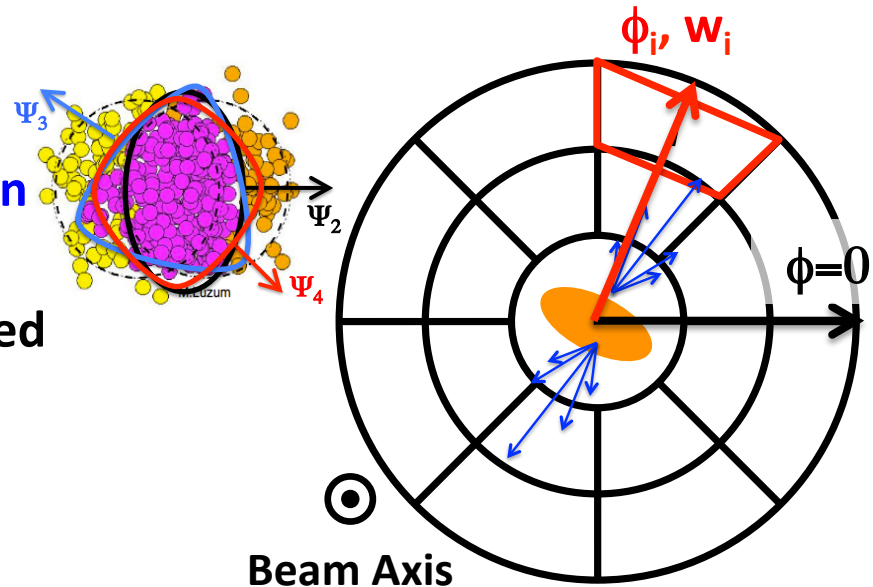
Flow subtracted
correlations

Pair yield per a
trigger

Unfolding of event-
plane resolution

Event-Plane

- ❖ Expansion to the initial short-axis direction by pressure gradient
 - EP is a direction most particles are emitted after freeze-out
 - EP is determined by flow signal itself

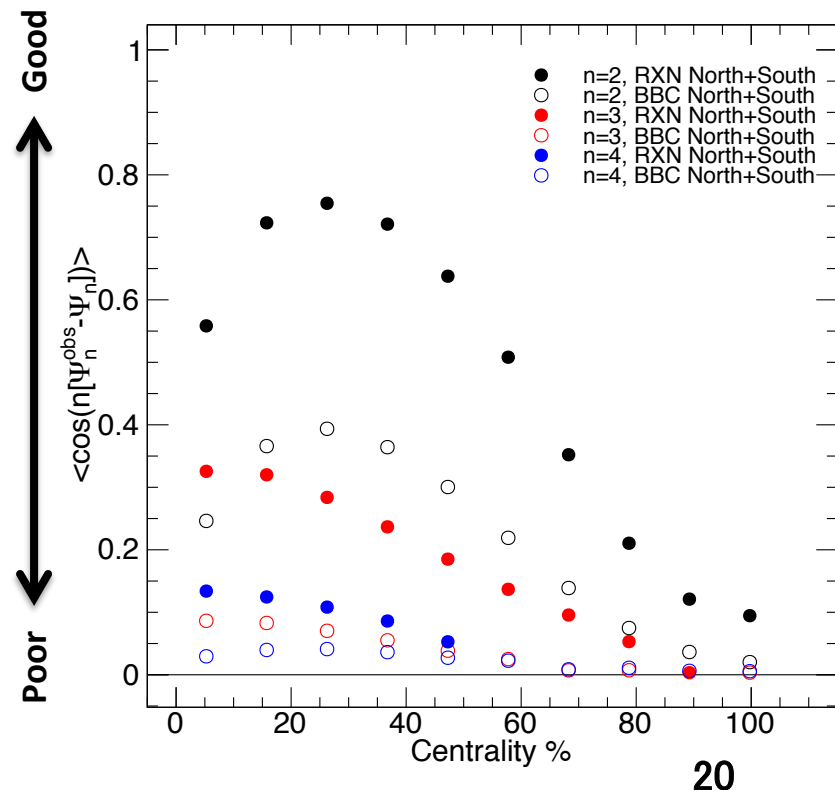


- ❖ EP is determined by RXN and BBC detectors
 - RXN ($1 < |\eta| < 2.8$) : 24 segments x 2 sectors
 - BBC ($3 < |\eta| < 3.9$) : 64 segments x 2 sectors

$$\Psi_n = \frac{1}{n} \tan^{-1} \left(\frac{\sum_i w_i \cos(n\phi_i)}{\sum_i w_i \sin(n\phi_i)} \right)$$

ϕ_i : Azimuthal angle of i^{th} segments

w_i : Weight (Charge etc.) of i^{th} segments



Flow Measurements

- ✧ Rapidity ranges of CNT, RXN, & BBC
 - Rapidity gap between particles & EP to avoid auto-correlations by jets



✧ Raw flow harmonics

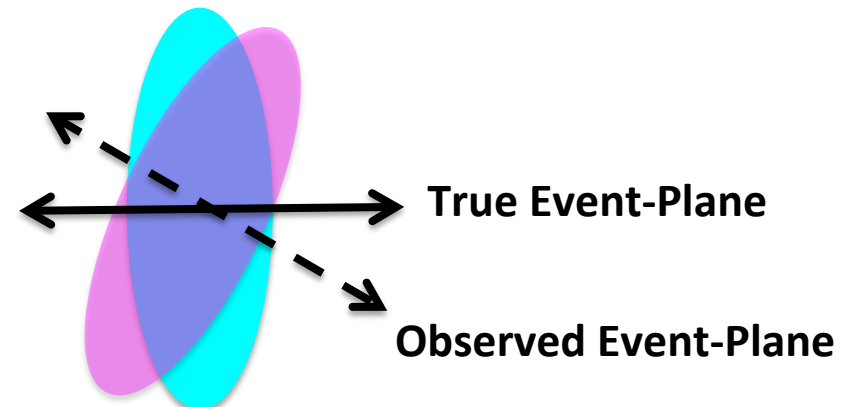
$$v_n^{raw} = \langle \cos n(\phi - \Psi_n^{obs}) \rangle$$

✧ Resolution correction

- Smearing due to limited resolution

$$v_n = \frac{\langle \cos n(\phi - \Psi_n^{obs}) \rangle}{\langle \cos n(\Psi_n - \Psi_n^{obs}) \rangle}$$

Event-Plane Resolution

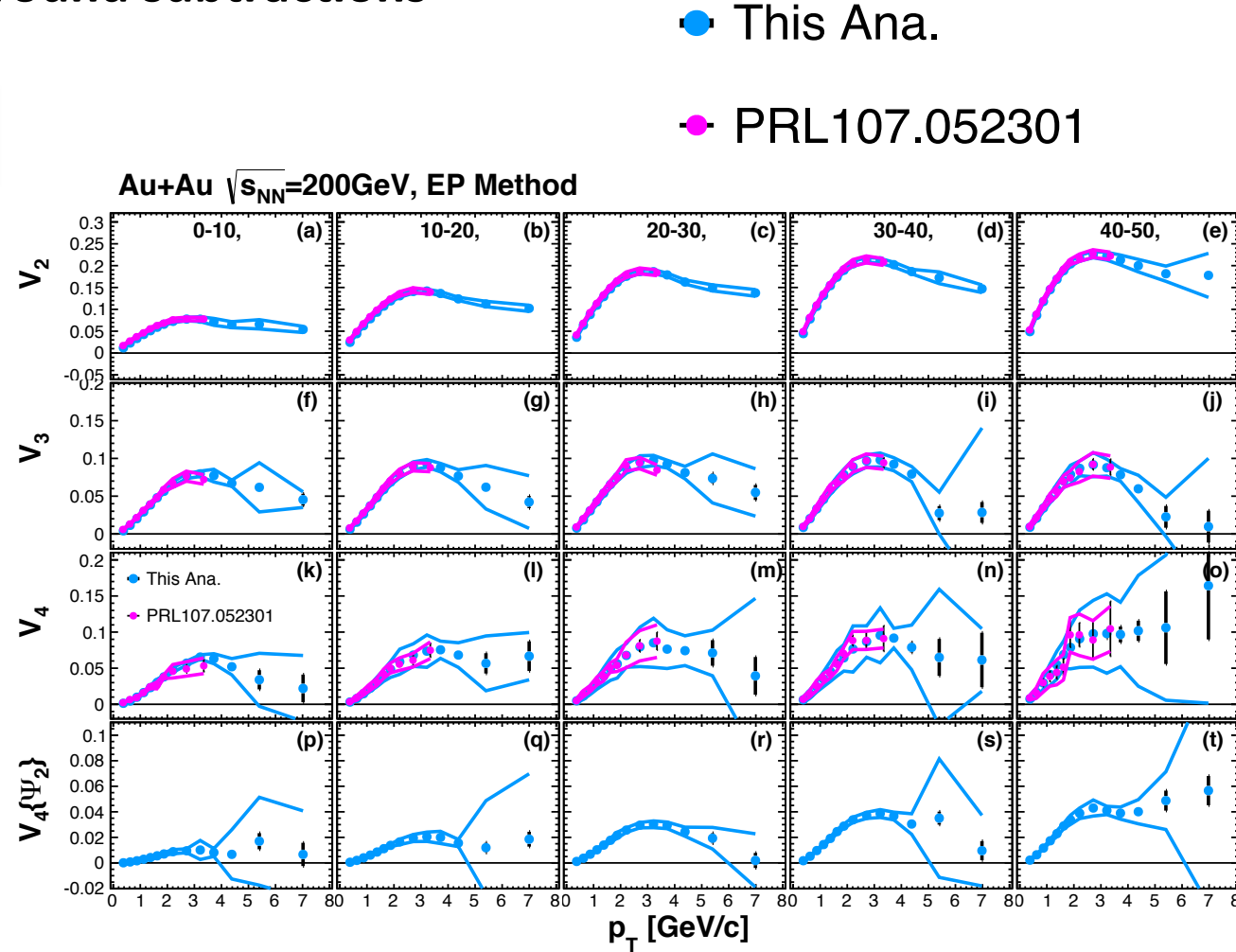


v_n Results

- ◇ Consistent results with previous PHENIX measurements
 - Used for background subtractions

Total systematics (%)
at $p_T=1-2 \text{ GeV}/c$

| Centrality | 0-10% | 40-50% |
|-----------------|-------|--------|
| v_2 | 4.3 % | 2.7% |
| v_3 | 4.9% | 12% |
| v_4 | 10% | 34% |
| $v_4\{\Psi_4\}$ | 15% | 6.5% |



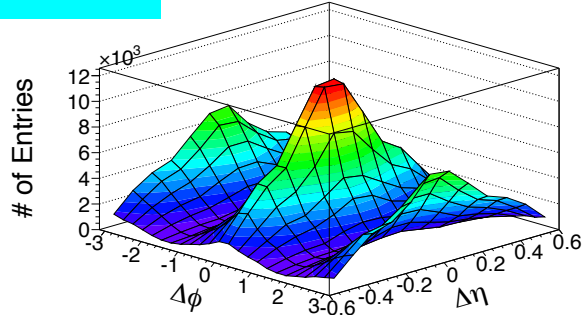
Two-Particle Correlations

Definition

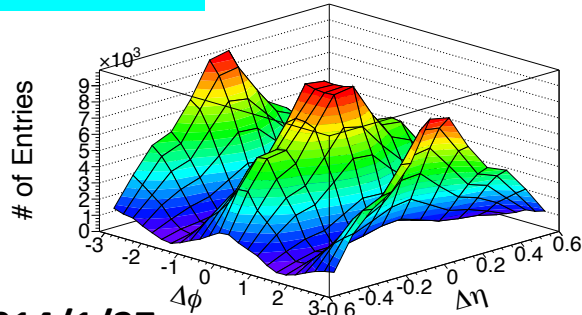
Ratio of two-particle probability over single-particle ones

$$C(\Delta\phi, \Delta\eta) = \frac{P(\phi^a, \phi^t | \eta^a, \eta^t)}{P(\phi^a | \eta^a)P(\phi^t | \eta^t)}$$

Real Pair



Mixed Pair



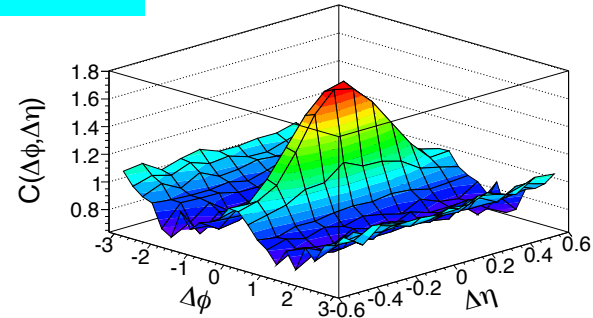
Experimental Def.

Ratio of real pair distribution over mixed one

$$C(\Delta\phi, \Delta\eta) = \frac{N_{mix}^{ta}}{N_{real}^{ta}} \frac{d^2 N_{real}^{ta} / d\Delta\phi d\Delta\eta}{d^2 N_{mix}^{ta} / d\Delta\phi d\Delta\eta}$$
$$\Delta\phi = \phi^a - \phi^t, \Delta\eta = \eta^a - \eta^t$$

Correlations = Real/Mixed

Event mixing also corrects acceptance effects by choosing similar events: centrality, collision points

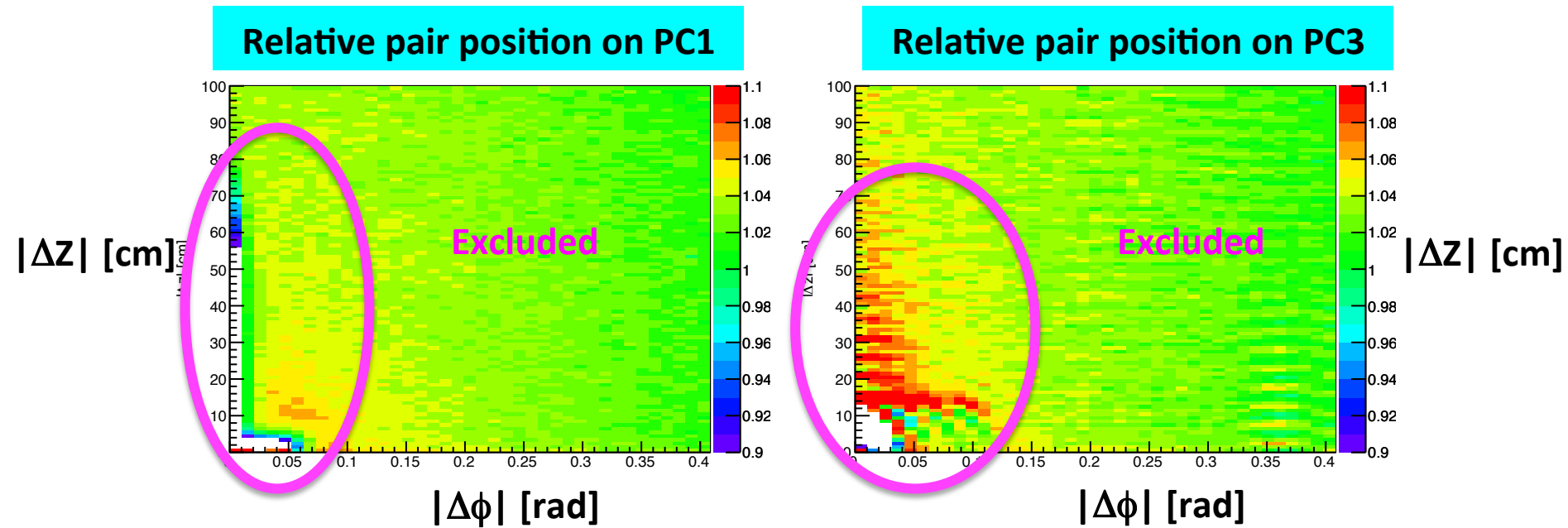


Pair Yield Per a Trigger

Dimension : Number of Particles

$$\frac{1}{N^t} \frac{d^2 N^{ta}}{d\Delta\phi d\Delta\eta} = \frac{1}{2\pi\varepsilon} \frac{N^{ta}}{N^t} C(\Delta\phi, \Delta\eta)$$

Pair Selection on Tracking Detectors



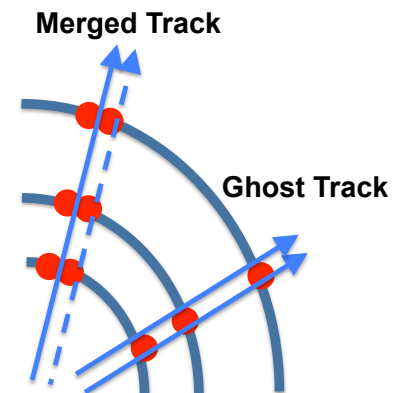
✧ Ghost track

- A **single** particle is counted as **two** tracks

✧ Merged tracks

- **Two** particles are counted as **one** track

✧ Real/Mix pair ratio should be 1 if an ideal detector



Flow Subtraction & Pair Yield per a Trigger (PTY)

✧ Pure flow background

$$F(\Delta\phi) = 1 + \sum 2v_n^t v_n^a \cos(n\Delta\phi)$$

✧ Flow subtractions by ZYAM

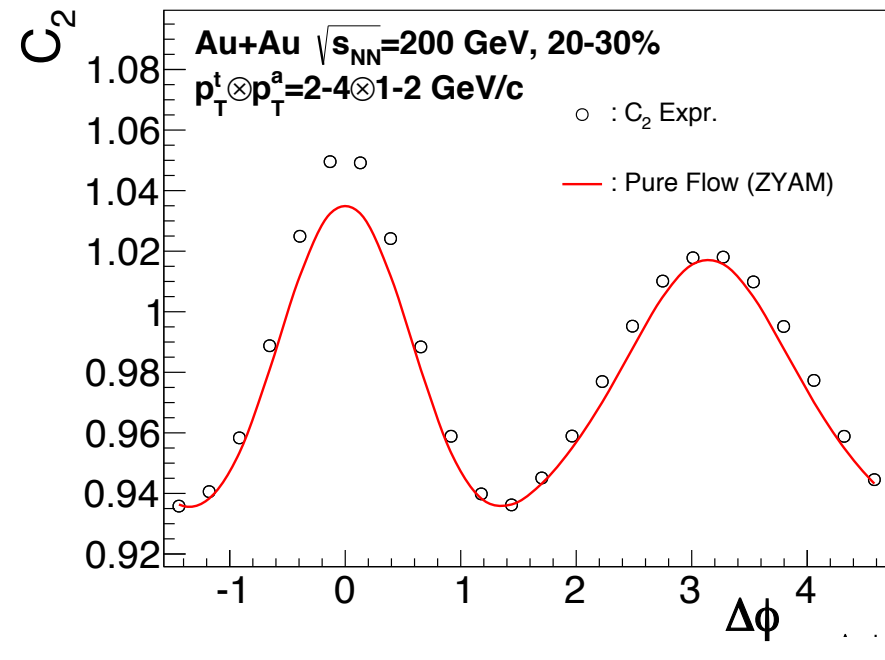
— Zero Yield At Minimum Assumption

$$j(\Delta\phi) = C(\Delta\phi) - b_0 \left[1 + \sum_{n=1} 2v_n^t v_n^a \cos(n\Delta\phi) \right]$$

✧ Pair yield per a trigger (PTY)

— Dimension : number of particles

$$\frac{1}{N^t} \frac{dN^{ta}}{d\Delta\phi} = \frac{1}{2\pi\varepsilon} \frac{N^{ta}}{N^t} j(\Delta\phi)$$

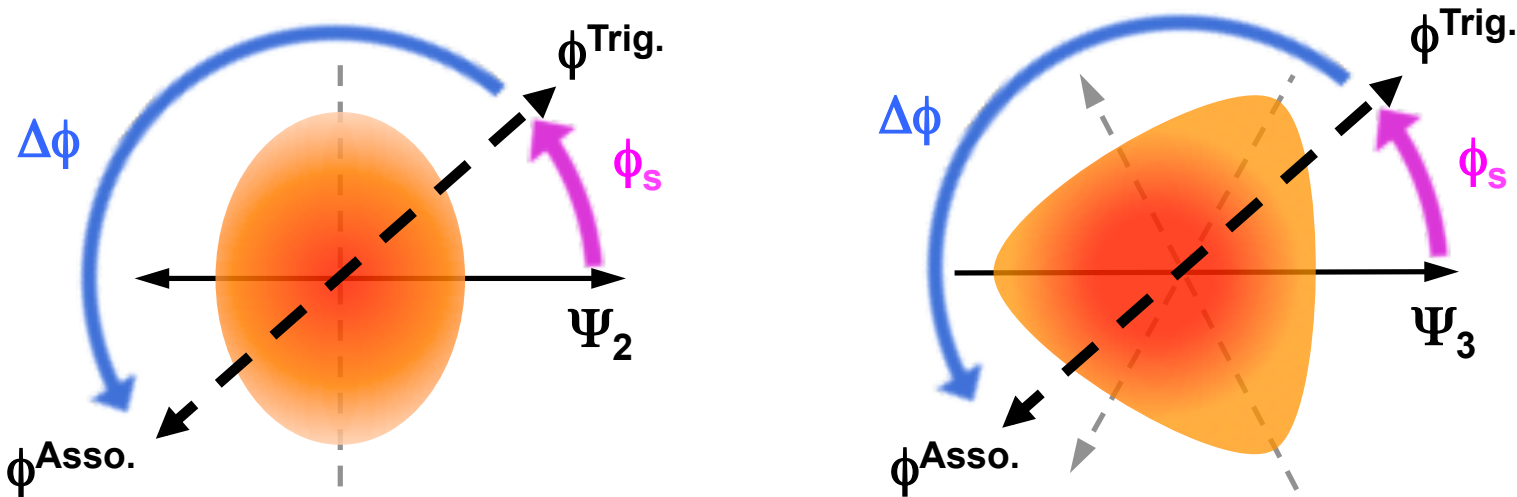


ε : Tracking efficiency of associate particles

N^t : Number of triggers

N^{ta} : Number of pairs

Trigger Selection with respect to Event-Plane

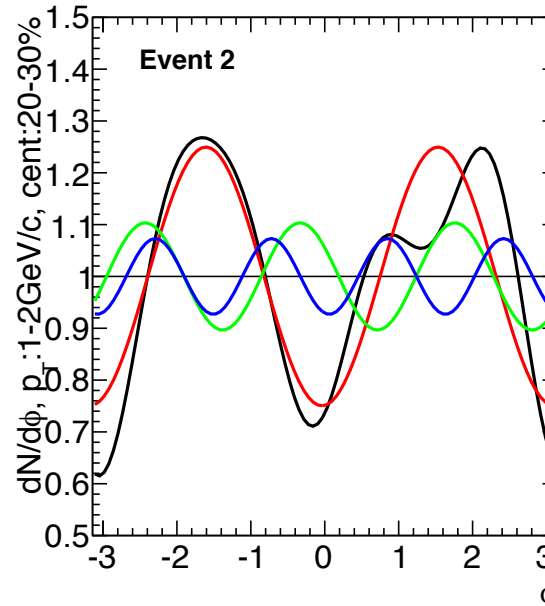
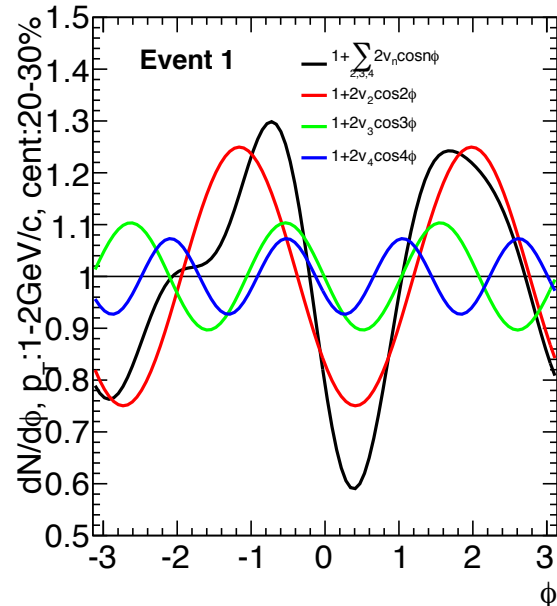


- ✧ Expansion to the short-axis direction by pressure gradient
 - EP : direction most particles are emitted after freeze-out
- ✧ Selecting trigger particles with respect to Ψ_2 & Ψ_3
 - 8 bins : $\phi^{trig} - \Psi_n : [-\pi/n, \pi/n]$
- ✧ Control of path length of trigger and associate particles
- ✧ Three p_T combinations: 2-4x1-2, 2-4x2-4, 4-10x1-2 GeV/c

Flow Backgrounds with respect to EP

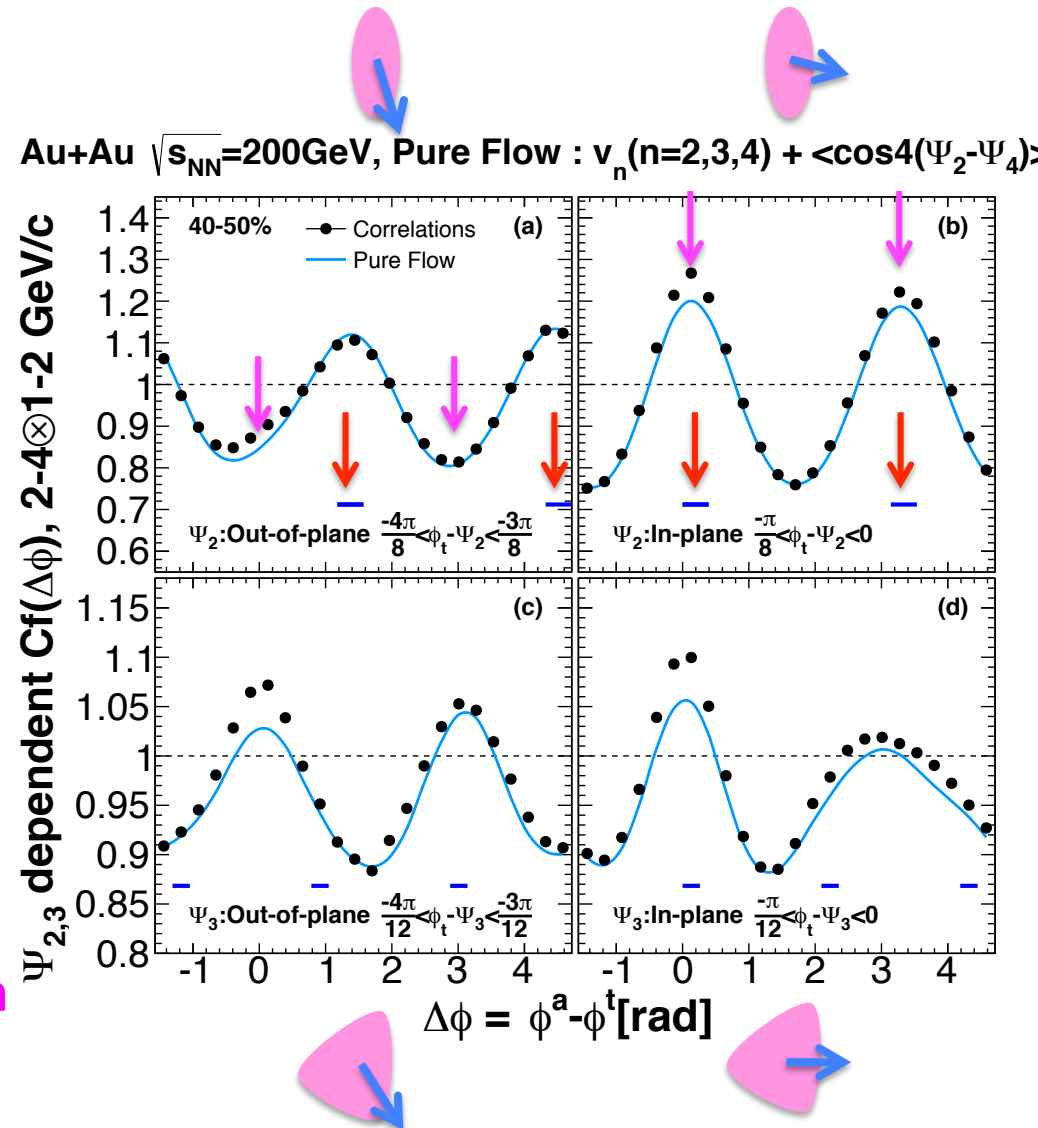
- ❖ A Monte Carlo simulation employed
- ❖ Azimuthal distribution using
 - Measured v_n
 - Observed correlation between EP
 - $\langle 4(\Psi_2 - \Psi_4) \rangle = v_4\{\Psi_2\}/v_4\{\Psi_4\}$
 - $\langle 6(\Psi_2 - \Psi_3) \rangle = 0$
- ❖ Determine trigger particle relative to EP taking into account EP resolutions
- ❖ Calculate two-particle correlations

$$\frac{dN}{d\phi} \propto 1 + \sum_{n=2,3,4} 2v_n \cos n(\phi - \Psi_n)$$



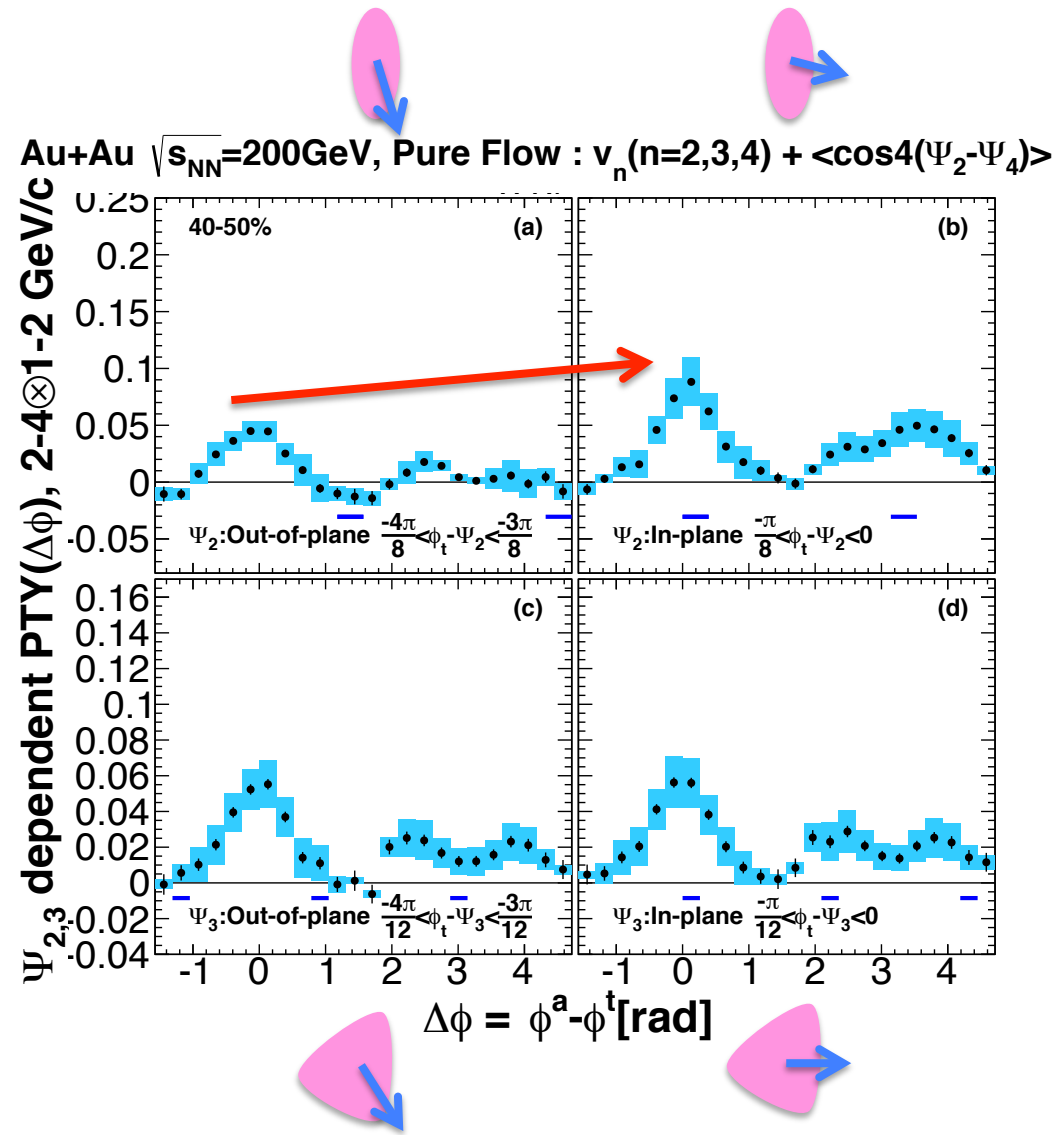
Flow Backgrounds with respect to EP

- ❖ Good reconstruction of Ψ_2 , Ψ_3 dependent correlations by MC simulation
 - Before PTY normalization
 - ❖ Except around $\Delta\phi=0, \pi$ where contribution of jet exists
- Correlations
——— Pure Flow
- : EP Direction
→ : Back-to-Back Direction



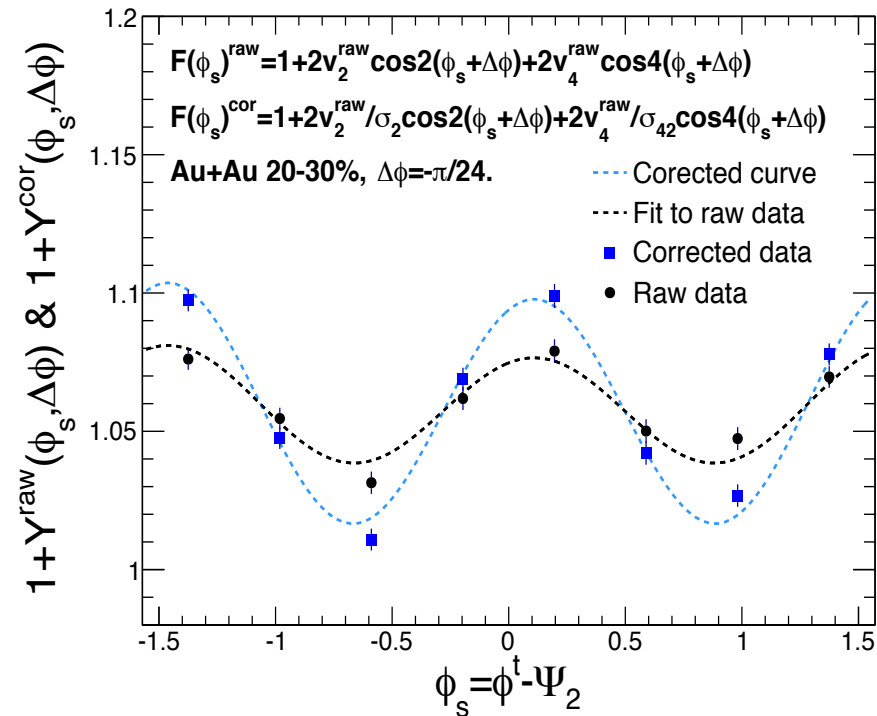
Two-Particle Correlations with respect to EP

- ❖ Flow subtracted Ψ_2, Ψ_3 dependent correlations
- ❖ Clear Ψ_2 dependence
- ❖ No Ψ_3 dependence?
- ❖ Smearing by neighboring trigger bins due to limited EP resolution
 - Needs unfolding !!



Unfolding Methods of EP Resolution

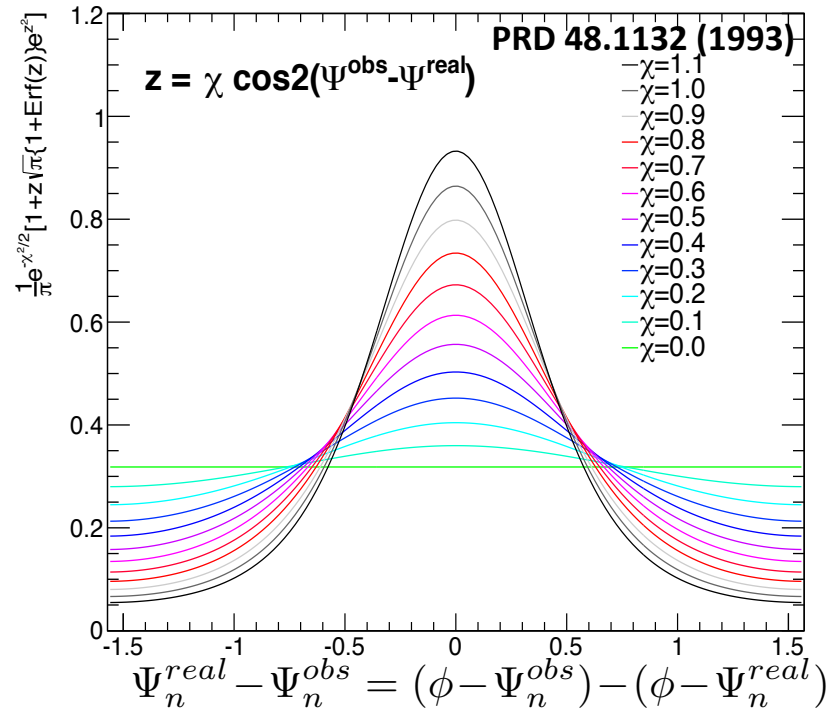
Fitting Method



❖ Azimuthal anisotropy of correlation yield corrected by the event-plane resolution

Method by PRC.84.024904 (2011)

Iteration Method



- ❖ Trigger smearing matrix “S”
- ❖ True & Observed Correlations “A” & “B”
 - Vector elements : Trigger bin
- ❖ Solve simultaneous equations via iteration

$$B = SA \quad \xrightarrow{\text{blue arrow}} \quad A = S^{-1}B$$

Systematic Uncertainties

✧ Flow v_n measurements

- Systematic difference within RXN segments
- Rapidity dependence of EP : RXN-BBC difference
- Matching cut of CNT particles

✧ Two-particle correlations

- Systematics from v_n
- Matching cut of CNT particles

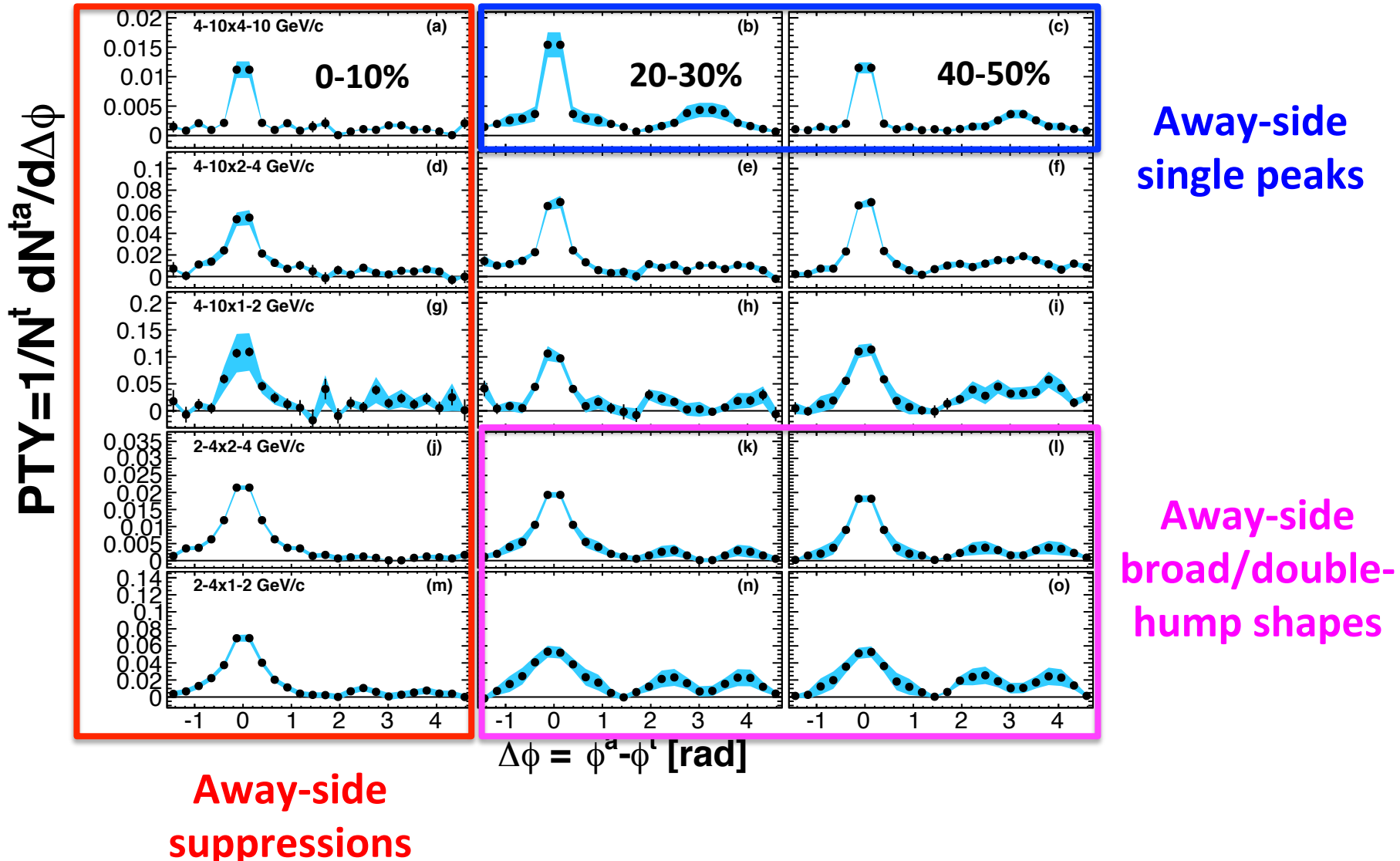
✧ Unfolding of event plane dependent correlations

- Difference of two methods : Fit & Iteration Methods
- Parameter in the iteration method

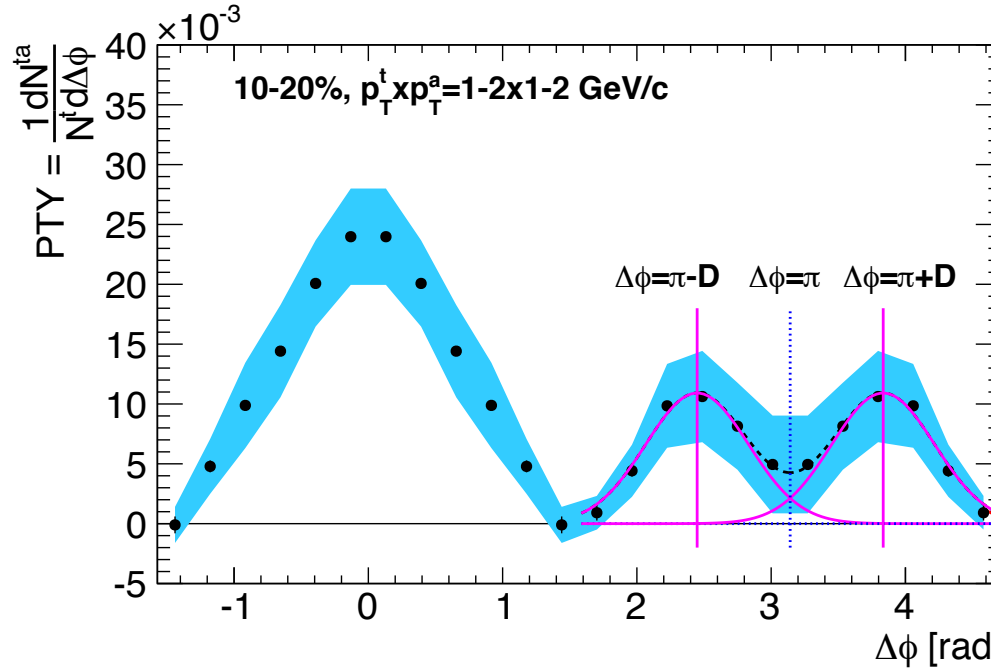
Results & Discussion

v_n ($n=2,3,4$) subtracted correlations

Au+Au $\sqrt{s_{NN}}=200$ GeV, v_n ($n=2,3,4$) subtracted



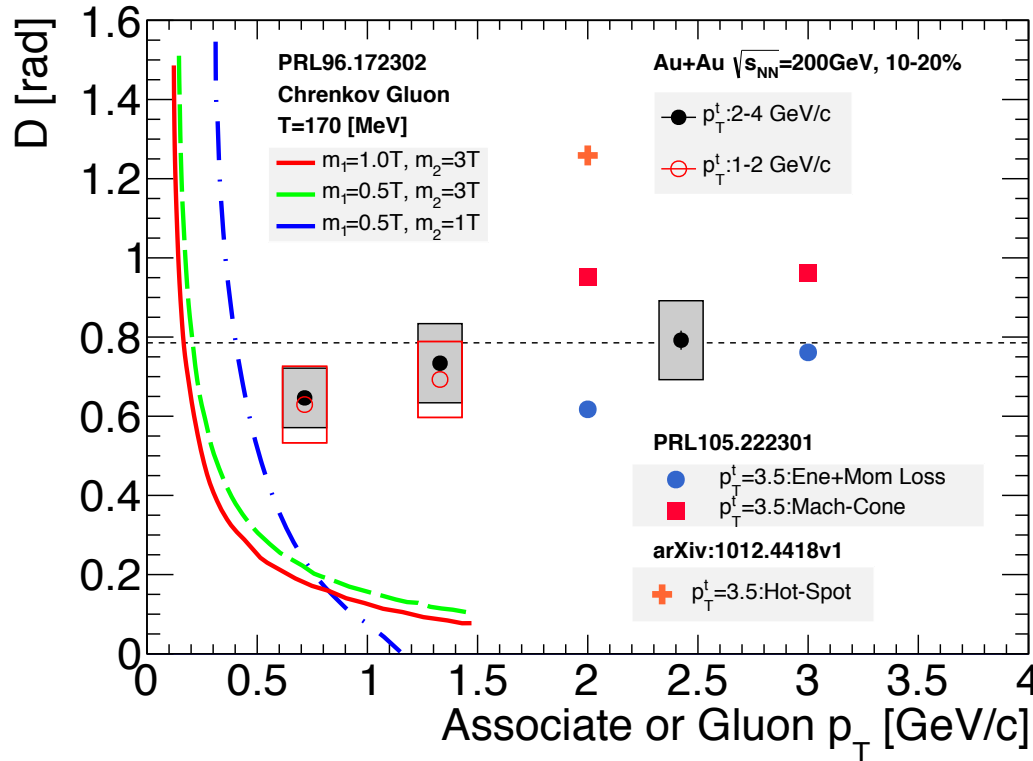
Extraction of Double-Hump Position



- ◇ Extraction of double-hump position via two-Gaussian fitting to away-side ($|\Delta\phi - \pi| < \pi$) at centrality 10%, where double-humps seen

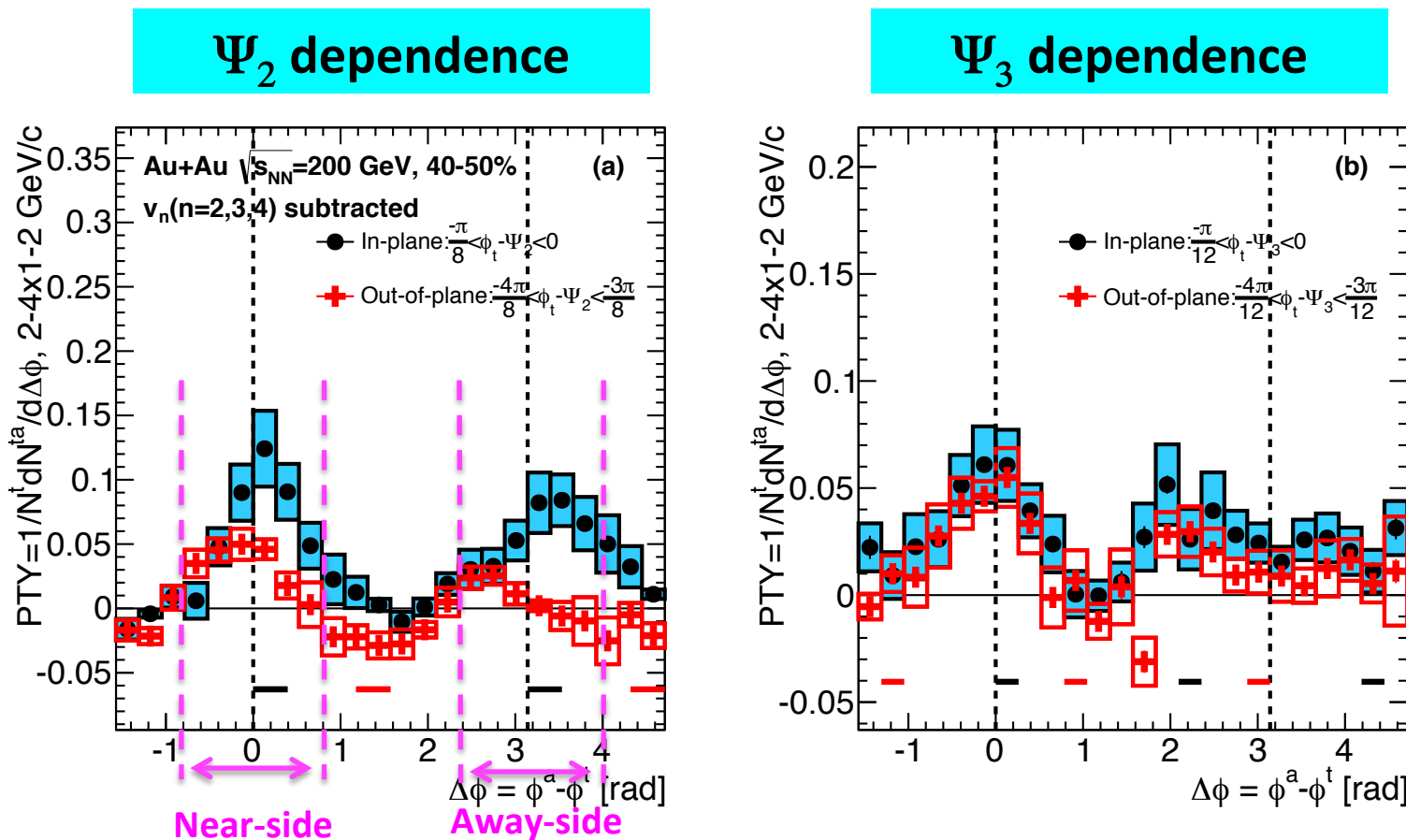
$$F(\Delta\phi) = A e^{-\frac{(\Delta\phi - \pi - D)^2}{\sigma^2}} + A e^{-\frac{(\Delta\phi - \pi + D)^2}{\sigma^2}}$$

Comparison with Models



- ✧ Cherenkov gluon : <25 % of experimental data at $p_T = 1 \text{ GeV}/c$
- ✧ Mach-cone & Energy-momentum loss :
 - Independence of p_T is similar to the experimental data
 - 20 % larger/smaller than experimental data at $p_T = 2 \text{ GeV}/c$
- ✧ Hot-spot : 50% larger than experimental data

Ψ_2 & Ψ_3 Dependent Correlations at $p_T: 2-4 \times 1-2$ GeV/c

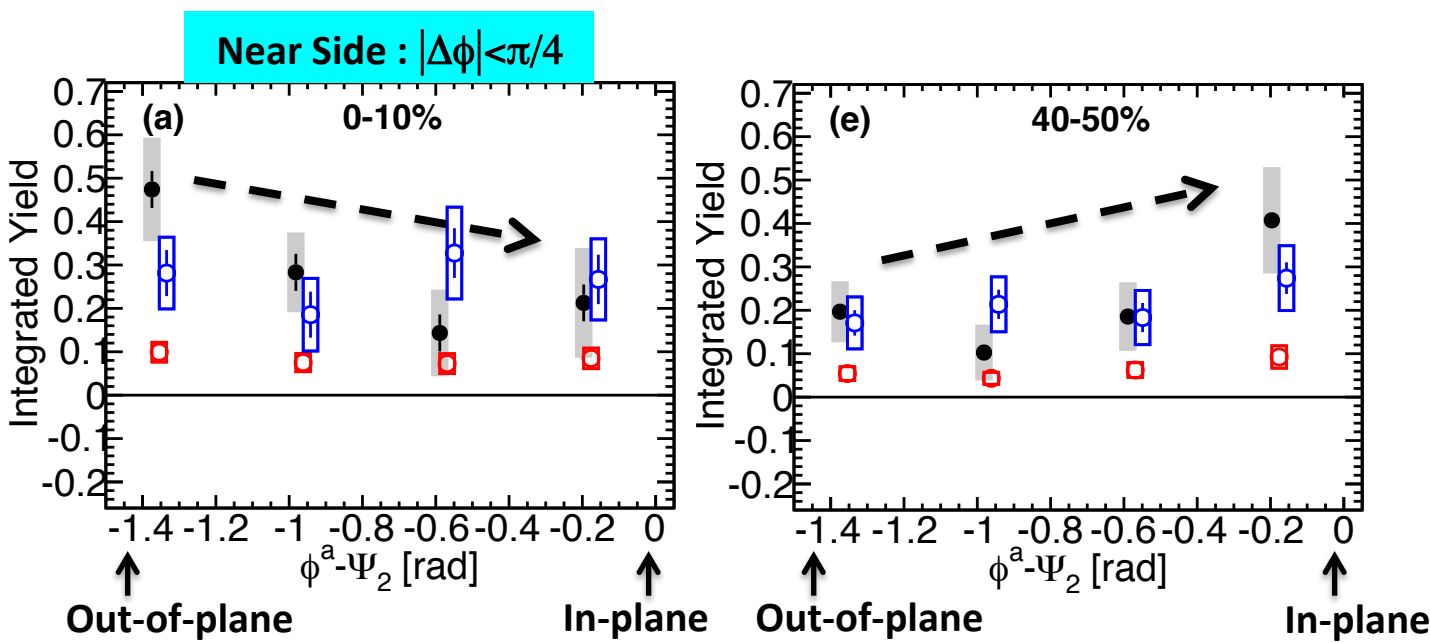


- Event-plane dependence is discussed via integrated near ($|\Delta\phi| < \pi/4$) and away ($|\Delta\phi - \pi| < \pi/4$) side yields vs associate angle from Ψ_2 and Ψ_3

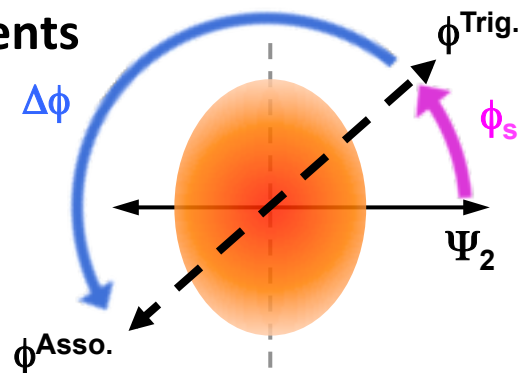
Near-Side Integrated Yield vs Associate Angle from Ψ_2

Au+Au 200GeV
 Ψ_2 dependence
Near Side : $|\Delta\phi| < \pi/4$

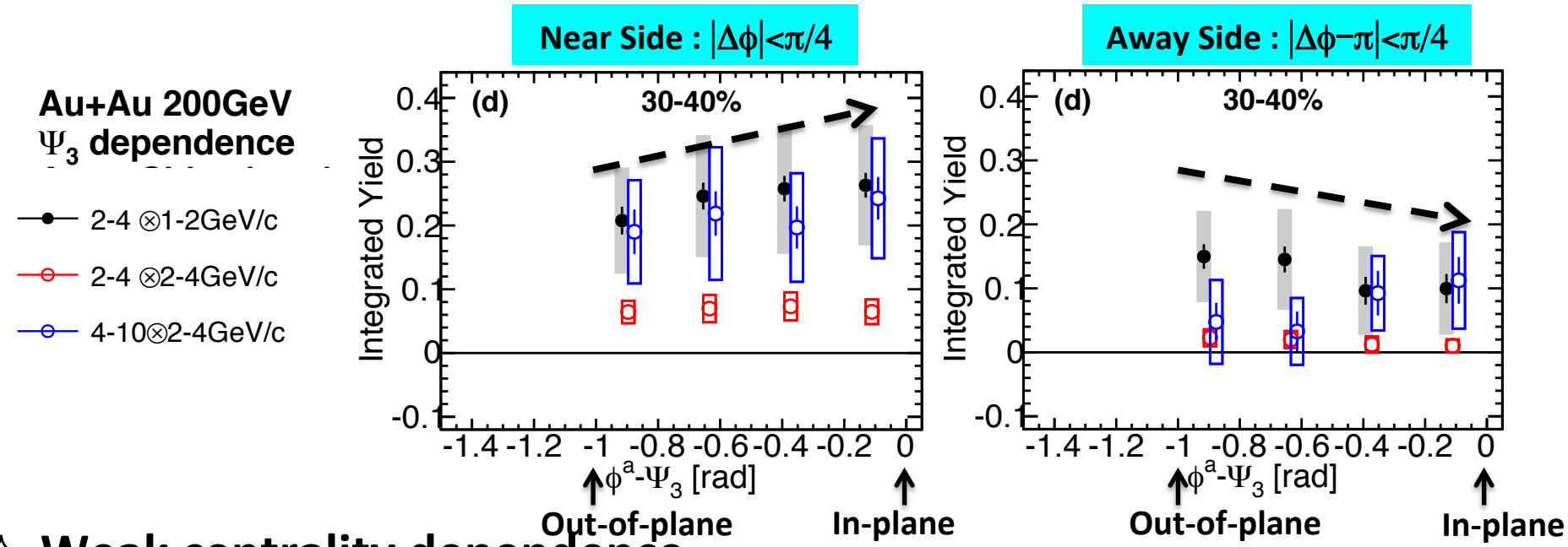
- 2-4 \otimes 1-2 GeV/c
- 2-4 \otimes 2-4 GeV/c
- 4-10 \otimes 2-4 GeV/c



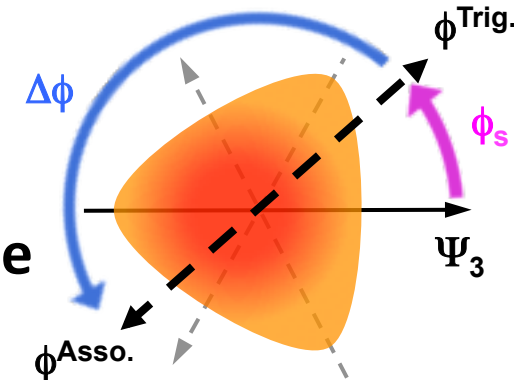
- ✧ Similar near and away-side trends
- ✧ p_T 2-4x2-4, 4-10x2-4 GeV/c : in-plane \geq out-of-plane
 - Qualitatively consistent with previous measurements
- ✧ p_T 2-4x1-2 GeV/c
 - 0-10% : Out-of-plane $>$ In-plane
 - 40-50% : In-plane $>$ Out-of-plane
 - More than 1σ significance of total systematics



Integrated Yield vs Associate Angle from Ψ_3



- Weak centrality dependence
- p_T 2-4x2-4, 4-10x2-4 GeV/c : in-plane \geq out-of-plane
- Event-plane dependence is not clearly seen
 - Flat within systematic uncertainties
- Centroids show different event-plane dependence between near and away-side



Azimuthal Anisotropy of PTY

- ✧ Integrated yield vs associate angle from EP is translated into azimuthal anisotropy v_n^{PTY}
- ✧ v_n^{PTY} can be compared with single particle v_n because the dimension of PTY is “# of particles”
- ✧ v_n^{PTY} is extracted via Fourier fitting

Ψ_2 dependence

$$F(\phi^a - \Psi_2) = a\{1 + 2v_2^{\text{PTY}} \cos 2(\phi^a - \Psi_2) + 2v_4^{\text{PTY}} \cos 4(\phi^a - \Psi_2)\}$$

Ψ_3 dependence

$$F(\phi^a - \Psi_3) = a\{1 + 2v_3^{\text{PTY}} \cos 3(\phi^a - \Psi_3)\},$$

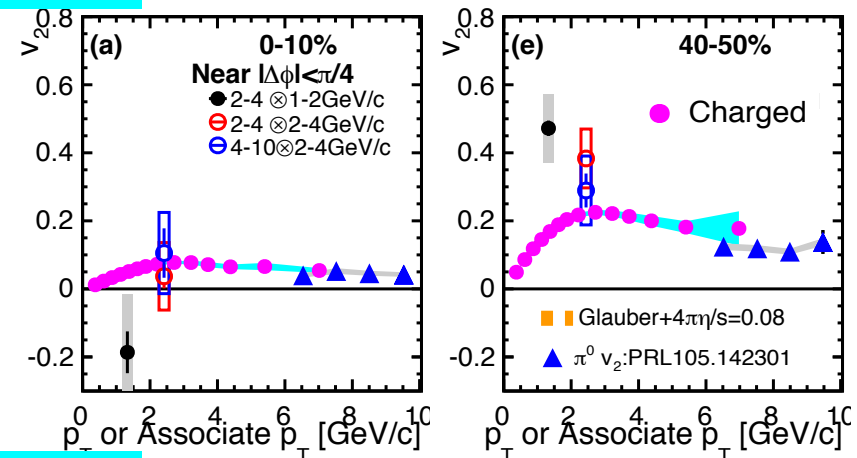
- ✧ Anisotropy of associate particles per a trigger → Anisotropy of associate particles per a event

$$v_n^{\text{PTY},\text{cor}} = v_n^{\text{PTY}} + v_n^{\text{trig}} \cos n(\phi^t - \phi^a)$$

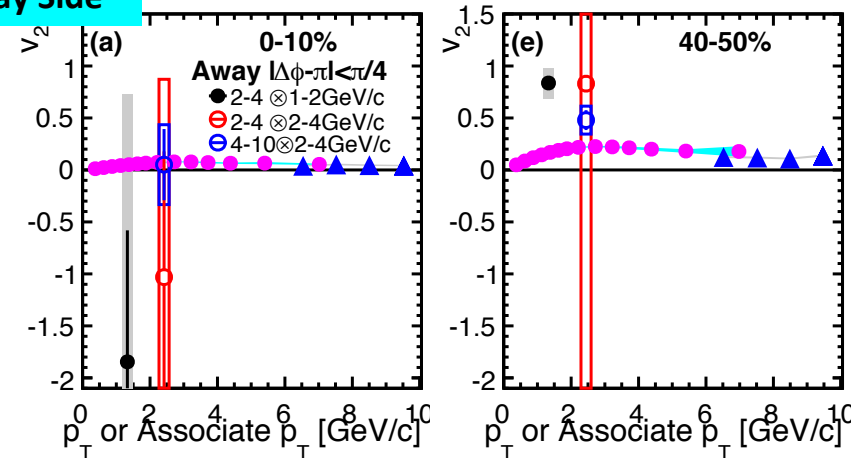
v_2^{PTY}

- ✧ Positive hadron v_2 (Hydrodynamics)
- ✧ Positive $\pi^0 v_2$ (Parton energy-loss)
 - Superposition of those assemblies
only positive v_2
- ✧ Near & away-side v_2^{PTY}
 - Positive value at 40-50%
 - Near-side negative value at 0-10%
- ✧ New effects need to be considered
- ✧ Possible re-distribution of deposited energy in longer path direction

Near Side

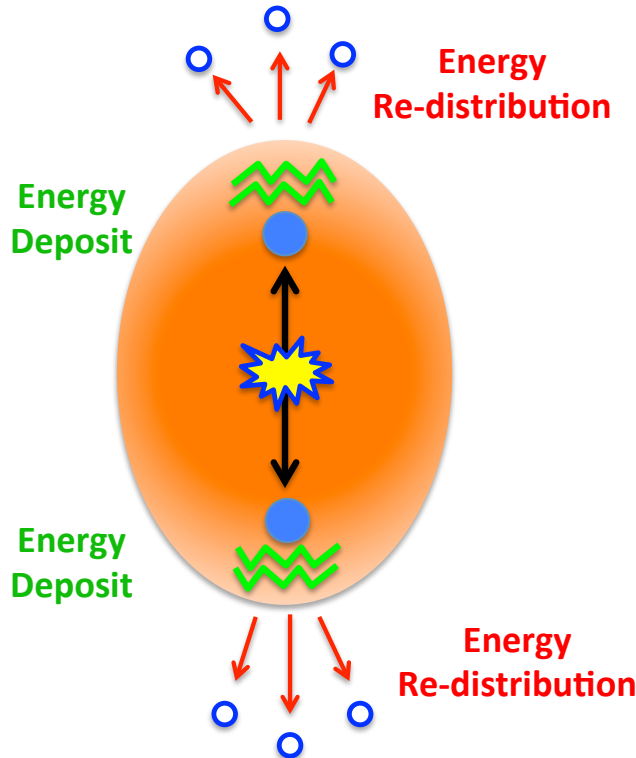


Away Side



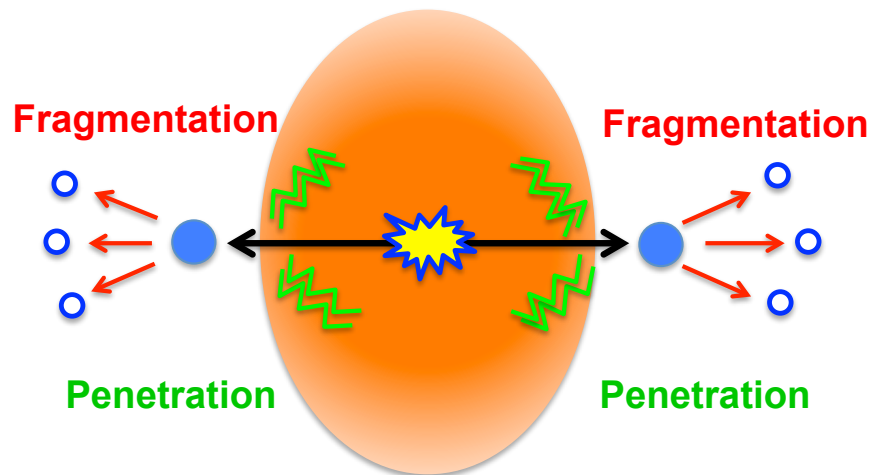
Interpretation of Ψ_2 Dependent Correlations

Central



Re-distribution
Dominance

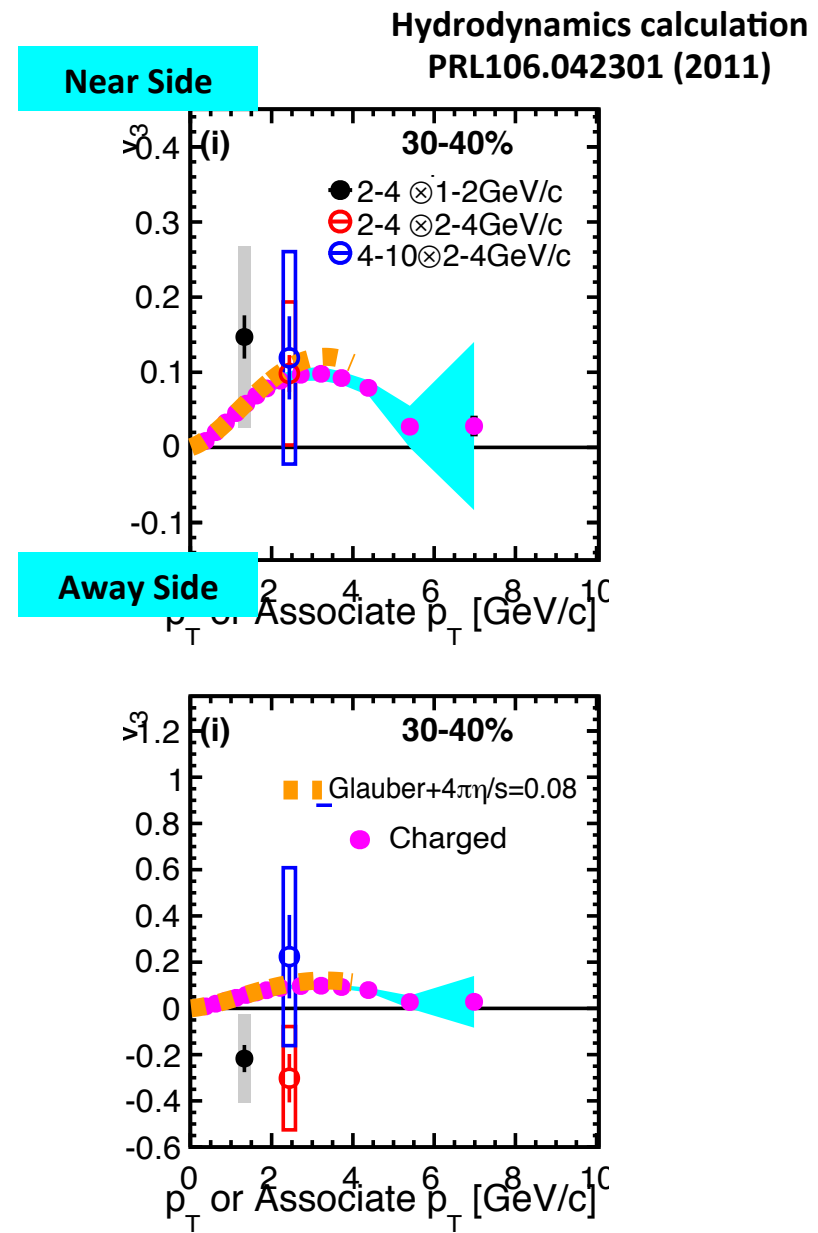
Mid-central



Penetration
Dominance

v_3^{PTY}

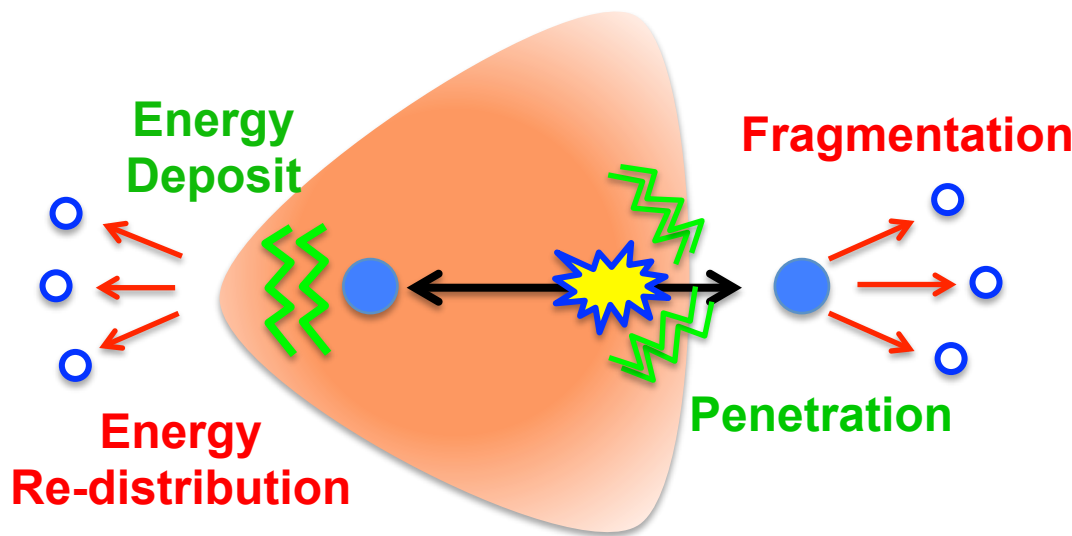
- ✧ Positive hadron v_3 (Hydrodynamics)
- ✧ Near & away-side v_3^{PTY} at 30-40%
 - Positive near-side
 - Negative away-side
- ✧ Weak centrality dependence
- ✧ Different near & away-side, as well as centrality dependences from those of v_2^{PTY}
- ✧ Possible different evolution processes between the 2nd- and 3rd-order geometry planes



Interpretation of Ψ_3 Dependent Correlations

Away-Side

Near-Side



**Re-distribution
Dominance**

**Penetration
Dominance**

Conclusion - I

- ◆ Two-particle correlations with v_n ($n=2,3,4$) subtractions are measured in Au+Au $\sqrt{s_{NN}}=200$ GeV collisions
- ✧ Away-side suppression in 0-10% independent of trigger and associate p_T combinations
- ✧ Single away-side peak of high p_T correlations in mid-central collisions
- ✧ Broad/double-peak structure at away-side of intermediate p_T correlations in mid-central collisions
- ✧ New experimental data to be compared among theoretical models

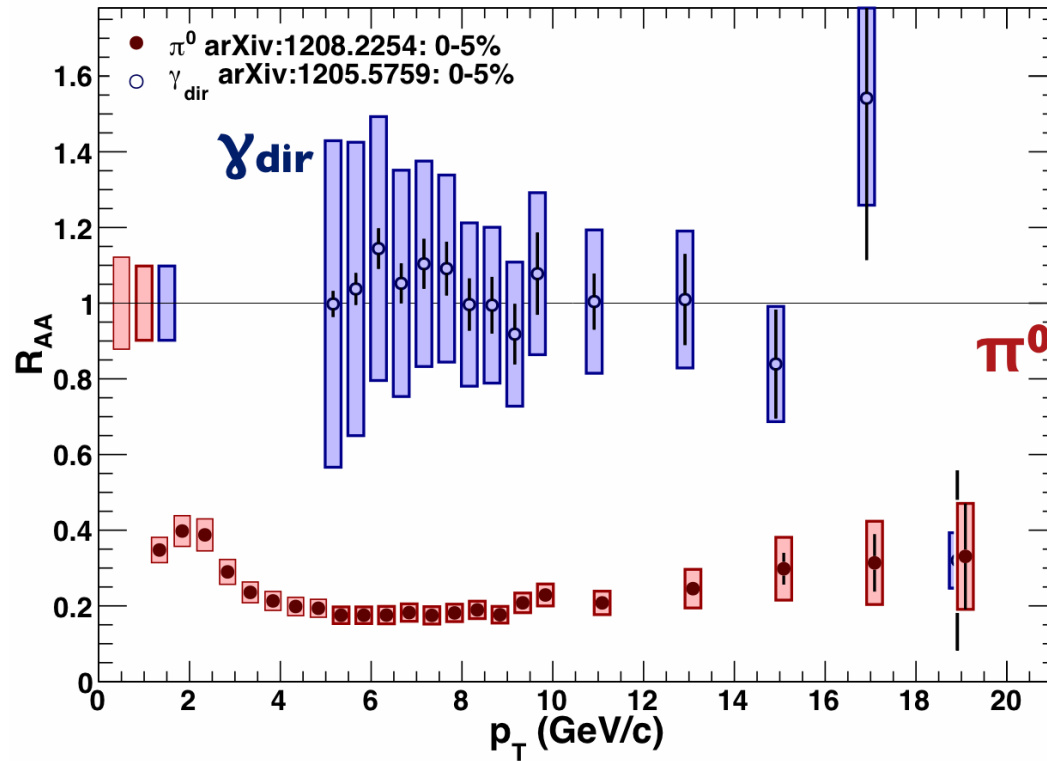
Conclusion - II

- ◆ Two-particle correlations with respect to the event-planes are also measured in Au+Au $\sqrt{s_{NN}}=200$ GeV collisions
- ✧ Path length dependence of high $p_T \Psi_2$ dependent correlations
 - qualitatively consistent with previous PHENIX measurements
- ✧ Intermediate $p_T \Psi_2$ dependence
 - Enhance of correlation yield in **out-of-plane** direction in **central** collisions
 - Re-distribution of deposited energy by hard-scattered partons
 - Enhance of correlation yield in **in-plane** direction in **mid-central** collisions
 - Penetration of hard-scattered partons via parton energy loss
- ✧ Intermediate $p_T \Psi_3$ dependence
 - Different path near and away-side as well as centrality dependences of correlations from those of Ψ_2 dependent case, which may suggest possible different evolution processes between the 2nd- and 3rd-order geometry planes

BACK UP

Nuclear Modification Factor R_{AA}

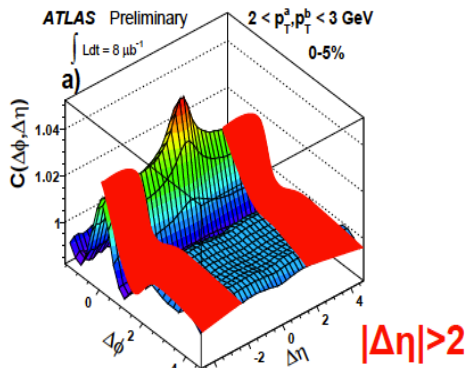
$$R_{AA} = \frac{d^2 N^{AA} / dp_T d\eta}{N_{coll} d^2 N^{pp} / dp_T d\eta}$$



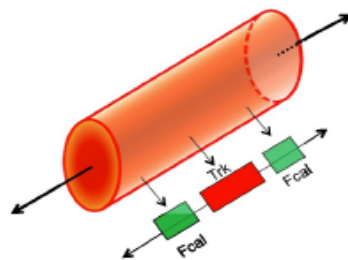
- ✧ Ratio of invariant yield scaled by that in p+p collision with scale
 - $R_{AA} < 1$ (suppression), $R_{AA} = 1$ (no change), $R_{AA} > 1$ (enhance)
- ✧ Suppression of hadron production
- ✧ No suppression of direct photon

Contributions of v_n ($n>2$) in correlations

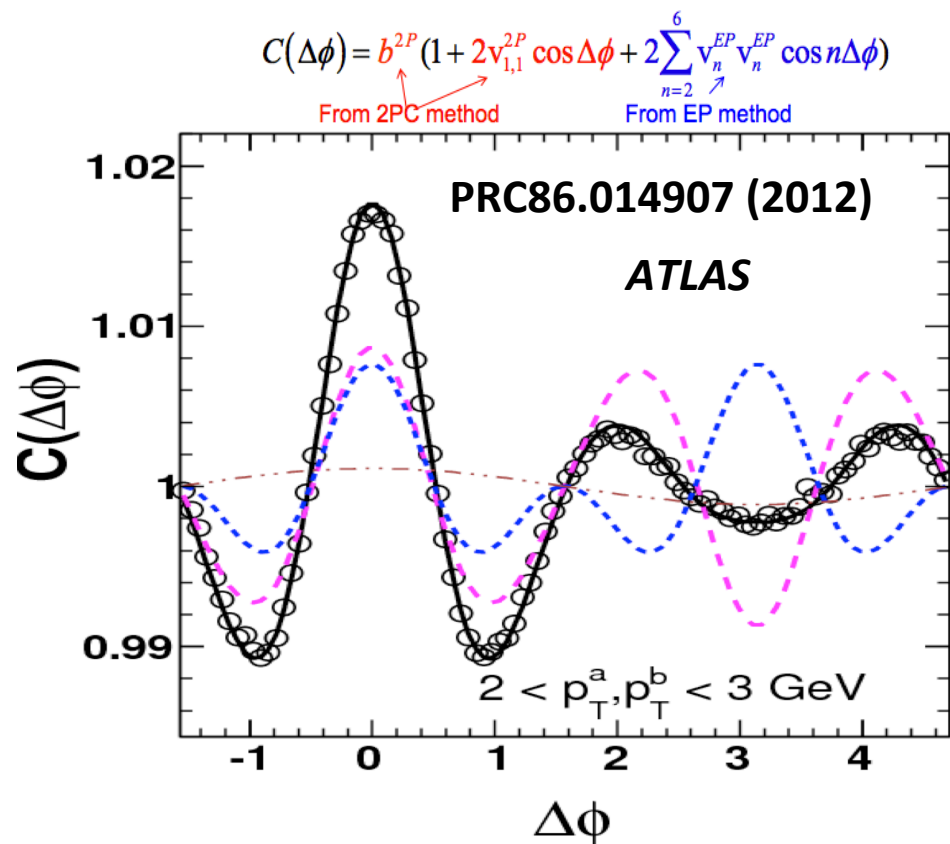
2Par. Correlation



v_n with EP Method



Track at $|\eta| < 2.5$ with EP
from full FCAL
 $3.3 < |\eta| < 4.8$



- ✧ Double-hump & ridge of long-rapidity correlation explained
- ✧ Short-rapidity correlation with v_n subtraction to discuss parton behavior

Data Set & Particle Selection

- ✧ PHENIX year 2007 Experiment
- ✧ Au+Au collisions at $\sqrt{s}_{NN}=200$ GeV
 - Minimum Bias trigger 4.4 billion events
- ✧ Charged hadron selection
 - 2 σ cut of track-hit matching
 - Electron veto
 - Energy/momentun cut of high p_T particles for background rejection
 - $E^{\text{EMC}} < 0.30 + 0.20 * p_T$ rejected for $p_T > 5.0$ GeV/c
 - Pair cut of miss-reconstructed hadron pairs

Tracking Efficiency

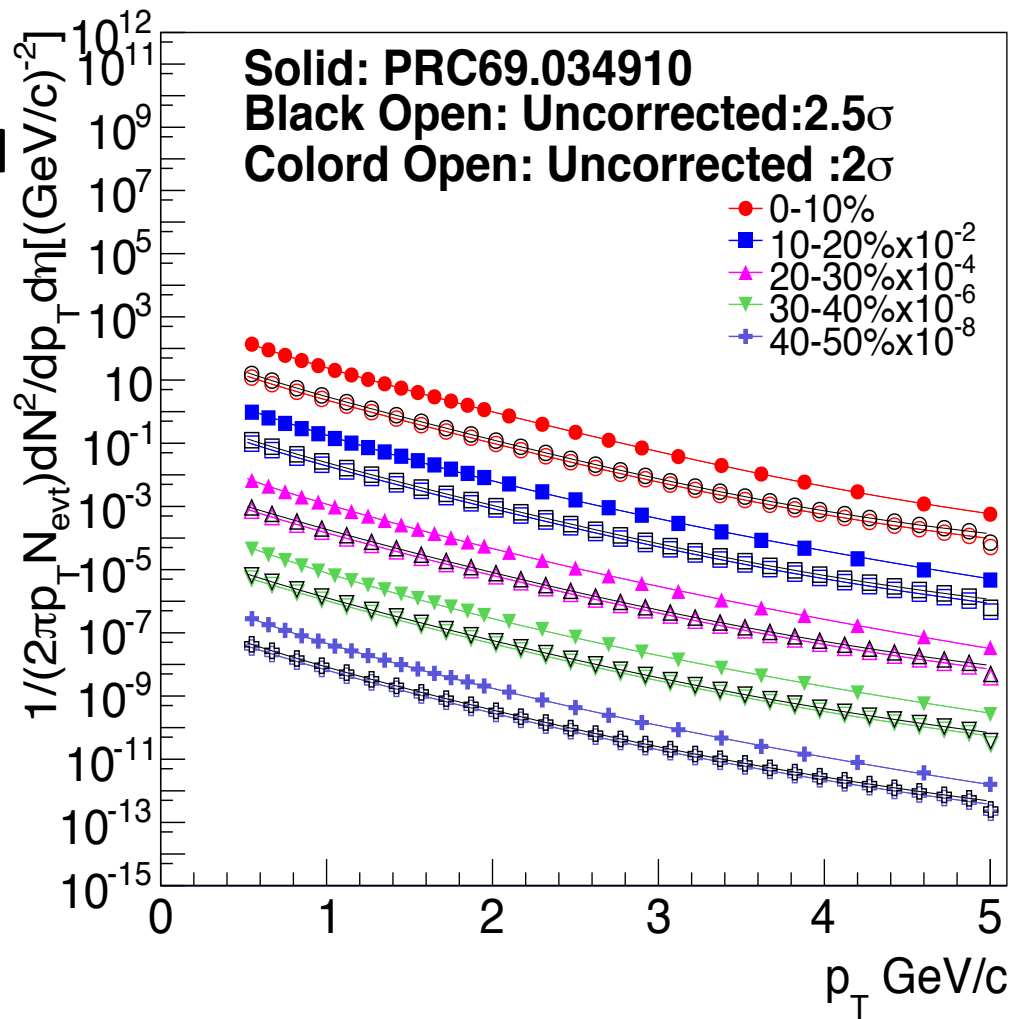
- Efficiency correction by ratio of uncorrected invariant yield over fully corrected ones

$$\varepsilon = \frac{\sigma^{uncor}}{\sigma^{cor}}$$

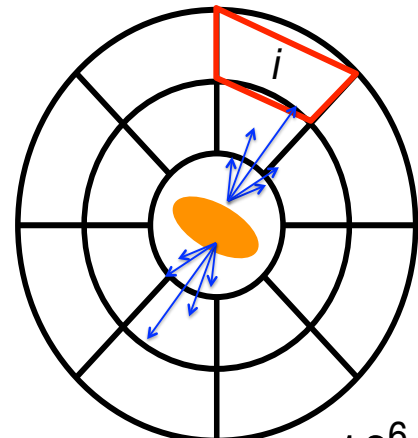
- Ratio calculated by fitting functions to the invariant yields

Fit Function

$$F(p_T) = p_0 * \left(\frac{p_1}{p_1 + p_T} \right)^{p_2}$$

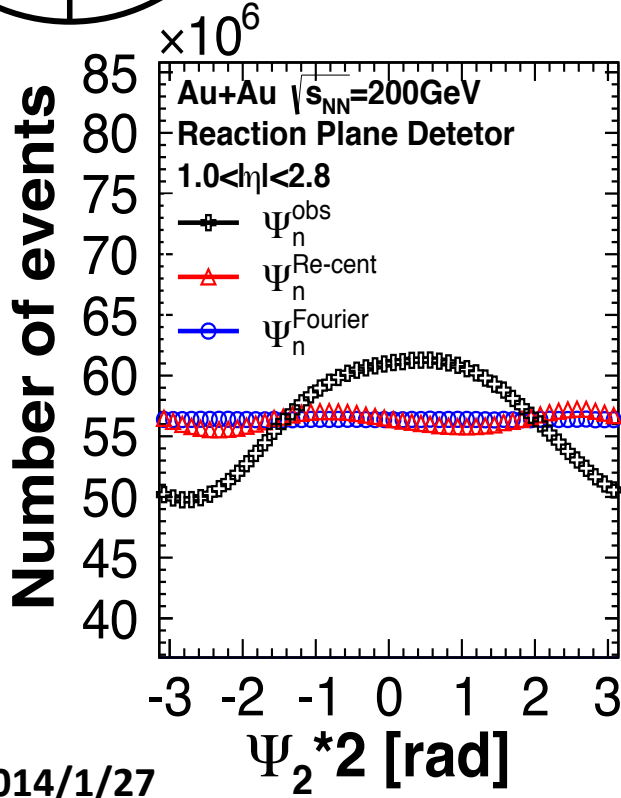


Event Plane Calibration



ϕ_i : Azimuthal angle

w_i : Weight (Charge etc.)



Raw distribution

$$Q_x = \sum_i w_i \cos(n\phi_i), Q_y = \sum_i w_i \sin(n\phi_i)$$

$$\Psi_n = \frac{1}{n} \tan^{-1} \left(\frac{Q_y}{Q_x} \right)$$

Re-centering

$$Q_x^{\text{Rec}} = \frac{Q_x - \langle Q_x \rangle}{\sigma_x}, Q_y^{\text{Rec}} = \frac{Q_y - \langle Q_y \rangle}{\sigma_y}$$

$$\Psi_n^{\text{Rec}} = \frac{1}{n} \tan^{-1} (Q_y^{\text{Rec}} / Q_x^{\text{Rec}})$$

Fourier correction

$$n\Psi_n^{\text{Fourier}} = n\Psi_n^{\text{Rec}} + n\Delta\Psi_n$$

$$n\Delta\Psi_n = \sum_k \{ A_k \cos(kn\Psi_n^{\text{Rec}}) + B_k \sin(kn\Psi_n^{\text{Rec}}) \}$$

$$A_k = -\frac{2}{k} \langle \cos(kn\Psi_n^{\text{Rec}}) \rangle, B_k = \frac{2}{k} \langle \sin(kn\Psi_n^{\text{Rec}}) \rangle$$

Event Plane Resolution

EP Resolution

PRC 58.1671 (1998)

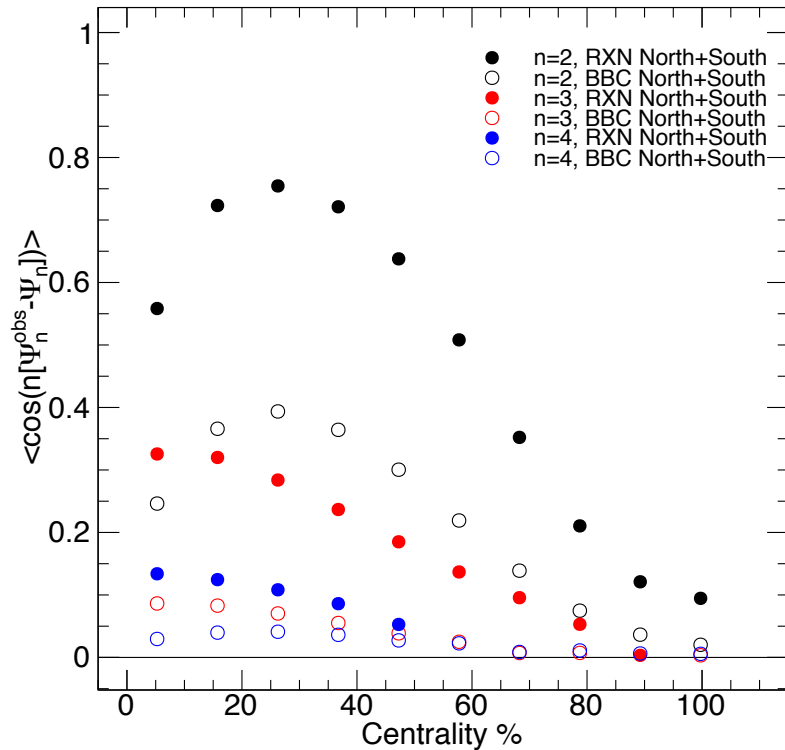
✧ Resolution $+/-\eta$

$$\begin{aligned}\sigma_n^{EP} &= \sqrt{\left\langle \cos kn(\Psi_n^{EP(+\eta)} - \Psi_n^{EP(-\eta)}) \right\rangle} \\ &= \left\langle \cos kn(\Psi_n^{EP+/-\eta} - \Psi_n) \right\rangle \\ &= \frac{\pi}{8} \chi_n^2 \left[I_{(k-1)/2} \left(\frac{\chi_n^2}{4} \right) + I_{(k+1)/2} \left(\frac{\chi_n^2}{4} \right) \right]^2\end{aligned}$$

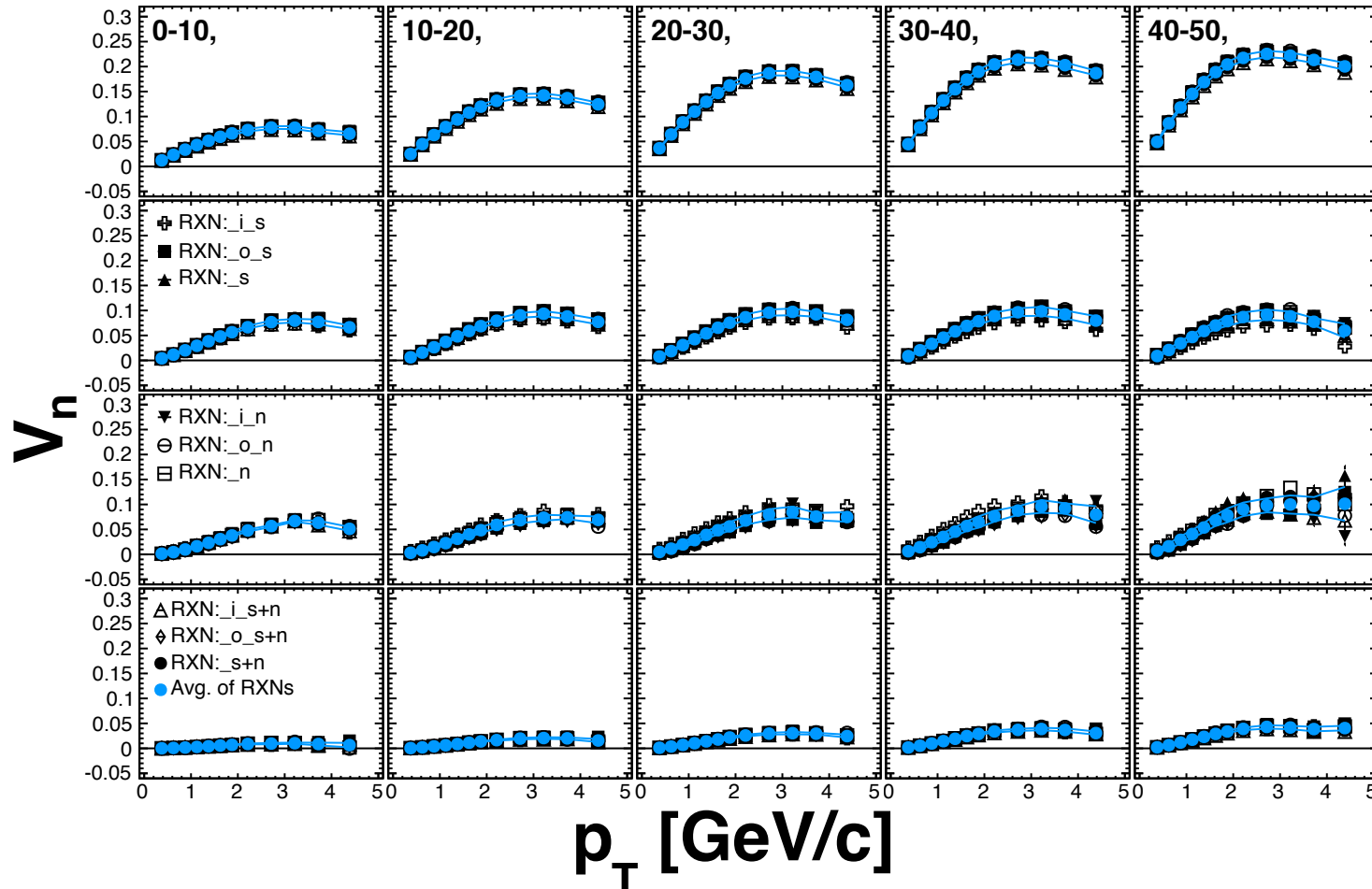
✧ Resolution $+&-\eta$

- $\chi_n \rightarrow \sqrt{2}\chi_n$

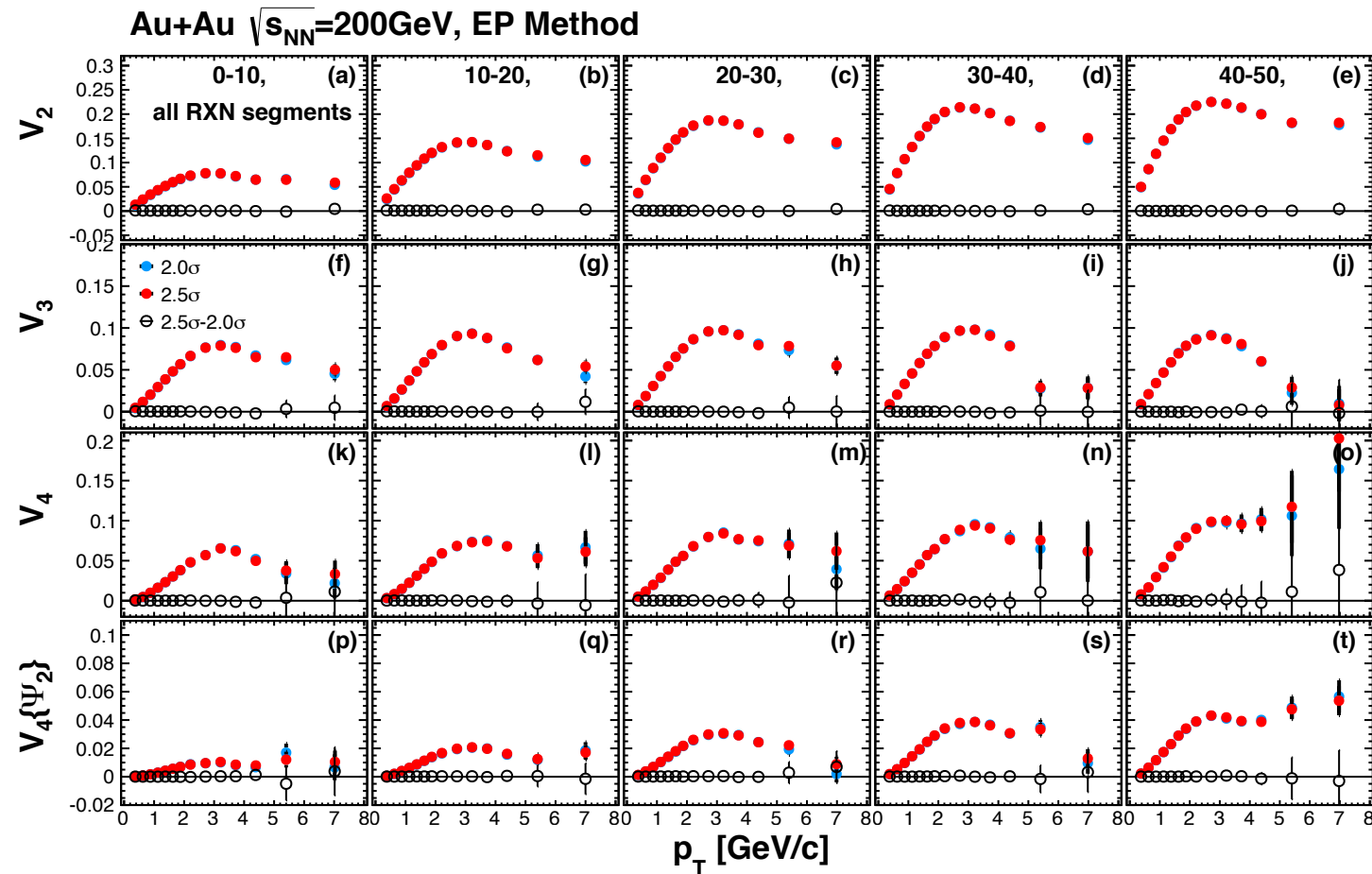
$$\sigma_n^{EP} = \frac{\pi}{8} 2\chi_n^2 \left[I_{(k-1)/2} \left(\frac{2\chi_n^2}{4} \right) + I_{(k+1)/2} \left(\frac{2\chi_n^2}{4} \right) \right]^2$$



v_n systematics : RXN segments



v_n systematics : Matching Cut



v_n systematics : RXN-BBC Difference

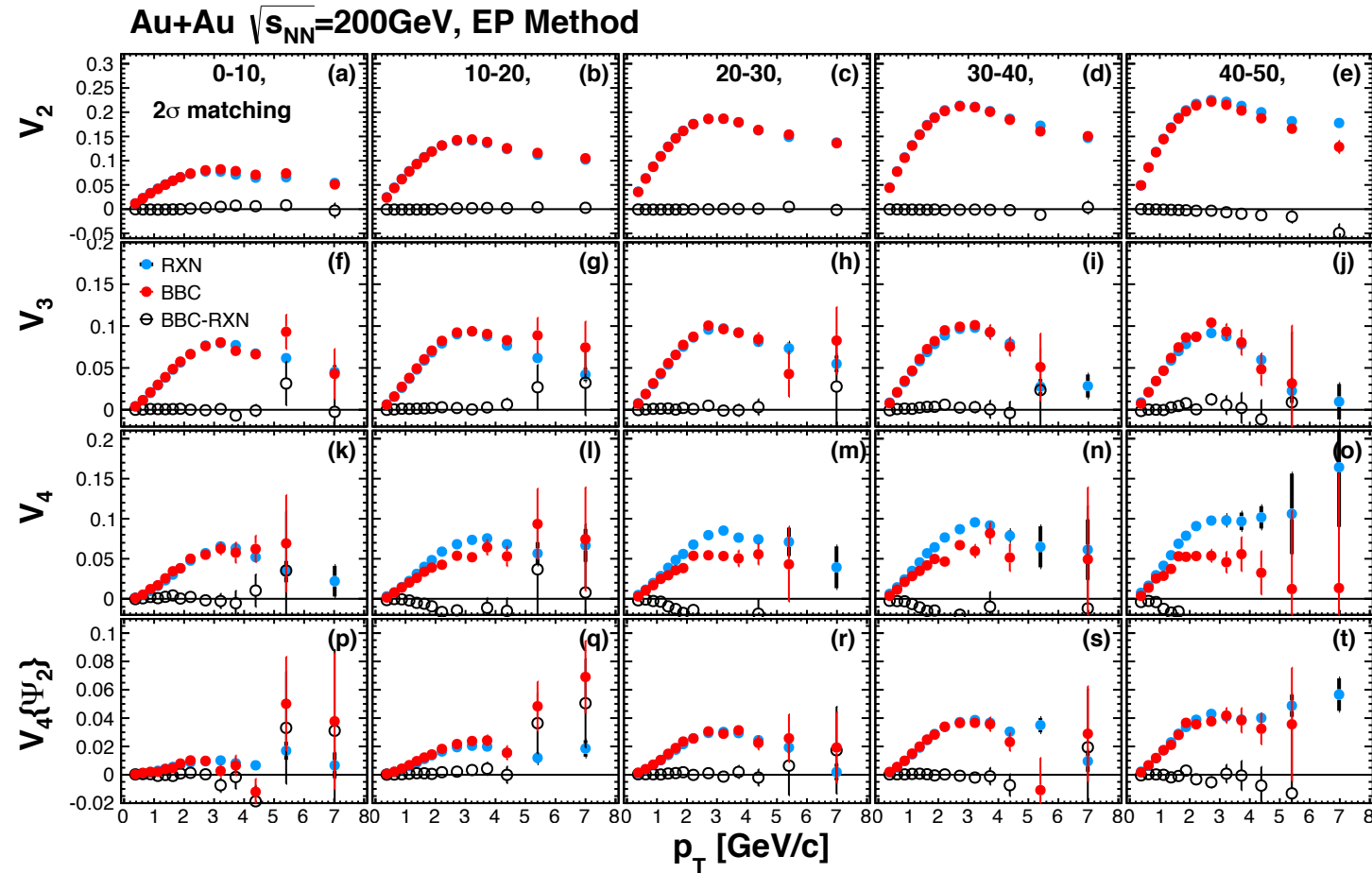


Table of total v_n systematic uncertainties

Table 3.8: Summary of percentile ratio of v_n systematic uncertainties

| Centrality % | p_T GeV/ c | v_2 sys. % | v_3 sys. % | v_4 sys. % | $v_4\{\Psi_2\}$ sys. % |
|--------------|----------------|--------------|--------------|--------------|------------------------|
| 0-10 | 0.5-1.0 | 5.449 | 6.387 | 24.87 | 48 |
| | 1.0-2.0 | 4.32 | 4.911 | 10.1 | 14.66 |
| | 2.0-4.0 | 4.536 | 4.131 | 4.412 | 11.39 |
| | 4.0-10.0 | 10.43 | 6.184 | 21.67 | 191.3 |
| 10-20 | 0.5-1.0 | 3.658 | 7.992 | 28.53 | 12.17 |
| | 1.0-2.0 | 2.891 | 6.431 | 20.16 | 12.27 |
| | 2.0-4.0 | 2.69 | 6.163 | 27.64 | 13.72 |
| | 4.0-10.0 | 3.124 | 13.62 | 19.09 | 32.09 |
| 20-30 | 0.5-1.0 | 2.811 | 9.469 | 35.48 | 9.633 |
| | 1.0-2.0 | 2.485 | 7.818 | 28.85 | 8.422 |
| | 2.0-4.0 | 2.391 | 6.822 | 28.03 | 6.577 |
| | 4.0-10.0 | 2.98 | 9.503 | 32.24 | 12.21 |
| 30-40 | 0.5-1.0 | 2.506 | 12.42 | 35.81 | 7.385 |
| | 1.0-2.0 | 2.462 | 9.695 | 29.88 | 6.509 |
| | 2.0-4.0 | 2.556 | 9.673 | 36.75 | 5.913 |
| | 4.0-10.0 | 2.934 | 14.18 | 44.32 | 31.73 |
| 40-50 | 0.5-1.0 | 2.575 | 13.8 | 32.96 | 6.338 |
| | 1.0-2.0 | 2.688 | 12.06 | 34.44 | 6.479 |
| | 2.0-4.0 | 3.224 | 11.7 | 45.4 | 10.71 |
| | 4.0-10.0 | 7.877 | 33.53 | 77.07 | 29.33 |

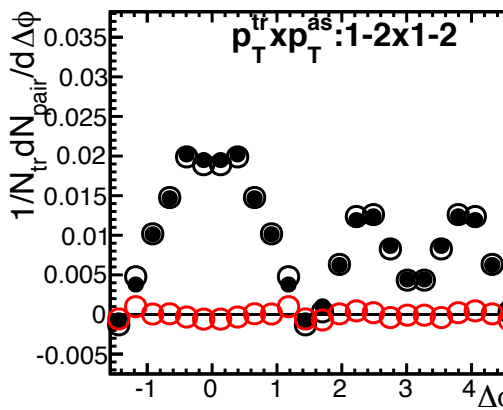
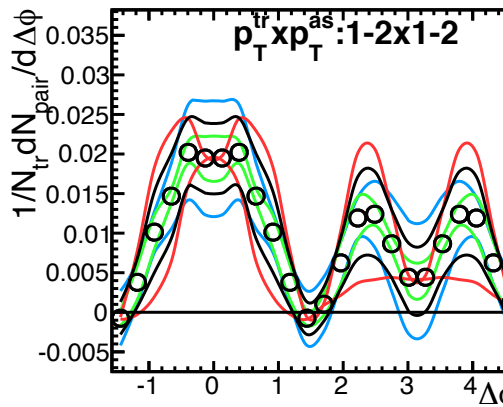
Systematics of Correlations

- ✧ Systematics propagated from v_n measurements

- Varying v_n value $\pm 1\sigma$ (# of harmonics $3 \times \pm 1\sigma = 6$ combinations)
- Systematics : RMS of above 6 combinations

- ✧ Systematics from matching cut
 - Systematics : Difference between $2.5\sigma - 2.0\sigma$ (main)

- ✧ Total Systematics
 - Quadrature-sum of above two systematics



EP Resolution in Monte Carlo

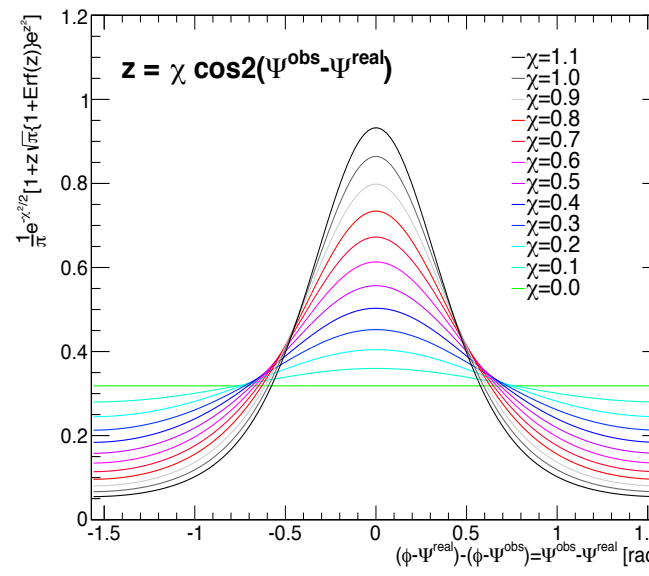
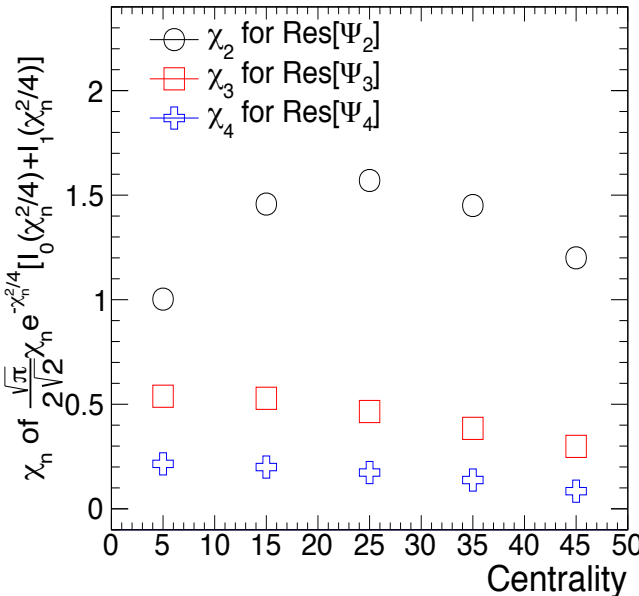
- ✧ Analytical formula of EP Resolution (RXN:S+N) as a function of χ_n
 - Convert Resolution to χ_n

PRC 58.1671 (1998)

$$\langle \cos [kn(\Psi_n^{obs} - \Psi_n^{real})] \rangle = \frac{\sqrt{\pi}}{2\sqrt{2}} \chi_n e^{-\chi_n^2/4} \left[I_{(k-1)/2} \left(\frac{\chi_n^2}{4} \right) + I_{(k+1)/2} \left(\frac{\chi_n^2}{4} \right) \right].$$

- ✧ Relative distribution between real and observed EP calculated using χ_n

$$\frac{dN^{eve}}{d[kn(\Psi_n^{obs} - \Psi_n^{real})]} = \frac{1}{\pi} e^{-\chi_n^2/2} \left[1 + z\sqrt{\pi}[1 + \text{erf}(z)]e^{z^2} \right] \quad z = \frac{1}{\sqrt{2}} \chi_n \cos n(\Psi_n^{obs} - \Psi_n^{real})$$



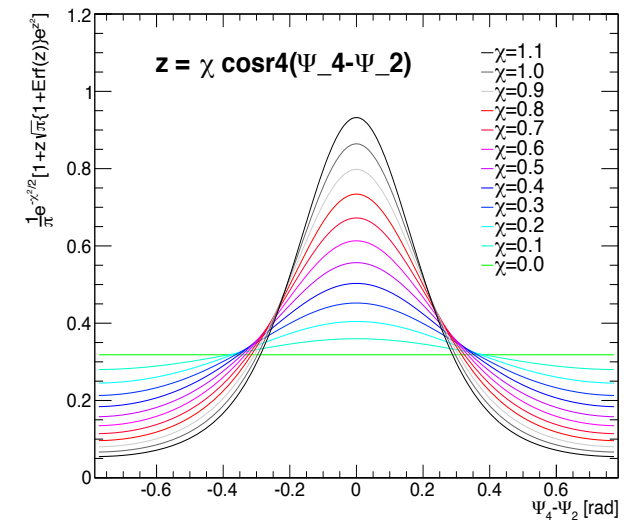
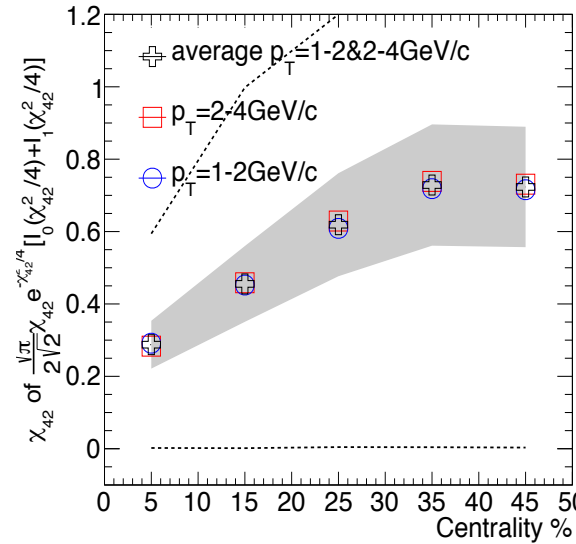
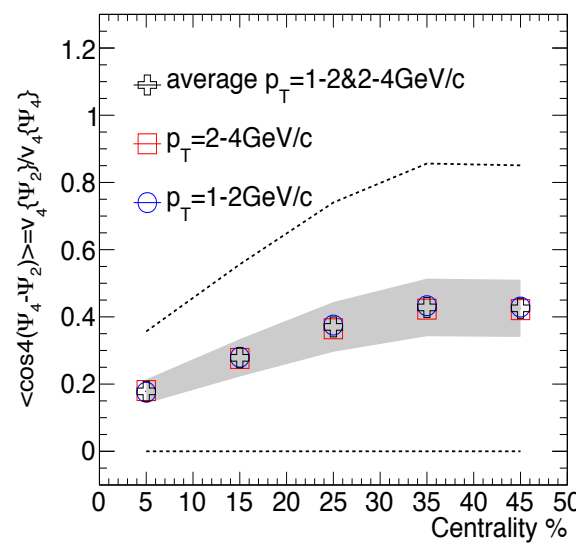
PRD 48.1132 (1993)

Ψ_2 - Ψ_4 correlation in Monte Carlo

- ✧ **Ψ_2 - Ψ_4 correlation at p_T 1-2&2-4GeV :** $\langle \cos [4(\Psi_2 - \Psi_4)] \rangle = v_4 \{\Psi_2\} / v_4 \{\Psi_4\}$
 - To avoid jet contribution to the Ψ_2 - Ψ_4 correlation
- ✧ Obtain χ_{42} & reconstruct relative distribution between Ψ_2 & Ψ_4

$$\langle \cos [4(\Psi_2 - \Psi_4)] \rangle = \frac{\sqrt{\pi}}{2\sqrt{2}} \chi_{42} e^{-\chi_{42}^2/4} \left[I_0 \left(\frac{\chi_{42}^2}{4} \right) + I_1 \left(\frac{\chi_{42}^2}{4} \right) \right]$$

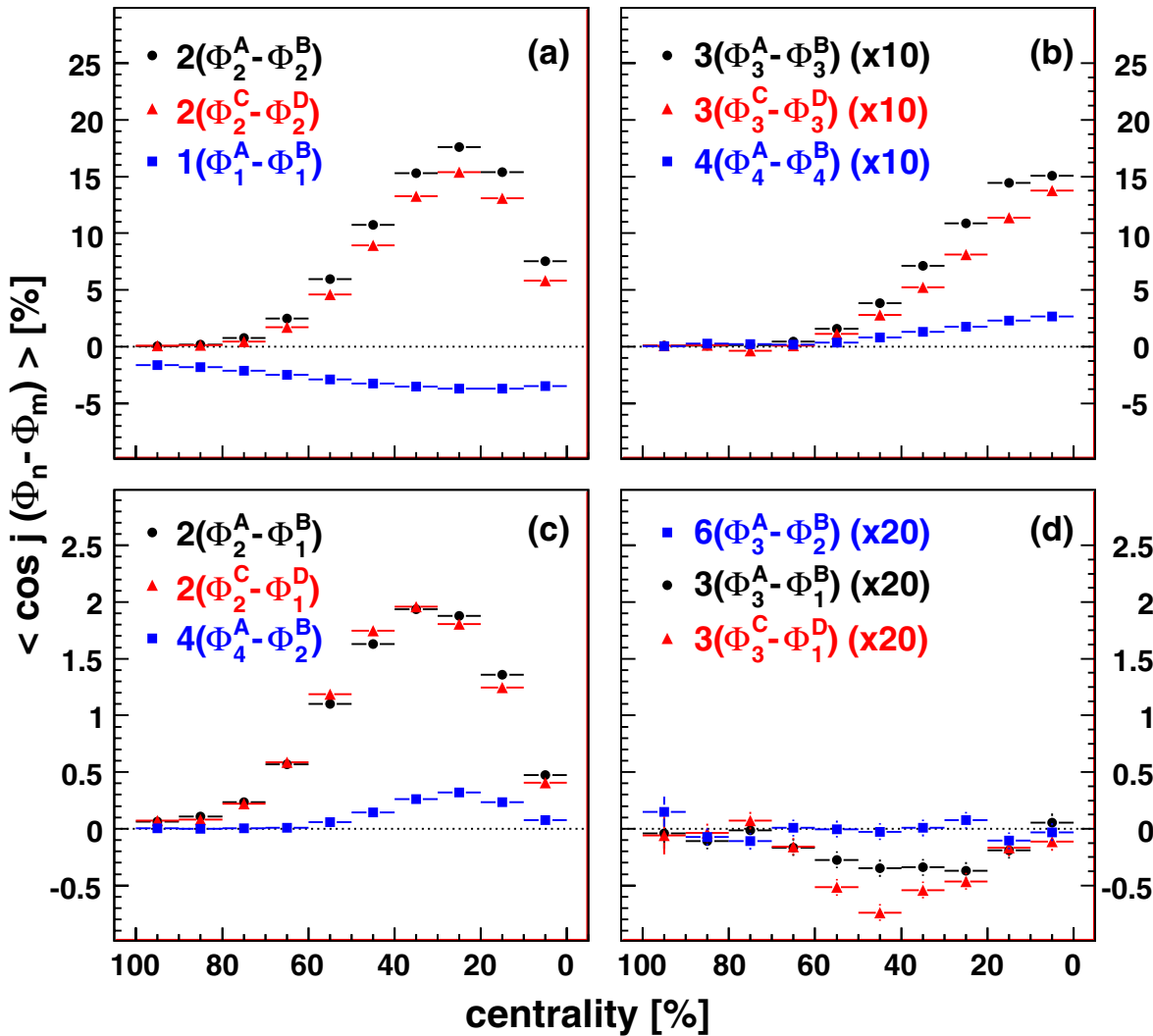
$$\frac{dN^{eve}}{d[kn(\Psi_n^{obs} - \Psi_n^{real})]} = \frac{1}{\pi} e^{-\chi_n^2/2} \left[1 + z\sqrt{\pi}[1 + \text{erf}(z)]e^{z^2} \right] \quad z = \frac{1}{\sqrt{2}} \chi_n \cos n(\Psi_n^{obs} - \Psi_n^{real})$$



Ψ_2 - Ψ_3 correlation

PRL107.252301 (2011)

- A : RXN North
- B : BBC South
- C : MPC North
- D : MPC South



EP Resolution Correction : Iteration-1

- Trigger bin is also smeared due to limited EP resolution as v_n
 - Add an offset $\lambda=1.0$ to correlation Y to avoid possible divisions by zero

Raw Correlation

$$\mathbf{A}(k) = \begin{pmatrix} 1 - Y(0, k) \\ 1 - Y(1, k) \\ 1 - Y(2, k) \\ 1 - Y(3, k) \\ 1 - Y(4, k) \\ 1 - Y(5, k) \\ 1 - Y(6, k) \\ 1 - Y(7, k) \end{pmatrix}, \quad k = 0, \dots, 23$$

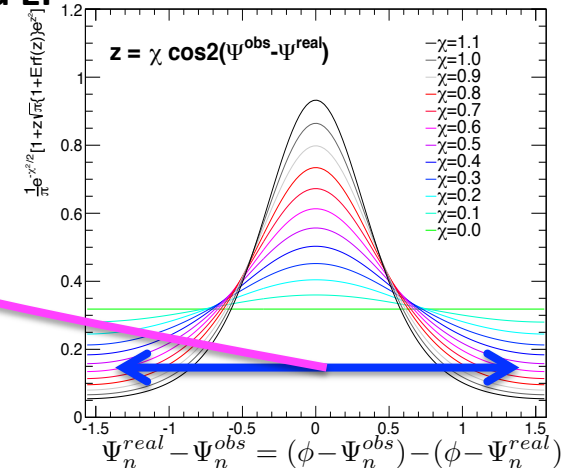
$\Delta\phi$ Bin

Smearing Effect

Trigger Bin

$$S = \begin{pmatrix} s_0 & s_1 & s_2 & s_3 & s_4 & s_3 & s_2 & s_1 \\ s_1 & s_0 & s_1 & s_2 & s_3 & s_4 & s_3 & s_2 \\ s_2 & s_1 & s_0 & s_1 & s_2 & s_3 & s_4 & s_3 \\ s_3 & s_2 & s_1 & s_0 & s_1 & s_2 & s_3 & s_4 \\ s_4 & s_3 & s_2 & s_1 & s_0 & s_1 & s_2 & s_3 \\ s_3 & s_4 & s_3 & s_2 & s_1 & s_0 & s_1 & s_2 \\ s_2 & s_3 & s_4 & s_3 & s_2 & s_1 & s_0 & s_1 \\ s_1 & s_2 & s_3 & s_4 & s_3 & s_2 & s_1 & s_0 \end{pmatrix}, \quad \sum_n s_n = 1, \quad s_n : \text{Ratio from } n^{\text{th}} \text{ away-bin}$$

: Calculated by relative distribution between real and observed EP



Smeared Correlation

$$\mathbf{B}(k) = \mathbf{S}\mathbf{A}(k)$$

Correction Matrix

$$\mathbf{C}(k) = (c_{ij})$$

$$c_{ij} = \begin{cases} \frac{A(i,k)}{B(i,k)} & (i = j) \\ 0 & (i \neq j) \end{cases}$$

Corrected Correlation

$$\mathbf{A}^{\text{cor}}(k) = \mathbf{C}(k)\mathbf{A}(k)$$

EP Resolution Correction : Iteration-2

- ✧ Start of iteration : experimental results (already smeared once)
- ✧ Obtained correction is not true
- ✧ Iteration until conversions of each coefficients
 - 300 Loops

Notation in Iteration

$$A \rightarrow A^{(n)}$$

$$B \rightarrow B^{(n)}$$

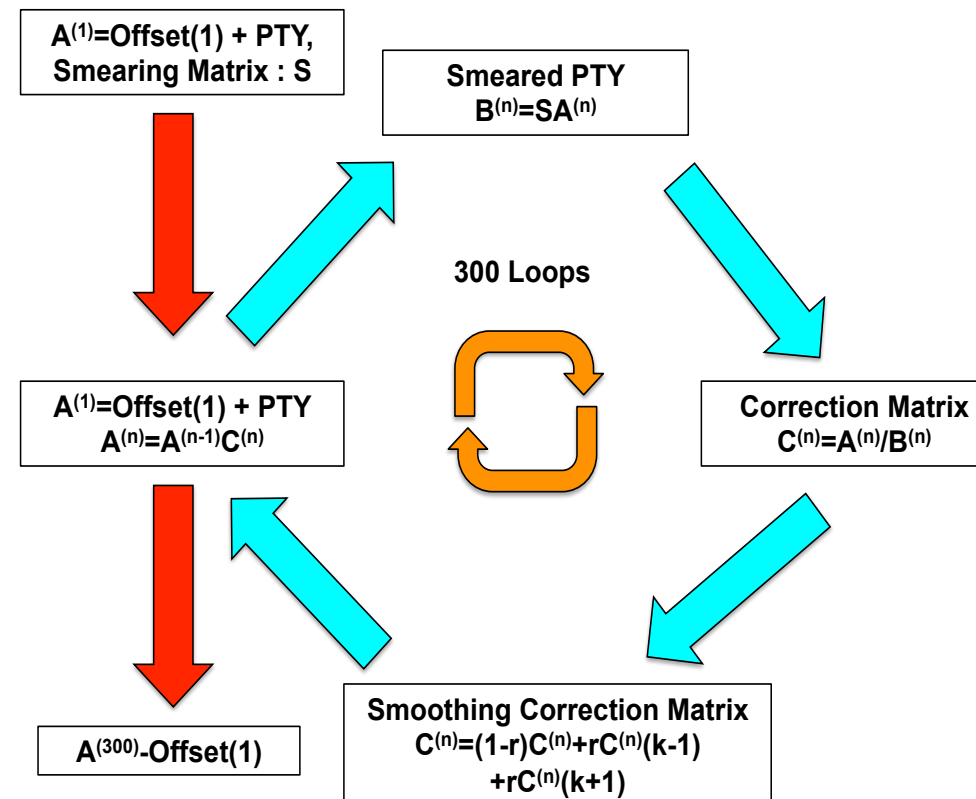
$$C \rightarrow C^{(n)}$$

$$A^{\text{cor}} \rightarrow A^{(n+1)}$$

Smoothing

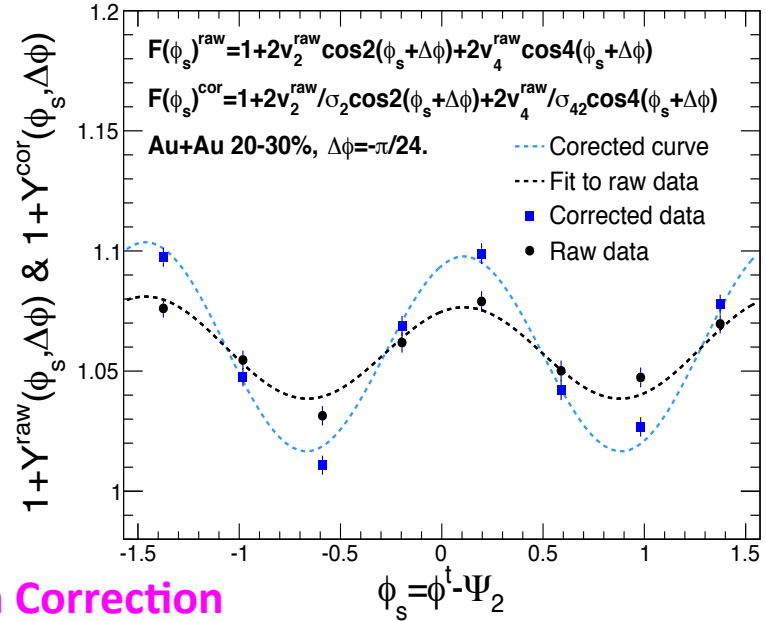
- ✧ Preventing a divergence of statistical fluctuations among $\Delta\phi$ bins
- ✧ $2r=0.20$ & 0.30

$$c_{ii}^{(n)}(k) = (1 - r)c_{ii}^{(n)}(k) + (r/2)c_{ii}^{(n)}(k-1) + (r/2)c_{ii}^{(n)}(k+1)$$



EP Resolution Correction : Fitting Method

- ❖ Assuming correlation yield has anisotropy with respect to EP
- ❖ Correction by EP resolution as done in v_n measurements
 - Method by PRC.84.024904(2011)
- ❖ Offset $\lambda=1.0$ to avoid possible division by zero



Ψ_2 dependent case

EP Resolution Correction

$$\lambda + Y^{cor}(\phi_s, \Delta\phi) = \frac{\lambda + b_0 [1 + 2v_2^Y / \sigma \cos 2(\phi_s + \Delta\phi) + 2v_4^Y / \sigma_{42} \cos 4(\phi_s + \Delta\phi)]}{\lambda + b_0 [1 + 2v_2^Y \cos 2(\phi_s + \Delta\phi) + 2v_4^Y \cos 4(\phi_s + \Delta\phi)]} (\lambda + Y(\phi_s, \Delta\phi))$$

Fitting

Ψ_3 dependent case

$$\lambda + Y^{cor}(\phi_s, \Delta\phi) = \frac{\lambda + b_0 [1 + 2v_3^Y / \sigma_3 \cos 3(\phi_s + \Delta\phi)]}{\lambda + b_0 [1 + 2v_3^Y \cos 3(\phi_s + \Delta\phi)]} (\lambda + Y(\phi_s, \Delta\phi))$$

Fitting

Consistency check : high- p_T trigger

- ❖ Three-Centralities
 - 0-20, 20-40, 40-60%

- ❖ Particle Selections
 - Trigger p_T : **5-10 GeV/c**
 - Associate p_T : **1-10 GeV/c**

- ❖ Subtracted Backgrounds
 - **Only v_2**

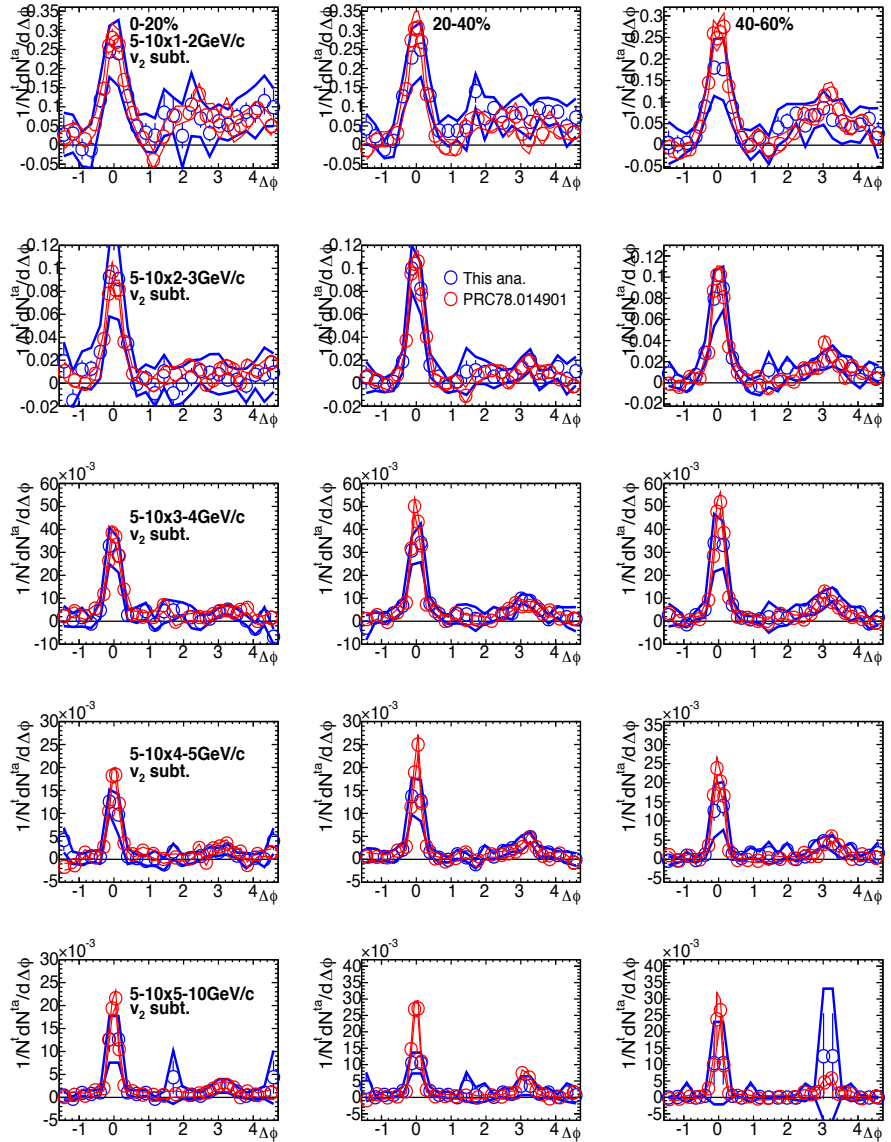
- ❖ Consistent with previous PHENIX results
(PRC78.014901)



: This Analysis



: PRC78.014901



Consistency check : mid- p_T trigger

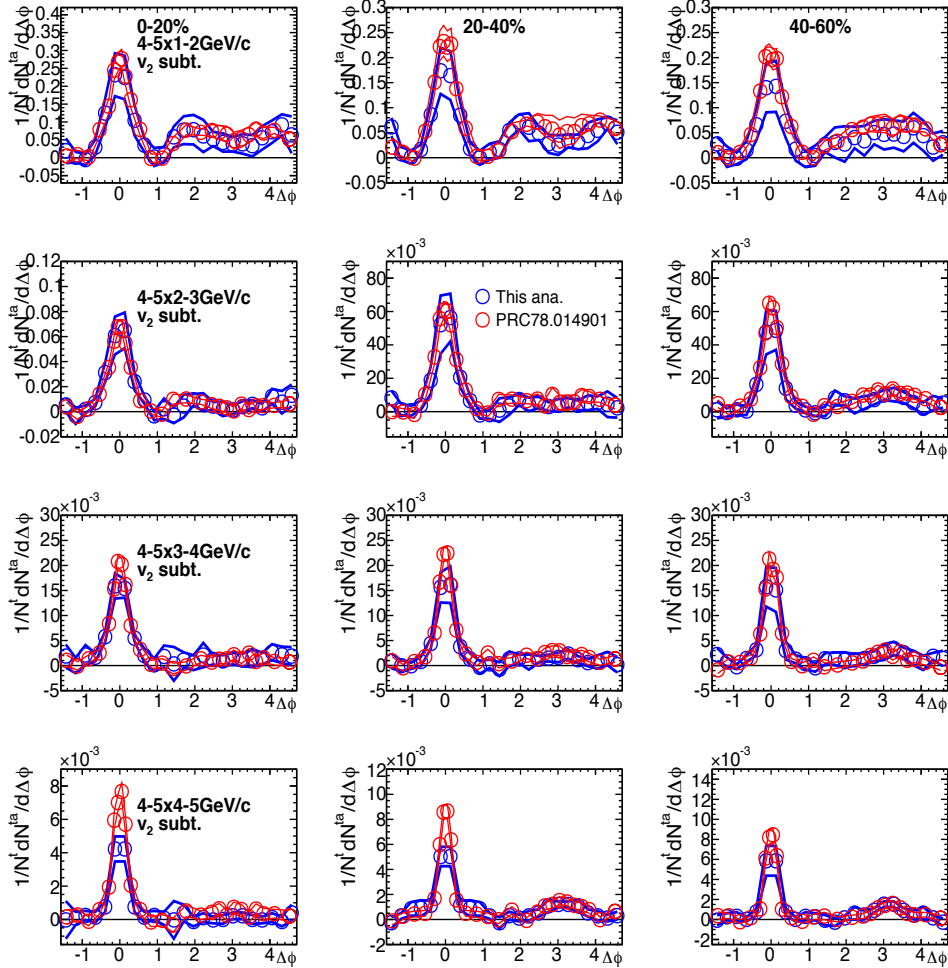
- ✧ Three-Centralities
 - 0-20, 20-40, 40-60%
- ✧ Particle Selections
 - Trigger p_T : **4-5 GeV/c**
 - Associate p_T : **1-5 GeV/c**
- ✧ Subtracted Backgrounds
 - Only **v_2**
- ✧ Consistent with previous PHENIX results
(PRC78.014901)



: This Analysis



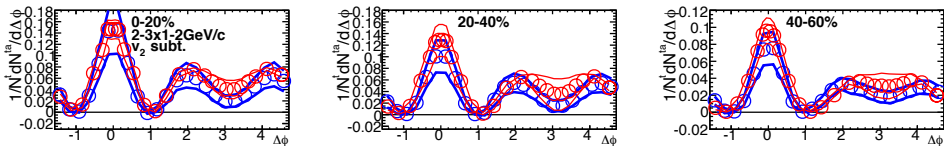
: PRC78.014901



Consistency check : low- p_T trigger

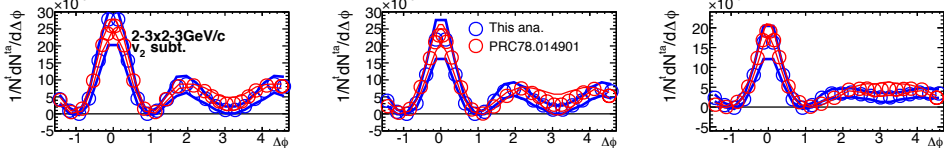
✧ Three-Centralities

- 0-20, 20-40, 40-60%



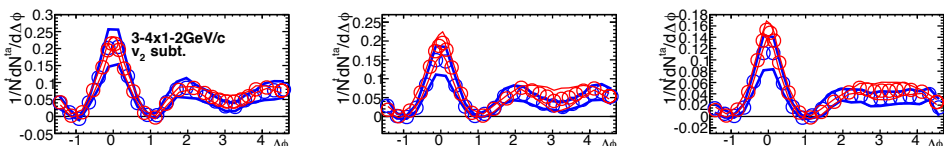
✧ Particle Selections

- Trigger p_T : **2-4 GeV/c**
- Associate p_T : **1-4 GeV/c**

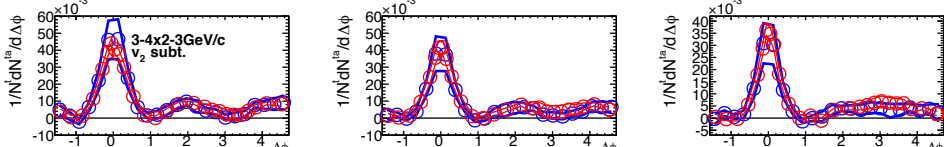


✧ Subtracted Backgrounds

- Only v_2



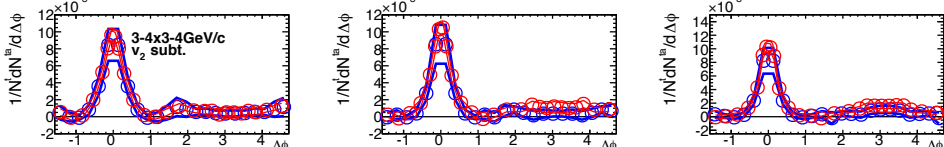
✧ Consistent with previous PHENIX results (PRC78.014901)



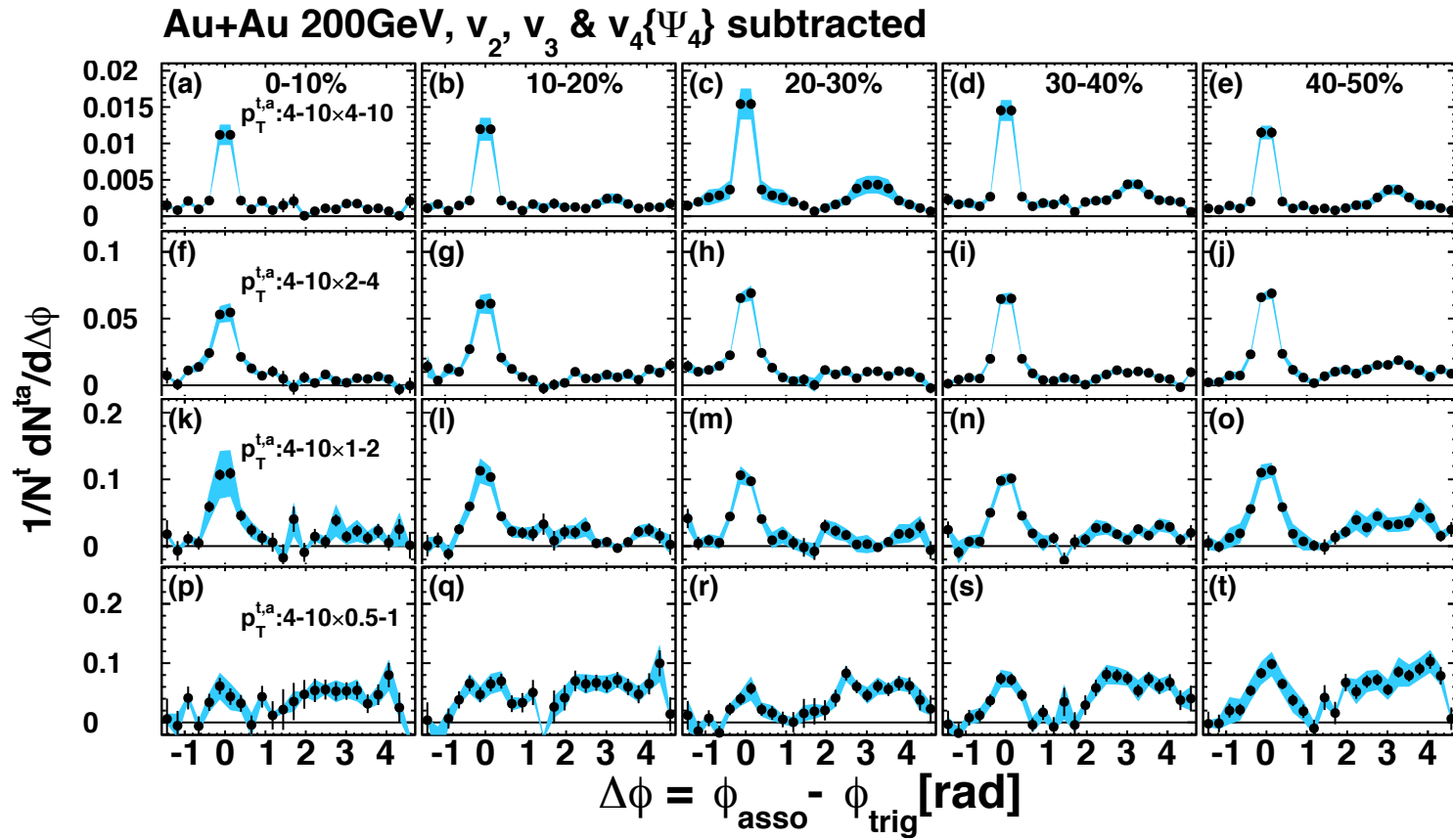
: This Analysis



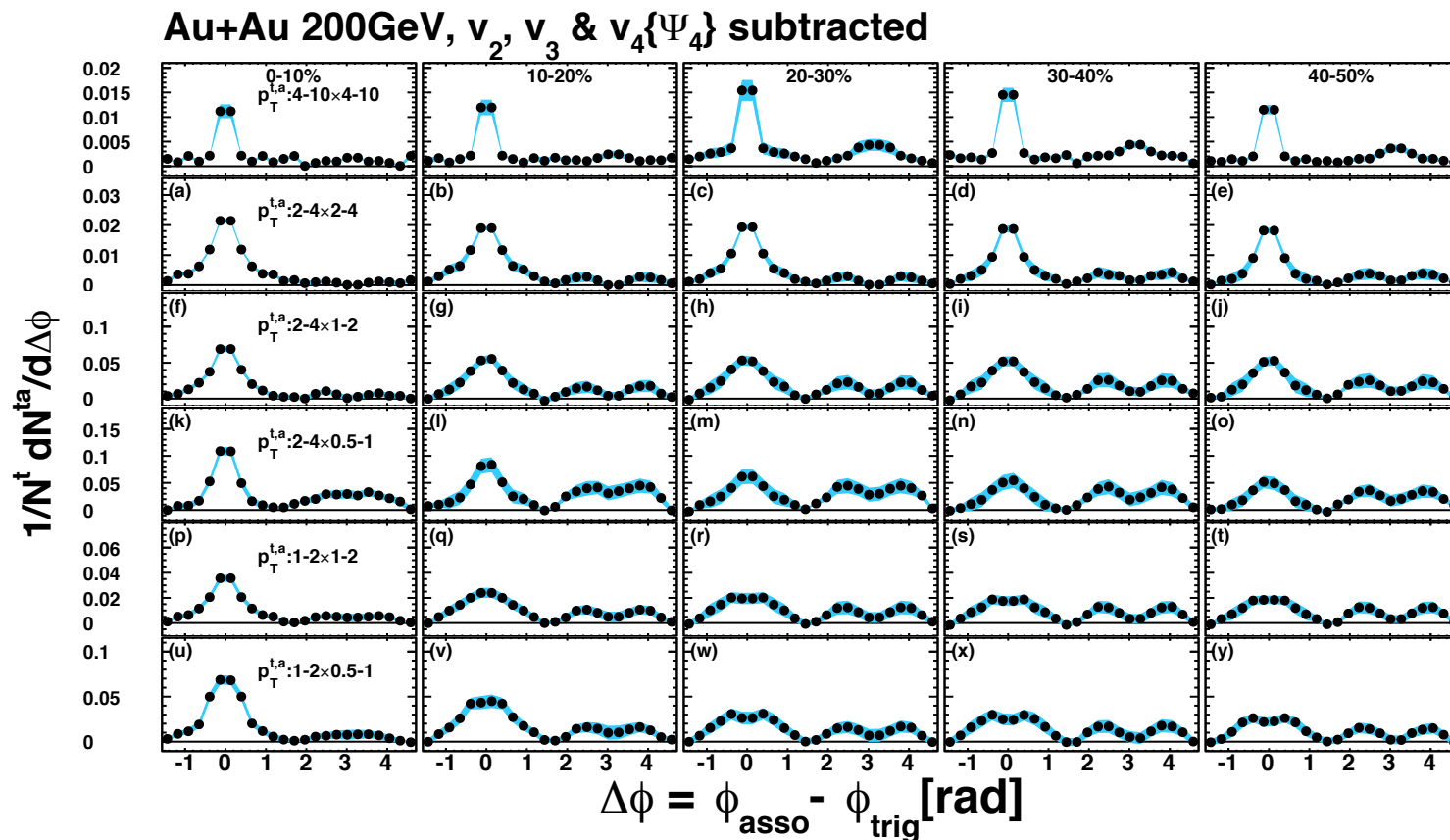
: PRC78.014901



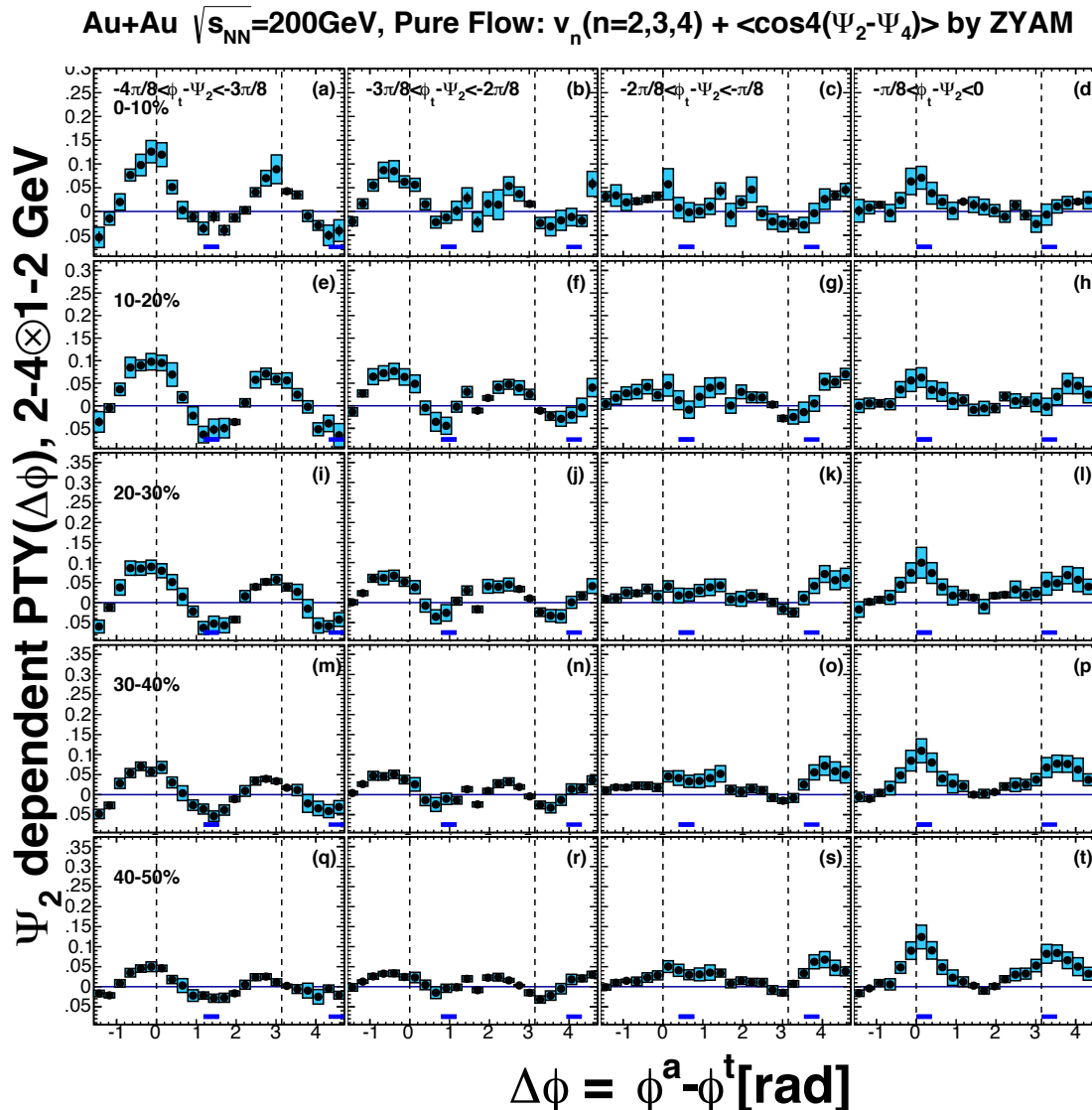
High p_T Trigger Two-Particle Correlations



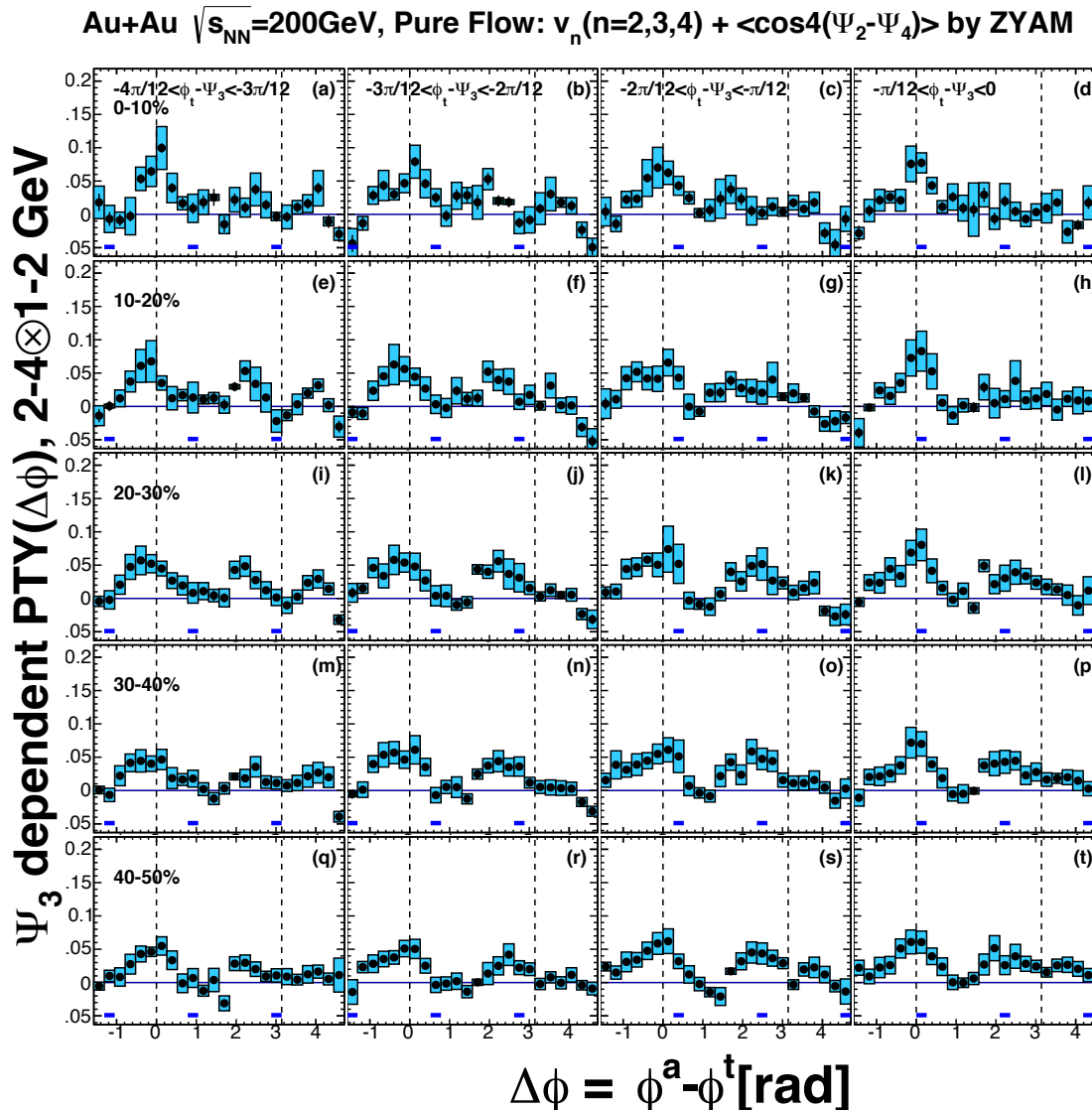
Intermediate p_T Two-Particle Correlations



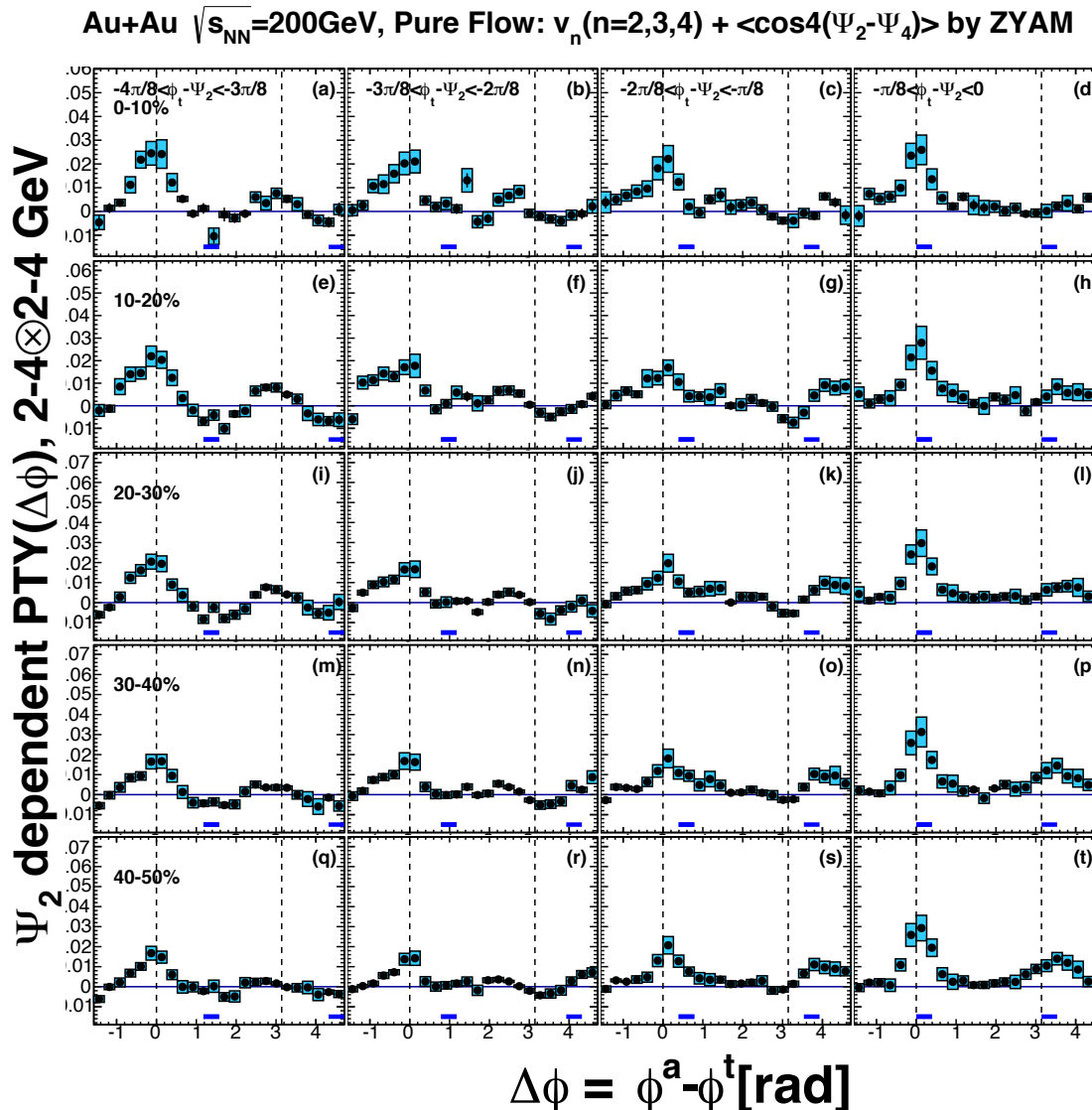
Ψ_2 Dependent Correlations : p_T 2-4x1-2 GeV/c



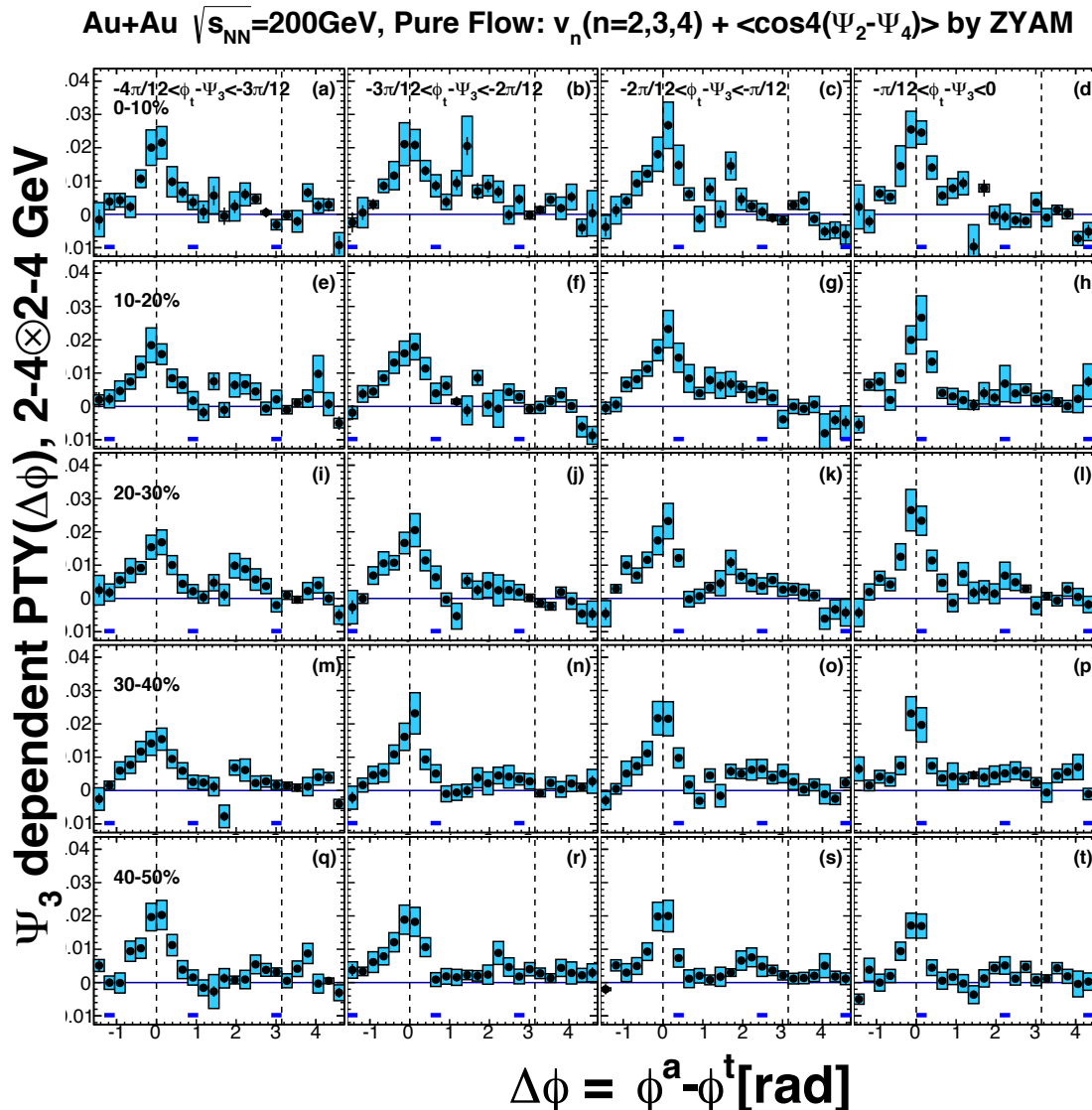
Ψ_3 Dependent Correlations : p_T 2-4x1-2 GeV/c



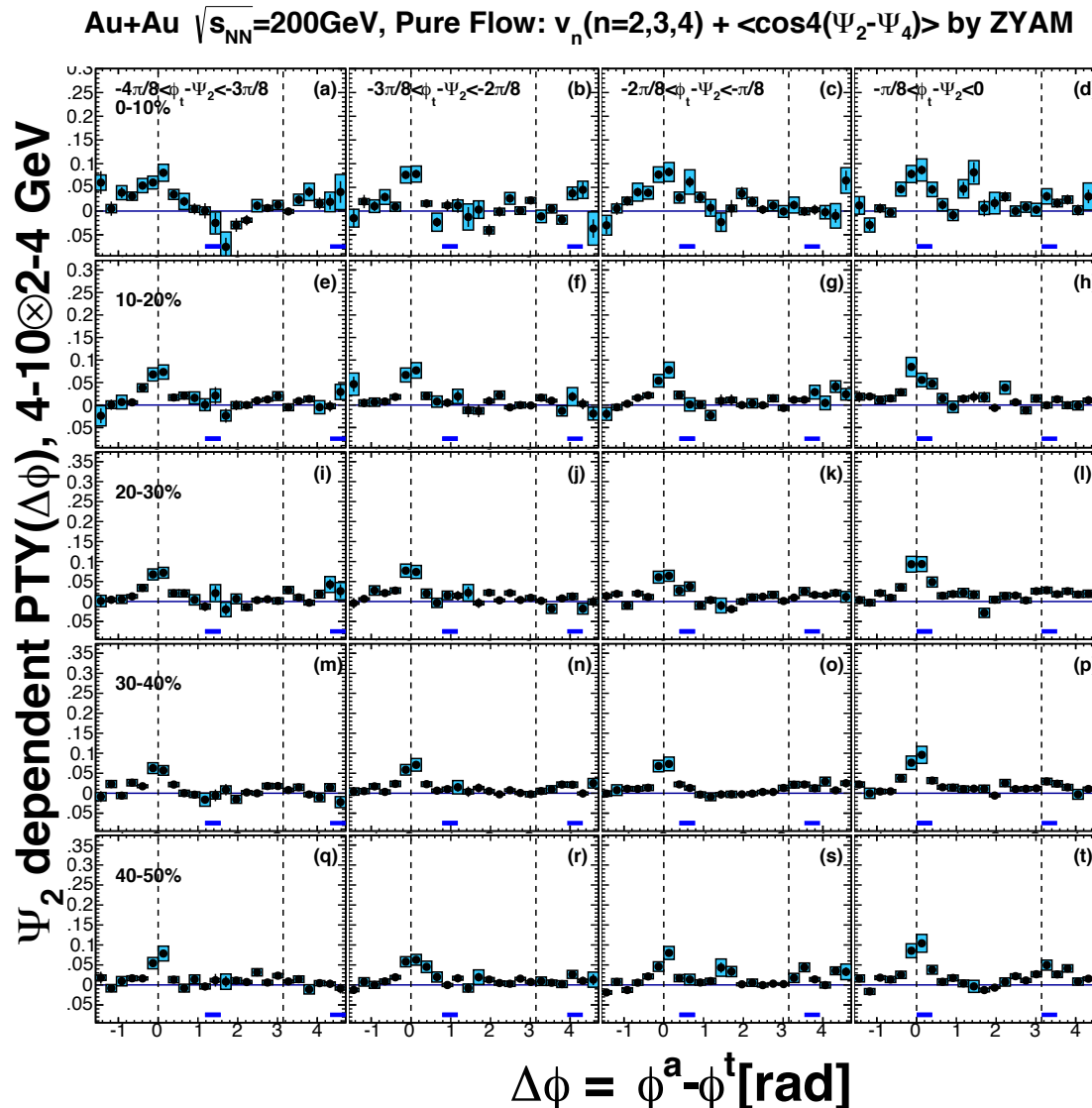
Ψ_2 Dependent Correlations : p_T 2-4x2-4 GeV/c



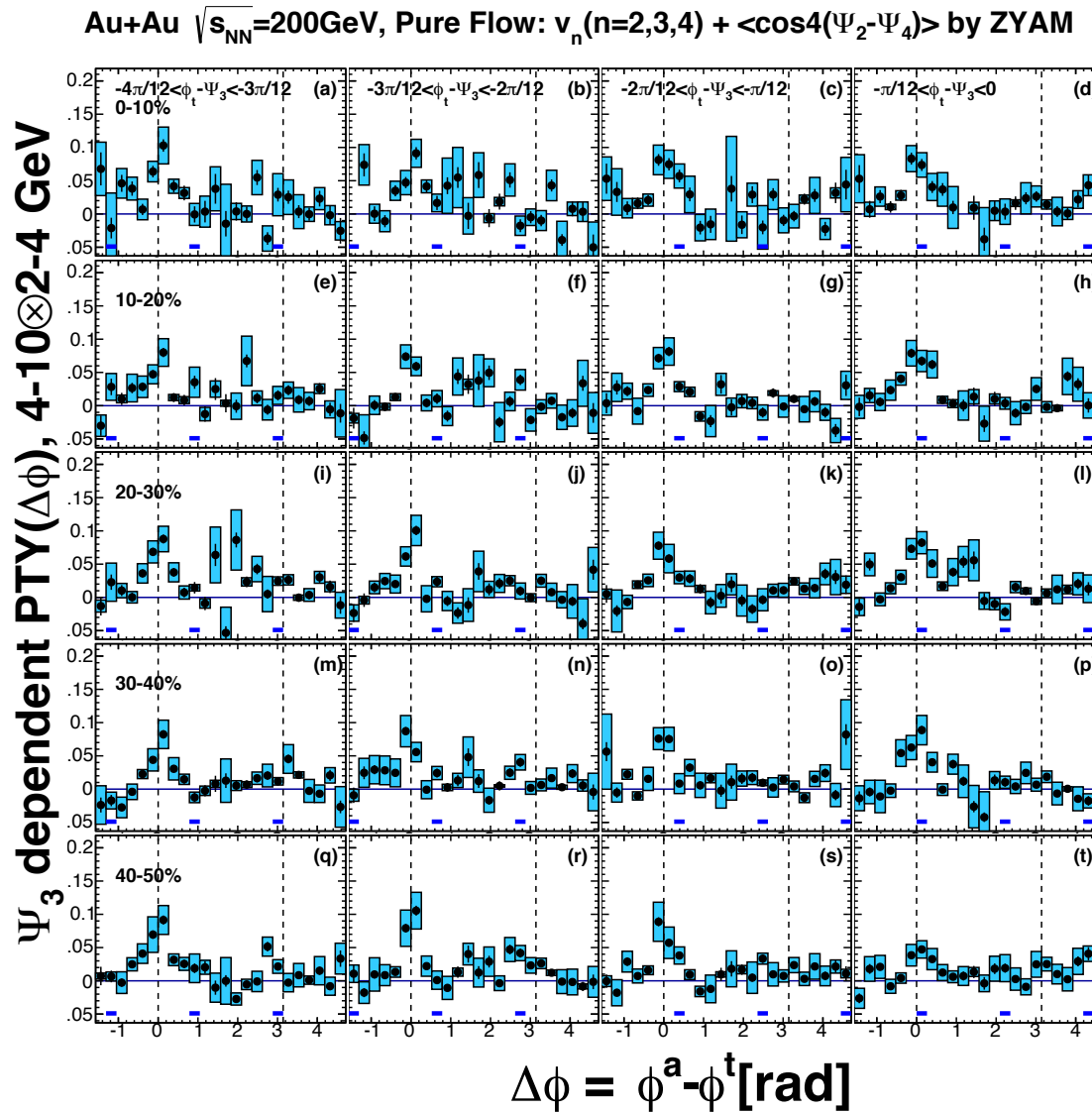
Ψ_3 Dependent Correlations : p_T 2-4x2-4 GeV/c



Ψ_2 Dependent Correlations : p_T 4-10x2-4 GeV/c

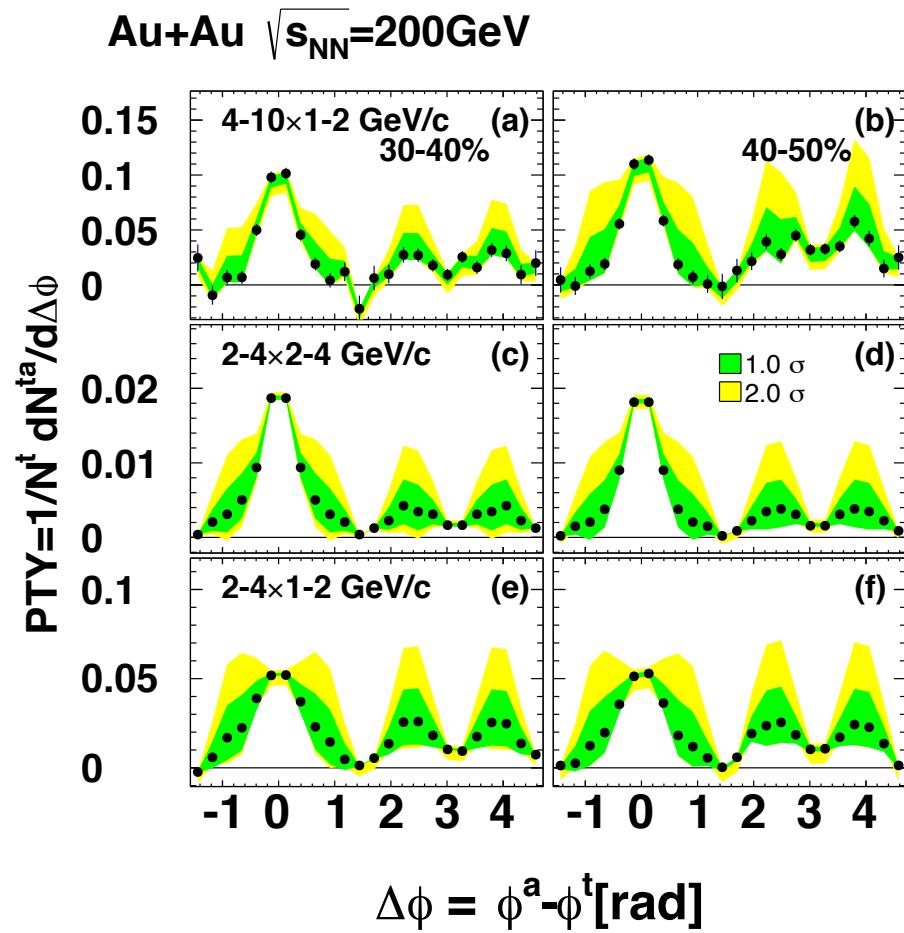


Ψ_3 Dependent Correlations : p_T 4-10x2-4 GeV/c



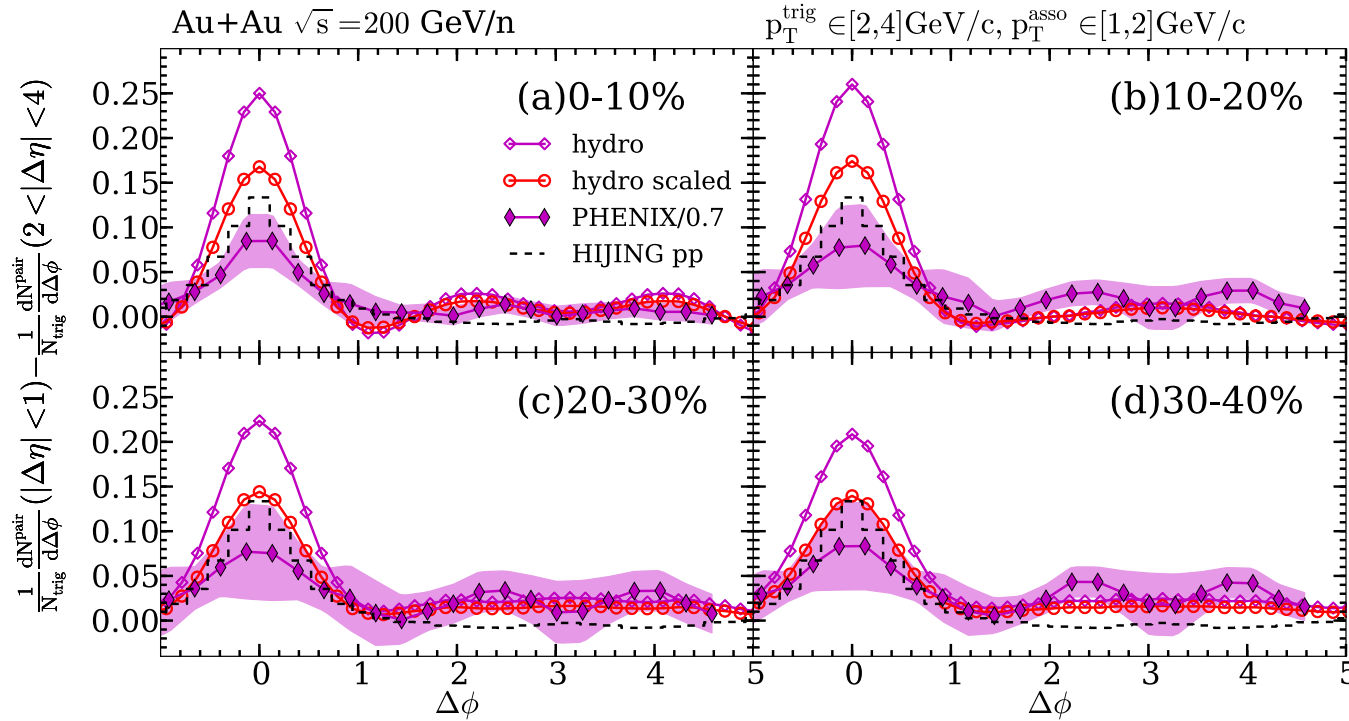
Significance of Double-Hump

- Examed the significance of Double-Hump in terms of v_4 systematics
- v_2 and v_3 are fixed in flow subtractions but v_4 is varied $\pm 1\sigma$
- Lower boundary of yellow band covers that of green band
- Significance is $\pm 1\sigma$ level of v_4 systematics



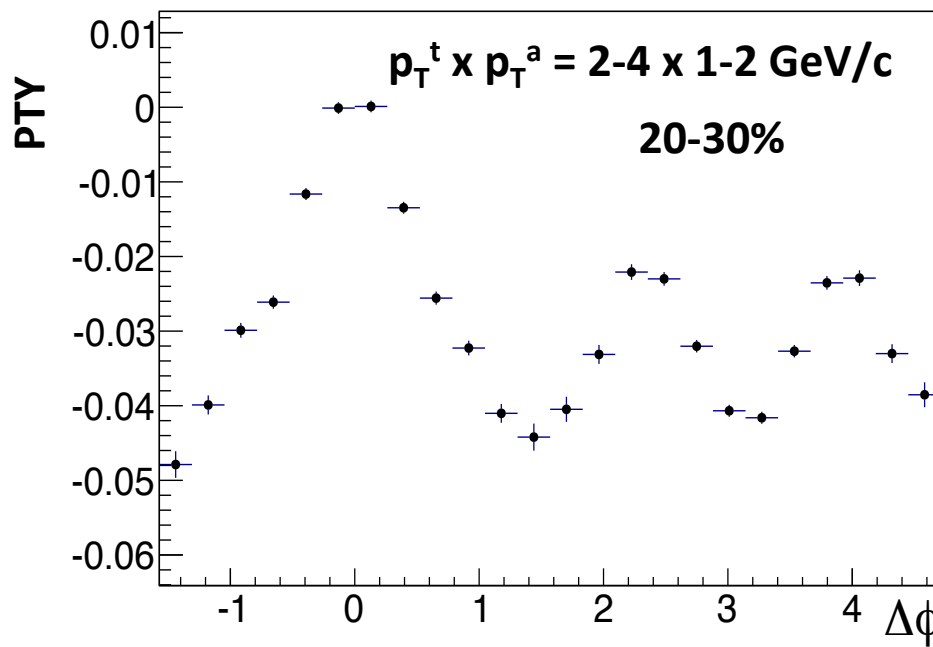
Latest Model for Two-Particle Correlations

arXiv:nucl-th/1309.6735v2 (2013)



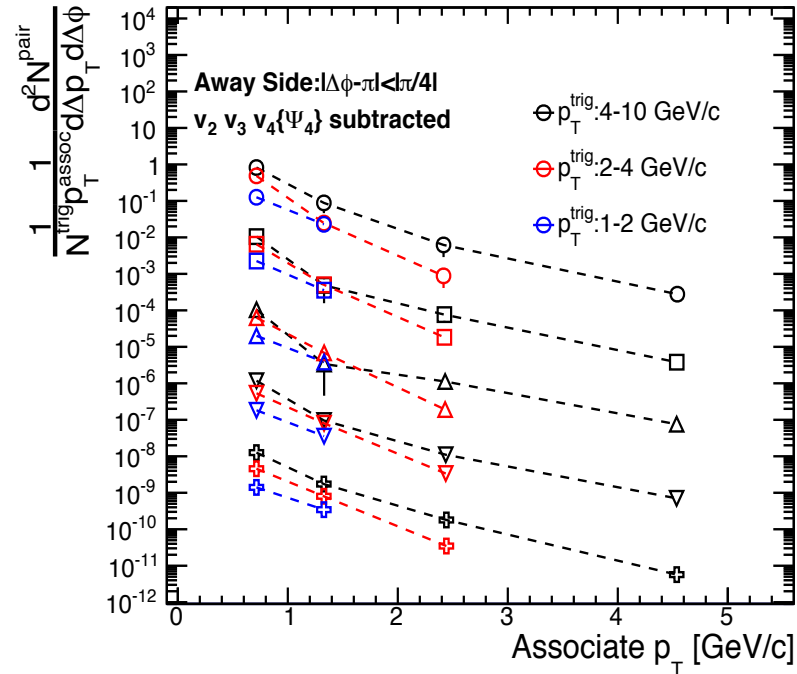
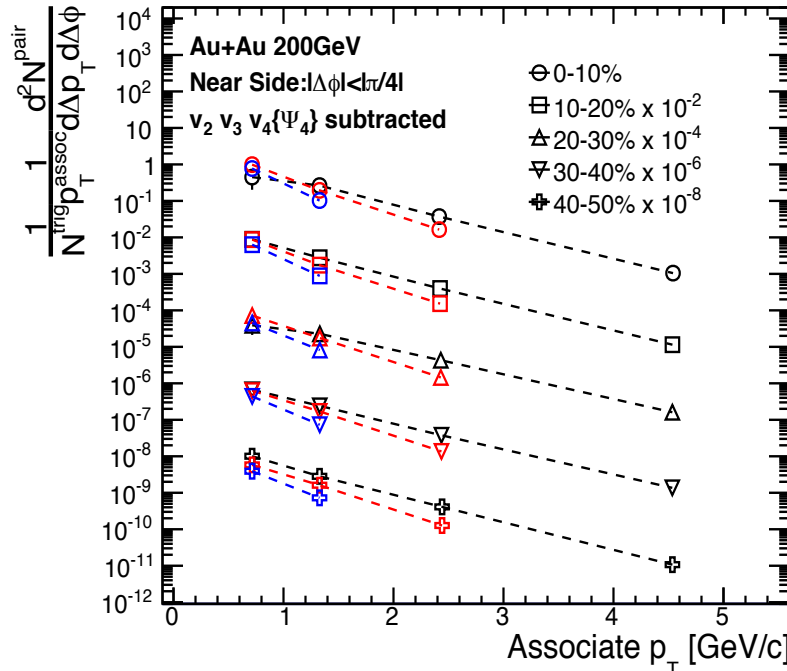
- ✧ Fluctuations of initial parton energy density
- ✧ Parton cascade
- ✧ Event-by-event (3+1)D hydrodynamics
- ✧ Parton Energy Momentum Loss

Zero Yield at Near-Side



- ✧ Correlation and Pure Flow is fitted at $\Delta\phi=0$
- ✧ Double-hump is not so sensitive to flow subtraction

Hardness of Correlation Yields



- p_T spectra of correlation yield

$$\frac{1}{p_T^a} \frac{dY}{d\Delta p_T} = \frac{1}{p_T^a} \frac{1}{(p_T^{a,\max} - p_T^{a,\min})} \int d\Delta\phi \frac{1}{N_{\text{trig}}} \frac{dN}{d\Delta\phi}$$

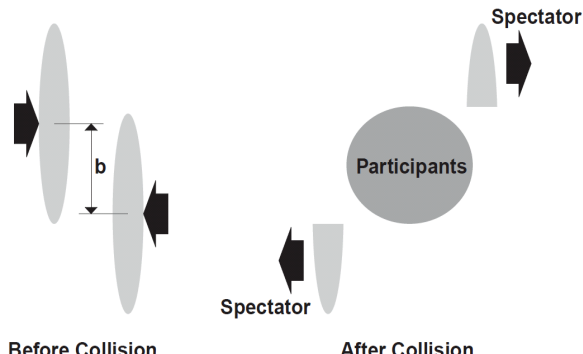
- ✧ Hardness increase with trigger and associate p_T
 - Different Physics depending on p_T

Glauber Model

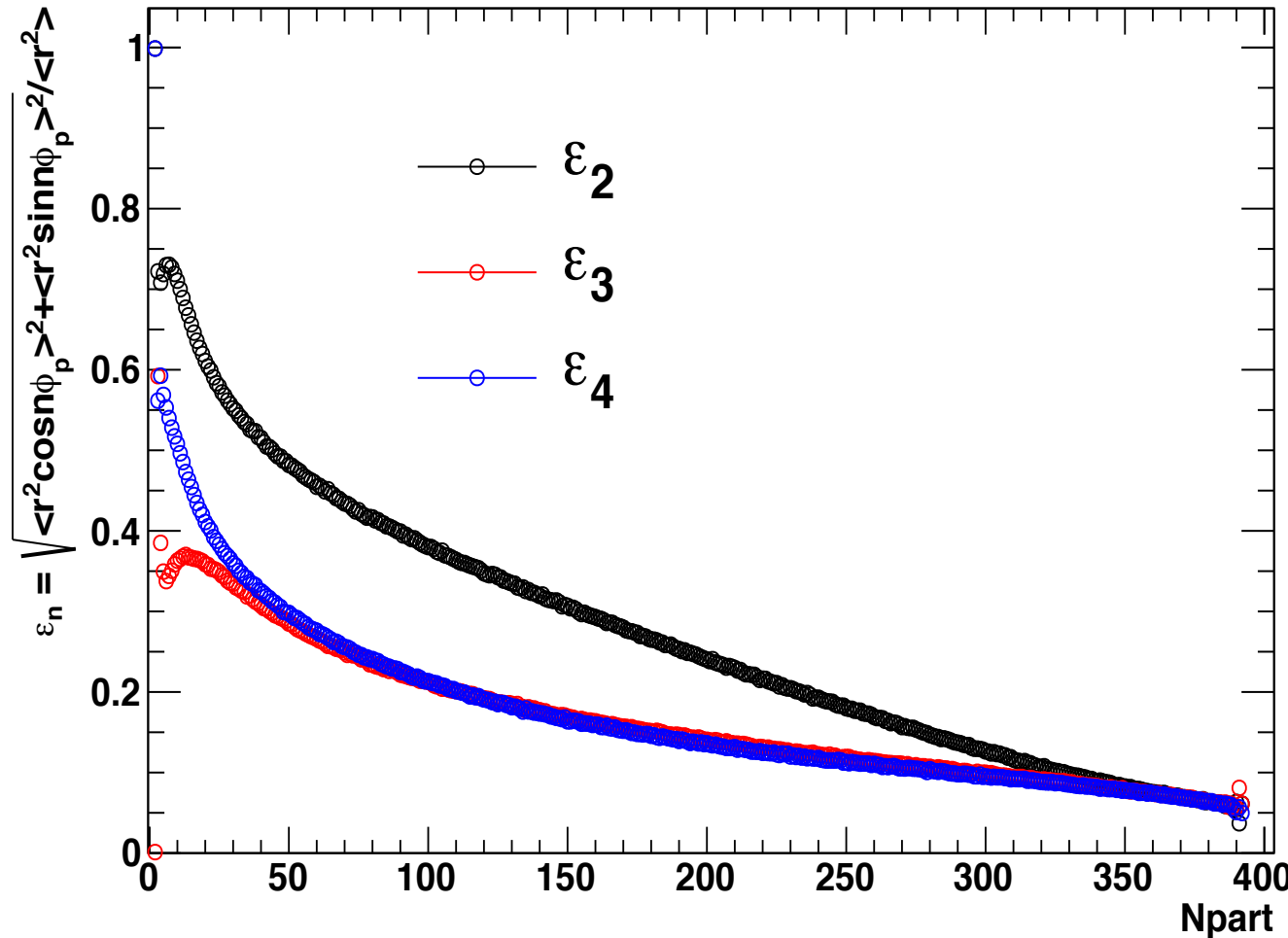
- ✧ Woods-Saxon Distribution
 - Nucleon density distribution
- ✧ Collision range
- ✧ Number of nucleons participated in a collision
- ✧ Number of binary nucleons collisions in a collision

$$\rho(r) = \frac{1}{1 + \exp \frac{r - r_a}{a}}$$
$$d < \sqrt{\frac{\sigma_{nn}}{\pi}}, \sigma_{nn} = 42mb$$
$$N_{part}$$

N_{coll}



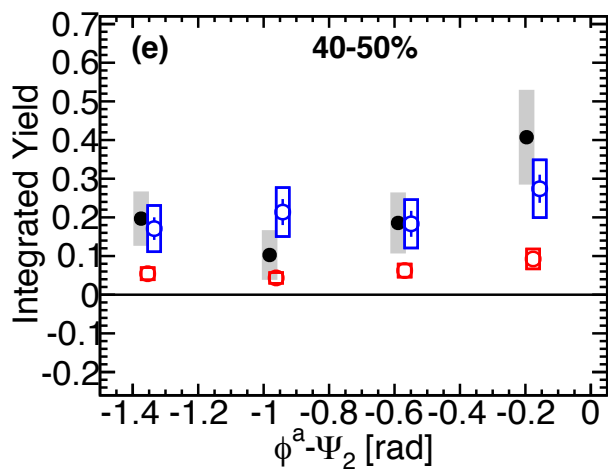
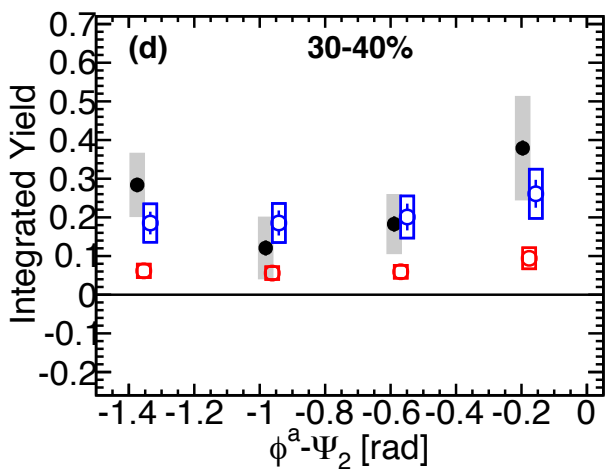
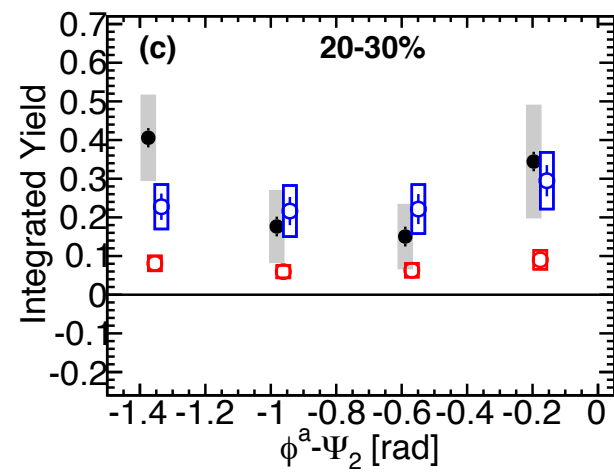
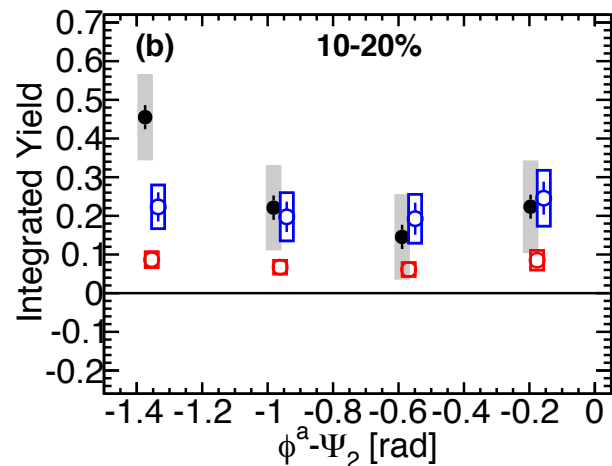
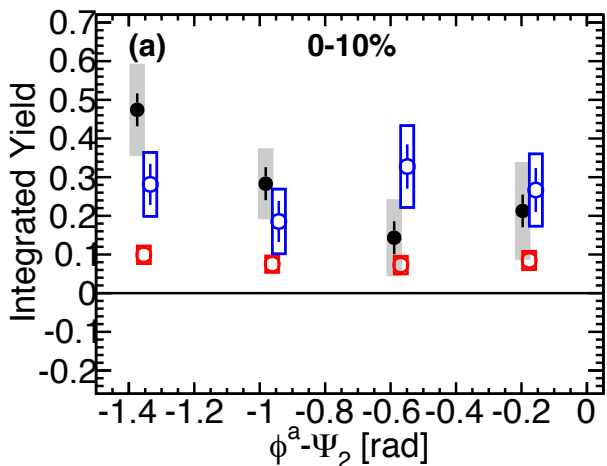
Participant Eccentricity by Glauber Model



Near-Side Integrated Yield vs Associate Angle from Ψ_2

Au+Au 200GeV
 Ψ_2 dependence
 Near Side : $|\Delta\phi| < \pi/4$

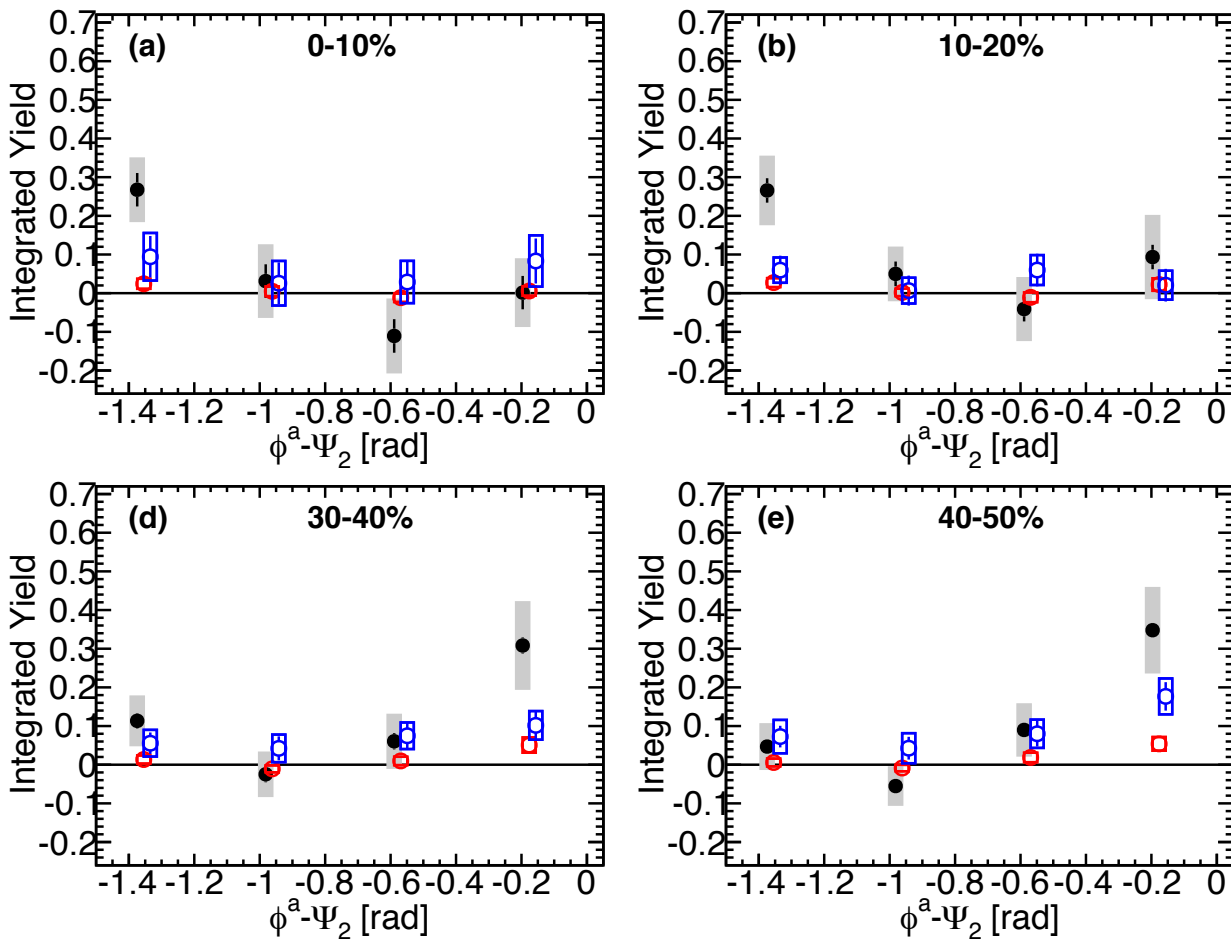
- 2-4 \otimes 1-2GeV/c
- 2-4 \otimes 2-4GeV/c
- 4-10 \otimes 2-4GeV/c



Away-Side Integrated Yield vs Associate Angle from Ψ_2

Au+Au 200GeV
 Ψ_2 dependence
 Away Side : $|\Delta\phi - \pi| < \pi/4$

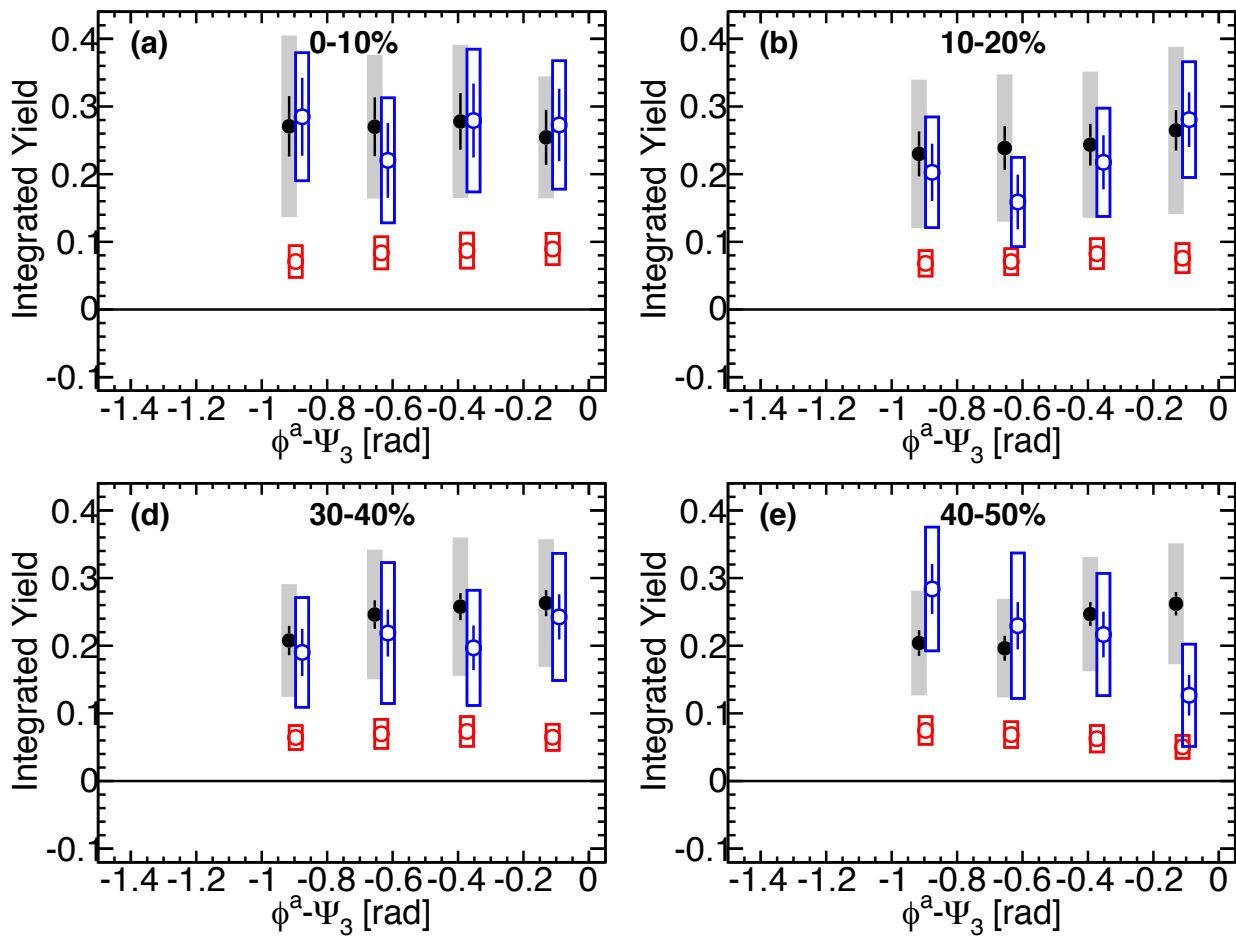
- 2-4 \otimes 1-2GeV/c
- 2-4 \otimes 2-4GeV/c
- 4-10 \otimes 2-4GeV/c



Near-Side Integrated Yield vs Associate Angle from Ψ_3

Au+Au 200GeV
 Ψ_3 dependence
 Near Side : $|\Delta\phi| < \pi/4$

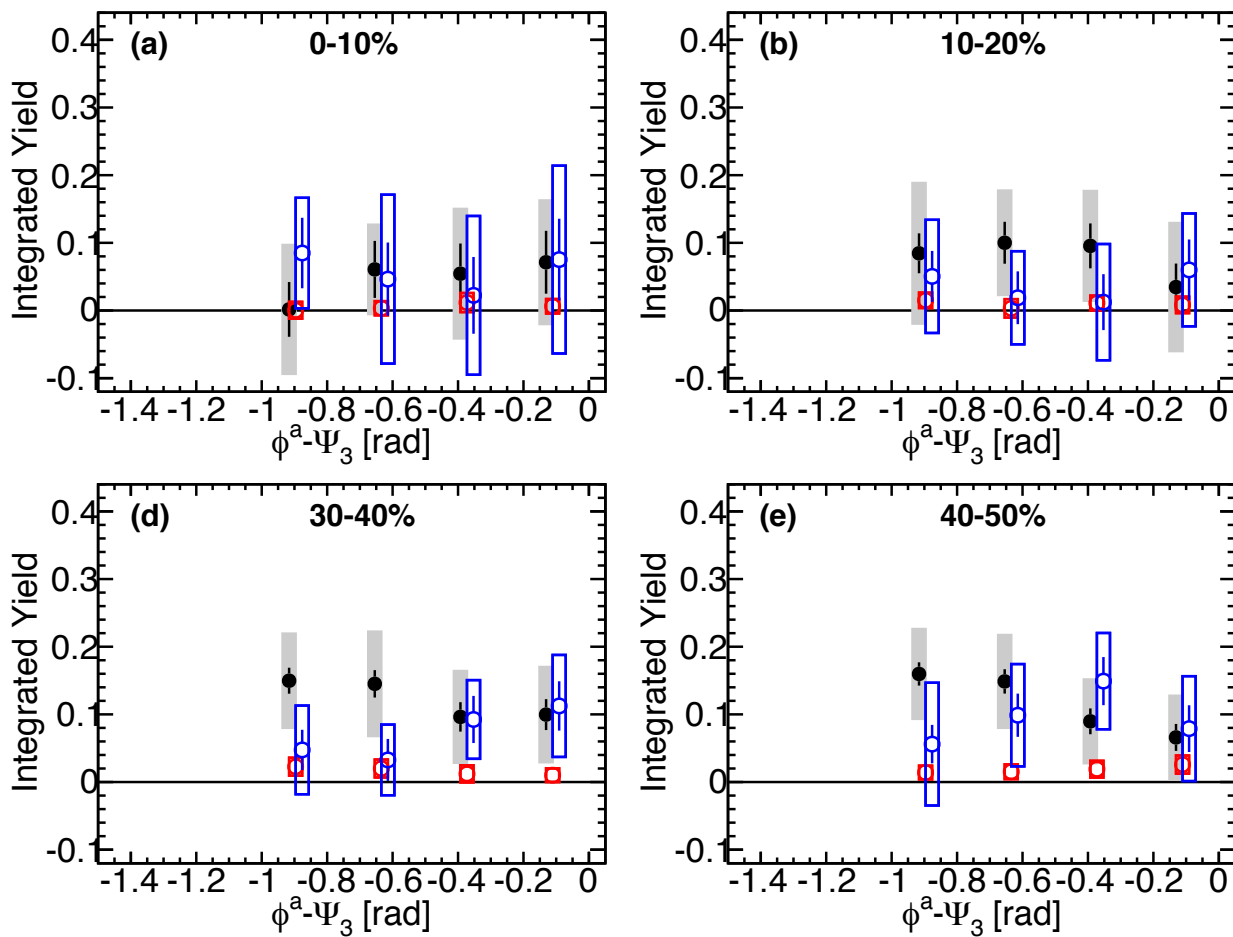
- 2-4 \otimes 1-2GeV/c
- 2-4 \otimes 2-4GeV/c
- 4-10 \otimes 2-4GeV/c



Away-Side Integrated Yield vs Associate Angle from Ψ_3

Au+Au 200GeV
 Ψ_3 dependence
 Away Side : $|\Delta\phi - \pi| < \pi/4$

- 2-4 \otimes 1-2GeV/c
- 2-4 \otimes 2-4GeV/c
- 4-10 \otimes 2-4GeV/c

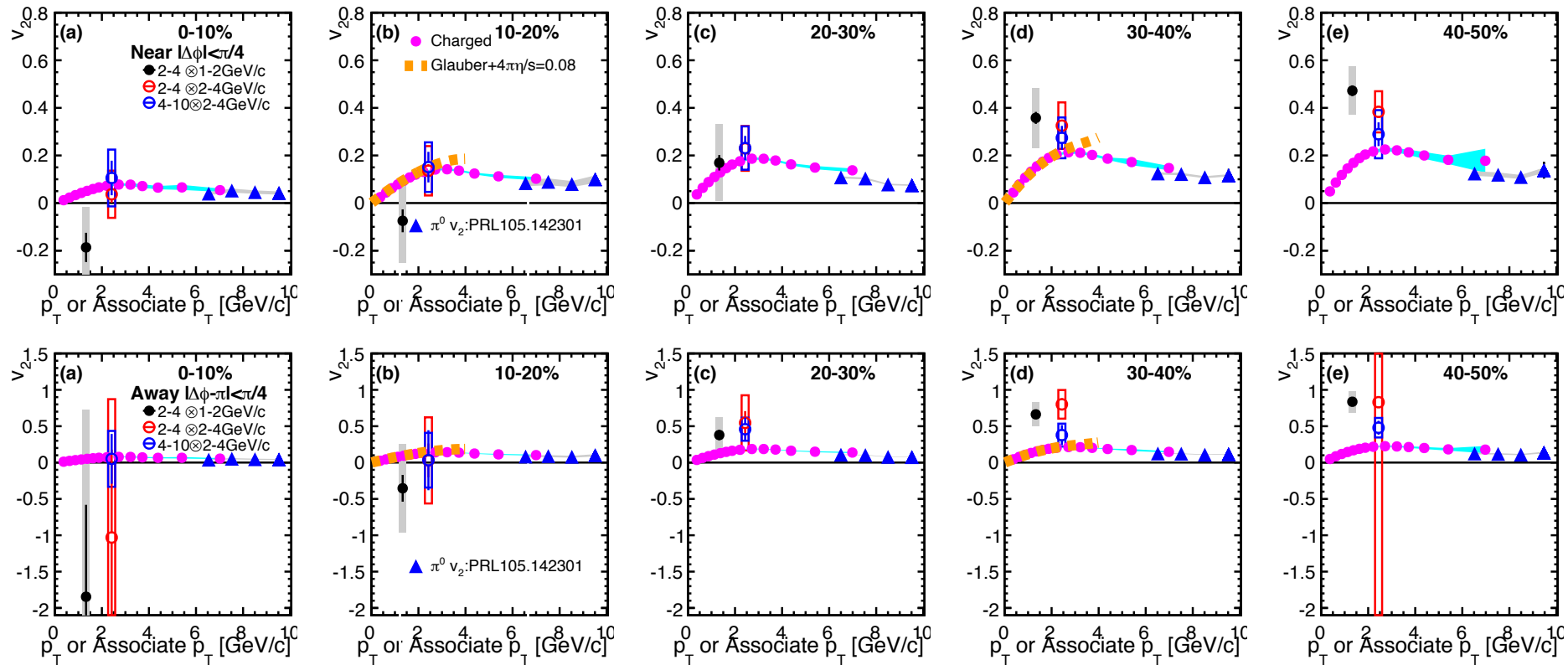


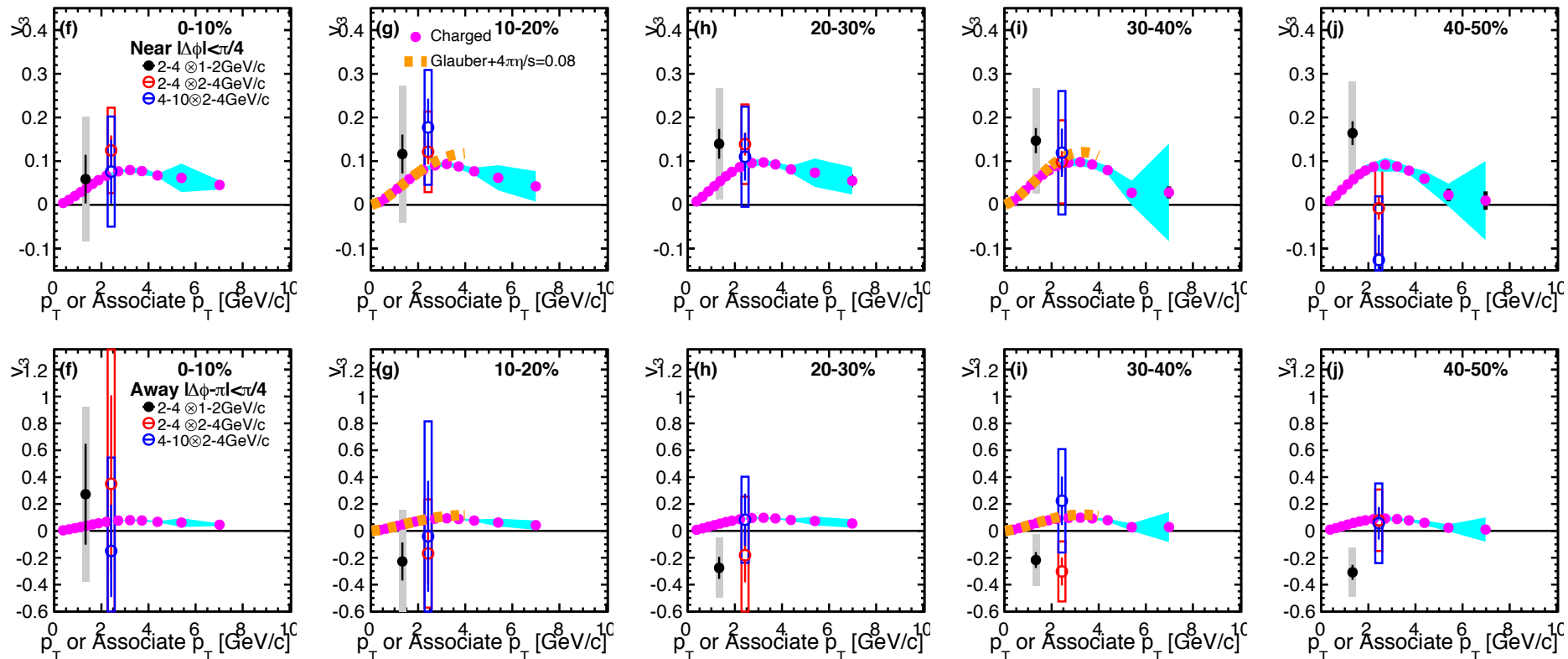
Anisotropy of particles per a jet →

Anisotropy of particles per a event

$$\begin{aligned} & \{1 + 2v_n^{PTY} \cos n(\phi^a - \Psi_n)\} \times \{1 + 2v_n^t \cos n(\phi^t - \Psi_n)\} \\ &= \{1 + 2v_n^{PTY} \cos n(\phi^a - \Psi_n)\} \times \{1 + 2v_n^t \cos n(\phi^a - \phi^t) \cos n(\phi^a - \Psi_n)\} \\ &\simeq 1 + 2v_n^{PTY} \cos n(\phi^a - \Psi_n) + 2v_n^t \cos n(\phi^a - \phi^t) \cos n(\phi^a - \Psi_n) \end{aligned}$$

$$v_n^{PTY,cor} = v_n^{PTY} + v_n^{trig} \cos n(\phi^t - \phi^a)$$





Gravity Position of Two-Particle Correlations

Definition

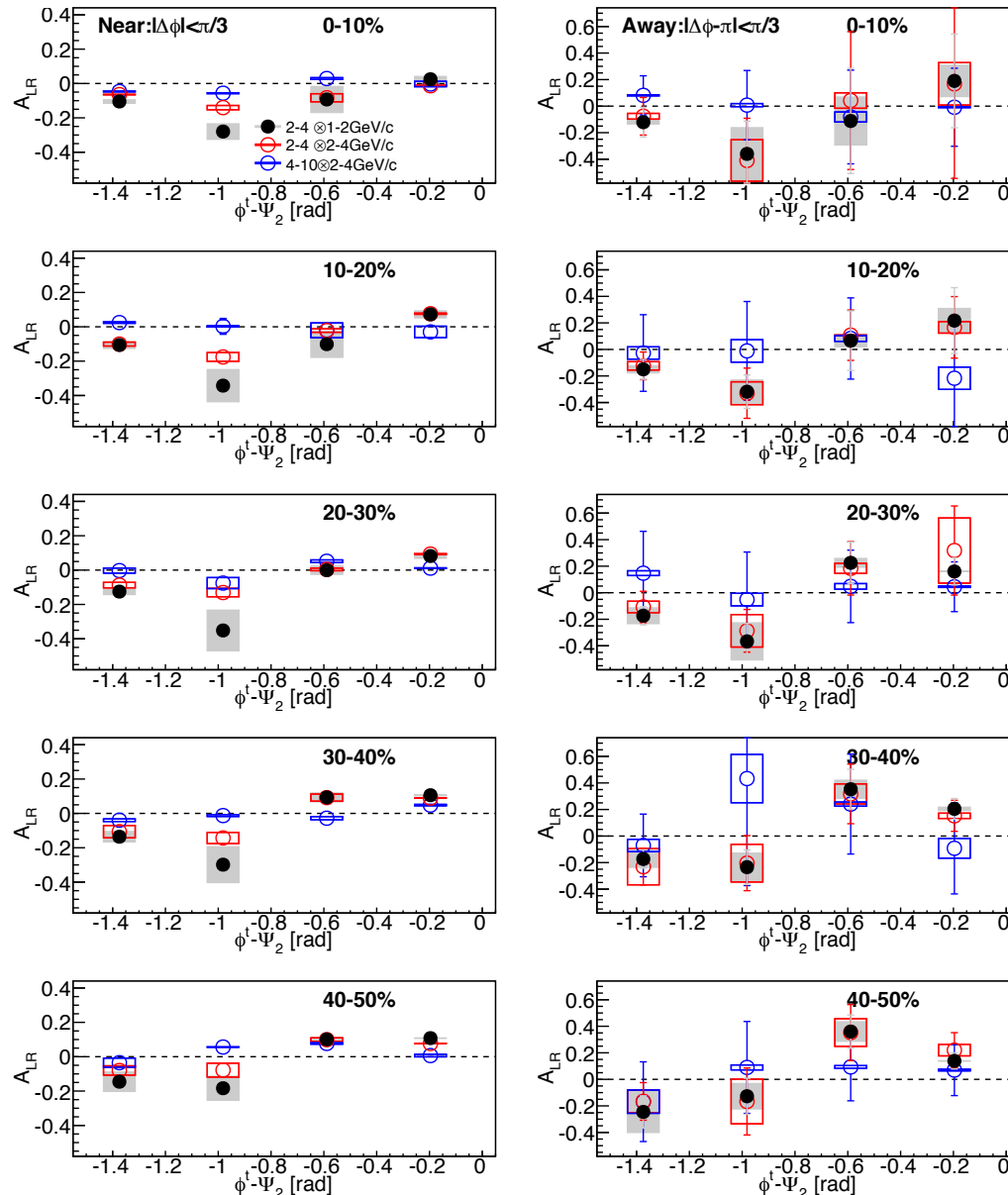
$$A_{LR} = \frac{\int d\Delta\phi \Delta\phi Y(\Delta\phi)}{\int d\Delta\phi Y(\Delta\phi)} - \begin{cases} 0 & \text{if near-side} \\ \pi & \text{if away-side} \end{cases}$$

Integral Ranges

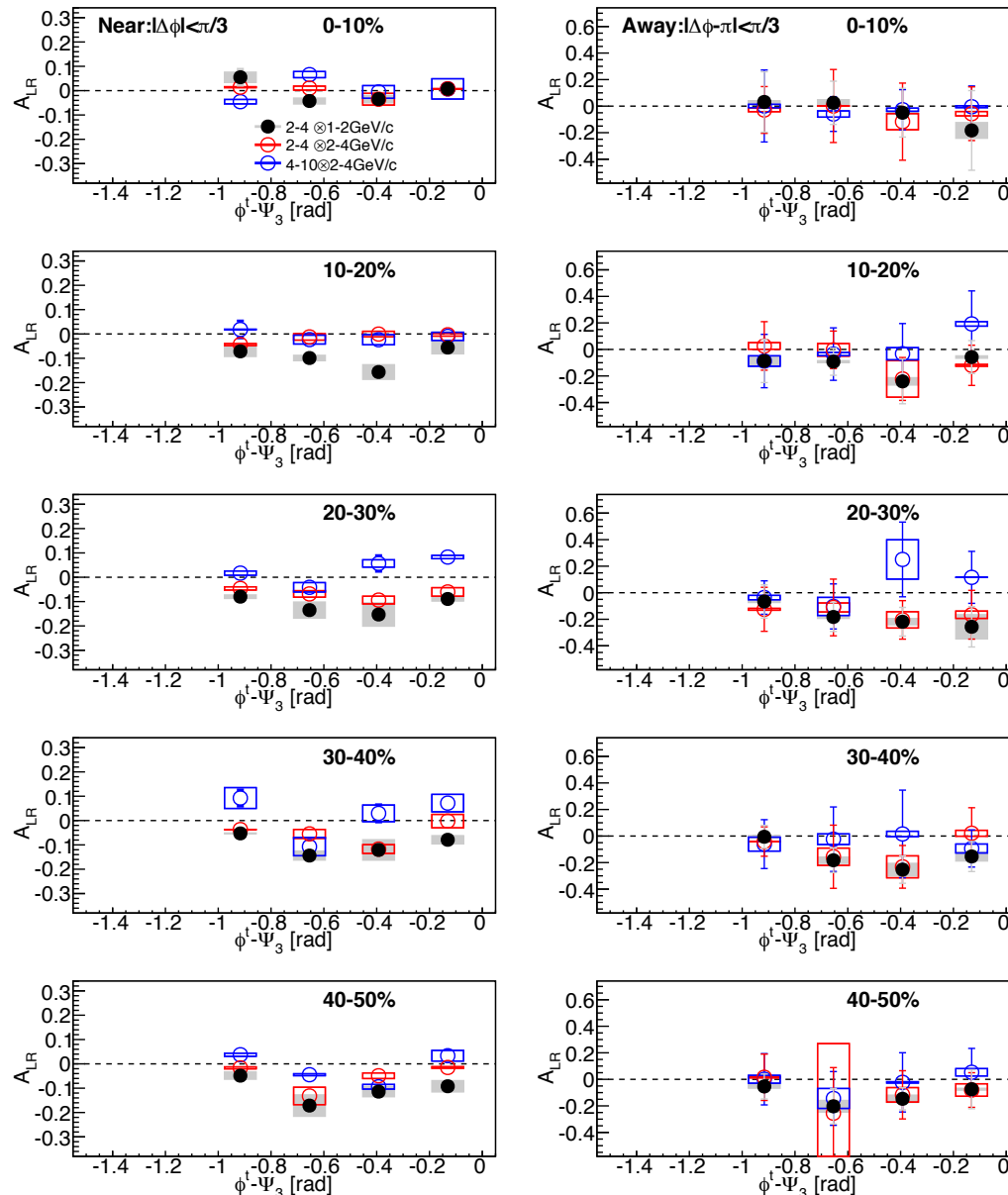
Near – Side : $|\Delta\phi| < \pi/3$

Away – Side : $|\Delta\phi - \pi| < \pi/3$

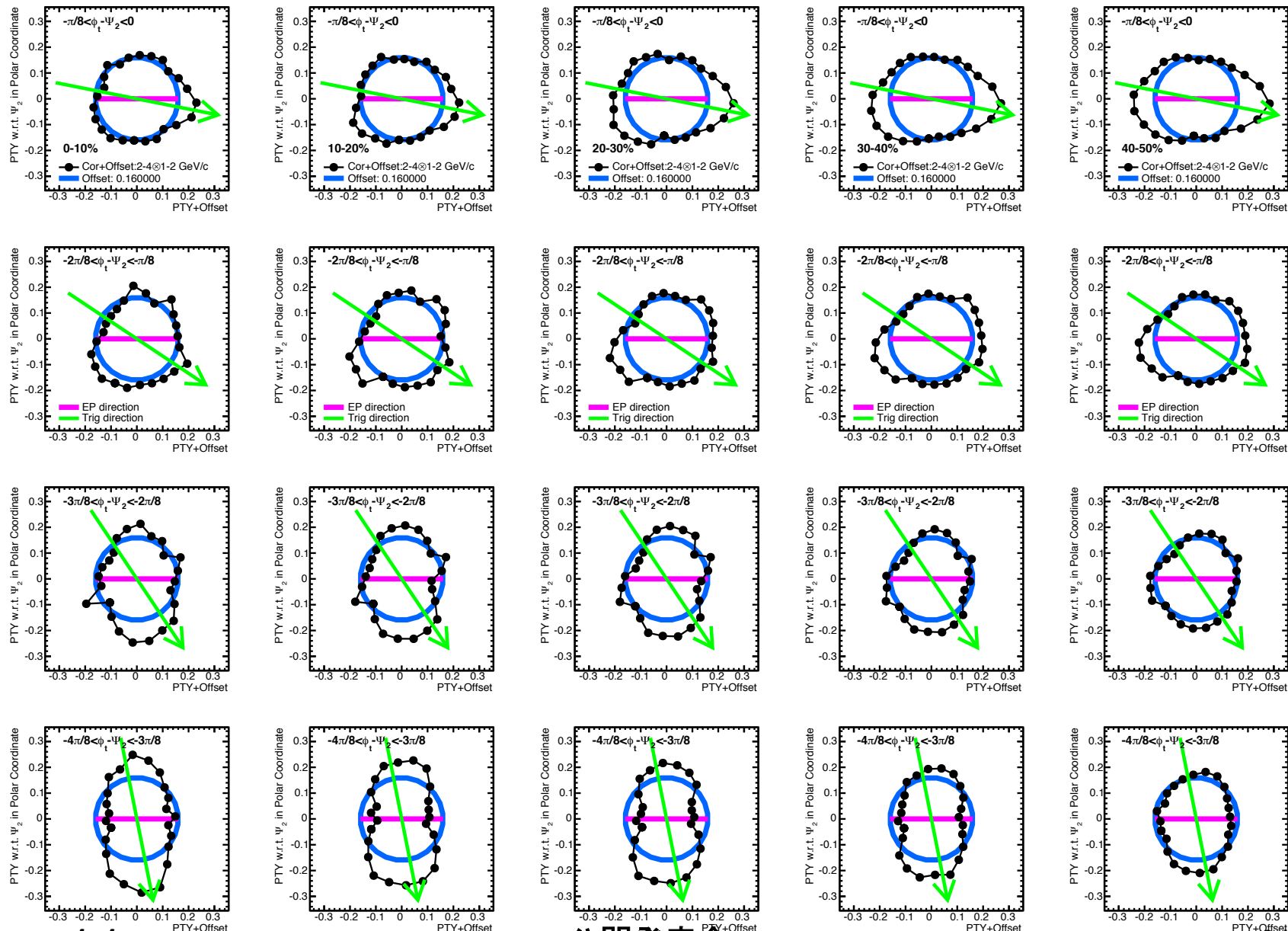
Gravity position vs trigger angle from Ψ_2



Gravity position vs trigger angle from Ψ_3



Ψ_2 Dependent Correlations : p_T 2-4x1-2 GeV/c



Ψ_3 Dependent Correlations : p_T 2-4x1-2 GeV/c

